NEW CHALLENGES IN THE SYNTHESIS OF NON-ISOCYANATE POLYURETHANES

A manuscript submitted to the

Universidad del Paìs Vasco (UPV/EHU)
Donostia-San Sebastián – España

and

Université de Bordeaux (UB)
Bordeaux – France

For the degree of

DOCTOR IN SCIENCES

Presented by

AMAURY BOSSION

Under the supervision of

Dr. Haritz Sardon (UPV/EHU)

Prof. Daniel Taton (UB)

Donostia, December 2018

To my family, love and friends

ACKNOWLEDGMENTS

This thesis represents the accomplishment of 3 years of "hard and happy" work carried out at POLYMAT (San Sebastian) and at the LCPO (Bordeaux) in Prof. David Mecerreyes' group and Prof. Daniel Taton's group, respectively. Throughout this thesis I have met so many people that have made this journey not only special but also unforgettable. This acknowledgement section won't be enough to explain all the gratitude I have for them.

Lehenik eta behin Haritz eskertu nahiko nuke, nire tesia lortzen lagundu, nigan sinetsi eta nire ideiak laborategian aplikatzen utzi didalako. Egia da hiru urte hauetan zehar gorabehera asko izan ditugula, baita hainbat bilera gogor ere, baina igarotako momentu pozgarri eta dibertigarriek aurre hartu diete momentu txar guztiei eta orain oroitzapen politak besterik ez zaizkit geratzen. Gainera, argi daukat hau guztia niregatik egin duzula, ni neu gaur egun naizen zientzialari eta pertsona izatera hel nedin. Horrenbestez, eta azkenik, bihotzez eskertu nahi dizut nire burua lan handiak egiteko gai dela erakusteko hainbeste aukera eman izana; zure laguntzari esker, oso harro nago nire lana eskuizkribu honetan aurkezteaz, benetan.

Je souhaite également remercier Daniel pour son aide, son encadrement et tout particulièrement pour m'avoir donné envie de réaliser cette thèse. Je me souviens encore des heures passées dans votre bureau à discuter longuement du pour et du contre de la thèse. Notamment je tiens à vous donner toute ma gratitude pour l'énorme opportunité que vous m'avez offerte cette année-là en me présentant cette offre de thèse européenne. Merci de m'avoir fait confiance dès le début. Ce fut un plaisir de travailler et de partager toutes ces longues discutions avec vous, même si cela n'a été que bien trop court. Sans vous tout cela n'aurait pas été possible !

Muchas gracias a David por permitirme ser parte de esta hermosa familia que he conocido en San Sebastián. Gracias por tus consejos, experiencia y por guiarme durante estos 3 años. Me aseguraré de mantener el lema "work hard and happy" en mi mente. Merci pour ton aide et ta bonne humeur tout au long de cette étape de ma vie.

Honez gain, Lourdes-ek Tesi honetan eskaini didan laguntza ere eskertu nahiko nuke, momentu zailenetan nire alboan egon baita beti; izan ere, zure aholkuak egokiak, erabilgarriak eta askotan ezinbestekoak izan dira eta izandako zailtasunei aurre egiten lagundu didate.

Je suis aussi très reconnaissant envers Prof. Henri Cramail, Dr. Etienne Grau, Cédric Le Coz et Gérard Dimier pour leurs soutiens, leurs idées et le temps passé ensemble à partager connaissances et bonne humeur au début de cette thèse et lorsque j'étais au LCPO.

I gratefully acknowledge all colleagues in POLYMAT: Daniele, Alvaro, Sara, Fermin, Coralie, Iñaki, Leire, Alex, Giulia, Stefano, Noé, Mehmet, Nora, Aitor Luca, Asier, Nerea, Ana S., Ana M., Isabel, Antonio, Guiomar, … ; mais aussi au LCPO: Martin, Sufi, Beste, Fiona, Mehdi, Dounia, Quentin S., Quentin P., Camille, Leila, Boris, Christopher, Cindy, Hélène, Arthur, … Thanks for the wonderful time spent together!

Of course, I could not end up these acknowledgements without talking about the people who made these years exceptional and who made me feel at home everyday: Naroa, Andere, Elena, Irma, Nicolas, Jérémy and Ion!

Una de mis gracias especiales a mi familia adoptiva, mi madre Naroa, mis hermanas Andere y Elena y mi abuela Irma. Naroa, mi chiquita, nuestra relación no comenzó tan temprano como debería hacerlo. Pero si tuviera que repetirlo, lo haría exactamente igual. Te convertiste en mi mejor amiga, la que siempre está aquí para escucharme y ayúdame sin importar nada. Nunca he tenido la oportunidad de conocer a alguien como tú en mi joven vida. Gracias por apoyarme, por todos estos momentos divertidos compartidos, por la larga conversación y por todo el amor y el

apoyo que me brindaste en los momentos difíciles. Espero que esta relación nunca termine.

Andere, mi hermana, la que estuvo aquí para mí desde mi llegada a San Sebastián. Estos años contigo fueron excepcionales. Nos reímos, peleamos, pero al final es lo que hacen los hermanos que se aman. Ahora entiendo, siempre trataste de empujarme a ser más independiente y crecer. ¡Gracias!

Elena e Irma mi hermana y abuela. Sin ustedes, esta familia no tendría sentido. Gracias por ser parte de este viaje, y por ser tan buenas personas. ¡Ojalá tuviera más tiempo para pasar con vosotras!

Esta tesis definitivamente no habría sido la misma sin ustedes, chicas. ¡Las amo y os extrañaré!

Merci à ma clique francophone, Jérémy et Nicolas pour m'avoir sorti de mon trou dès votre arrivée et pour tout le bon temps passé ensemble en soirée ou lors de nos sessions surf. Nicolas merci de m'avoir fait découvrir cette nouvelle passion, le surf, de m'avoir appris à parler comme un vrai Marseillais avec mes « wesh » et pour tous les fous rires. Un grand merci à Jérémy pour m'avoir patiemment écouté me plaindre tous les jours comme un bon français, pour ses conseils professionnels (et autres) et pour toutes ces bonnes bières belges vidées ensemble. Encore désolé de vous avoir battu à la Coupe du Monde, on se retrouve dans deux ans pour l'Euro ! Merci à vous deux ! On se revoit très vite à Paris où vous serez les bienvenus n'importe quand, ou lorsque je reviendrai vous montrer comment surfer les bonnes vagues de Zurriola !

Y muchas gracias Ion por tu ayuda y tu apoyo durante este último año. Gracias a tu ayuda una parte de esta tesis ha sido posible. He disfrutando mucho trabajando contigo, pero sobre todo de nuestras sesiones de videojuegos después del trabajo. ¡No solo eres un gran alumno sino una gran persona!

Merci à ma famille pour leur confiance, leur support and leur amour et sans qui tous cela n'aurait pas pu être possible !

Finally, I would like to thank everybody that are not mentioned here, who has been part of this journey and who has been important to the successful realization of this thesis.

I would also like to express my appreciation for the financial support from the European commission through the SUSPOL-EJD (642671).

Thank you, Muchas gracias, Merci beaucoup, Mila esker!!

TABLE OF CONTENT

ABBREVIATIONS

Catalysts

BEMP	2-*tert*-Butylimino-2-diethylamino-1,3-dimethylperhydro-1,3,2-diazaphosphorine
DBTDL	Dibutyltin dilaurate
DBU	1,8-Diazabicyclo[5.4.0]undec-7-ene
TBD	1,5,7-Triazabicyclo[4.4.0]dec-5-ene
t-BuP_2	1-*tert*-Butyl-2,2,4,4,4-pentakis(dimethylamino)-2λ^5,4λ^5-catenadi(phosphazene)
P_4	1-*tert*-Butyl-4,4,4-tris(dimethylamino)-2,2-bis[tris(dimethylamino)-phosphoranylidenamino]-2λ^5,4λ^5-catenadi(phosphazene)
PTSA	*p*-Toluenesulfonic acid
TEA	Triethylamine
TU	1-(3,5-Bis(trifluoromethyl)phenyl)-3-butylthiourea

Measurements techniques

DFT	Density functional theory
DLS	Dynamic light scattering
DSC	Differential scanning calorimetry
FTIR	Fourier transform infrared spectroscopy
LC-TOF-MS	Liquid chromatography-time-of-flight-mass spectrometry
NMR	Nuclear magnetic resonance
SAXS	Small angle X-ray scattering
SEC	Size exclusion chromatography
TEM	Transmission electron microscopy
TGA	Thermogravimetric analysis

Notations

Đ	Dispersity
Da	Dalton (1 Da = 1 g.mol^{-1})
G’	Storage modulus
G”	Loss modulus
mol. %	Mole percentage

M_n	Number-average molar mass
M_w	Weight-average molar mass
O/W	Oil-in-Water
W/O	Water-in-Oil
T_g	Glass transition temperature
wt. %	Weight percentage

Polymerization methods

ROP	Ring-opening polymerization
SAIP	Surfactant-assisted interfacial polymerization

Polymers

NIPU	Non-isocyanate polyurethane
PEG diamine	*O,O'*-Bis(2-aminoethyl)polyethylene glycol
PEG	Polyethylene glycol
PDMS diamine	Bis(3-aminopropyl) terminated poly(dimethylsiloxane)
PHU	Poly(hydroxyurethane)
PHUU	Poly(hydroxyurea−urethane)
PU	Polyurethane
PUU	Poly(urea-urethane)
WNIPU	Water-dispersible non-isocyanate polyurethane
WPU	Waterborne polyurethane

Reagents and solvents

$CDCl_3$	Deuterated chloroform
$(CD_3)_2CO$	Deuterated acetone
DGC	Diglycerol dicarbonate
DCM	Dichloromethane
DMAc	*N,N*-Dimethylacetamide
DMPA	2,2-Bis(hydroxymethyl) propionic acid
DOX	Doxorubicin
DOX·HCl	Doxorubicin hydrochloride
DMF	*N,N*-Dimethylformamide
DMSO	Dimethyl sulfoxide

$DMSO\text{-}d_6$	Deuterated dimethyl sulfoxide
ECF	Ethyl chloroformate
MDEA	*N*-Methyldiethanolamine
$MgSO_4$	Magnesium sulfate
MTC-tBAc	Trimethylenecarbonate-5-methyl-5-carboxy-*tert*-butylacetate
NaOH	Sodium hydroxide
$NaHCO_3$	Sodium bicarbonate
PFC	(Bis)-pentafluorophenyl carbonate
TAEA	Tris-(2-aminoethyl)amine
TBBA	*tert*-Butyl bromoacetate
THF	Tetrahydrofuran
TFA	Trifluoroacetic acid

Surfactants

DTAB	Dodecyltrimethylammonium bromide
CTAB	Cetyltrimethylammonium bromide
SDS	Sodium dodecyl sulfate
Tween 80	Polyoxyethylene (20) sorbitan monooleate

Others

EPA	Environmental protection agency
HAP	Hazardous air pollutant
VOC	Volatile organic compound

Chapter 1

Introduction

CHAPTER 1. INTRODUCTION

Whether it is in the packaging, building and construction, automotive, electronic, textile, household, leisure or medical industry, polymers are ibiquitous in our daily life. The World production of plastic materials reached 335 million tons in 2016 and the production growth is set to increase by 1.5 % in 2018 imparted primarily by the growing demand of the emerging countries.[1]

Among plastic materials, polyurethanes (PUs) represent the 6th most popularly used polymers in the World, with a global production that was estimated at 18 million tons in 2016. The demand for PUs is rising on average of 4.5 % per year. In Europe, this demand attained 7.5 % in 2016.[1] Since their first synthesis by Otto Bayer in 1937, PUs gained considerable interest due to their high versatility, good mechanical and physical properties, such as toughness, durability, biocompatibility, elasticity and abrasive resistance, and relatively low cost.[2] Owing to the wide range of monomeric building blocks employed for their synthesis, namely, diisocyanates and diols, PUs find numerous applications, for example, in rigid and flexible foams for insulation or the automotive industry, adhesives and sealants materials, coatings, or as biomedical materials (**Figure 1**).[3,4] PUs are conventionally synthesized by the reaction between a polyol, a polyisocyanate and a chain extenders in the presence of metal-based catalyst; this method is still currently in use by the chemical industry. Moreover, PU synthesis is usually achieved in solution, the use of a solvent being aimed at decreasing the overall viscosity of the reaction medium and enabling to reach high molecular weight polymers.[5]

In the last decade, however, researchers have strived to develop greener alternatives, to address concerns about the toxicity and the environmental impact of the reagents employed in PU synthesis.

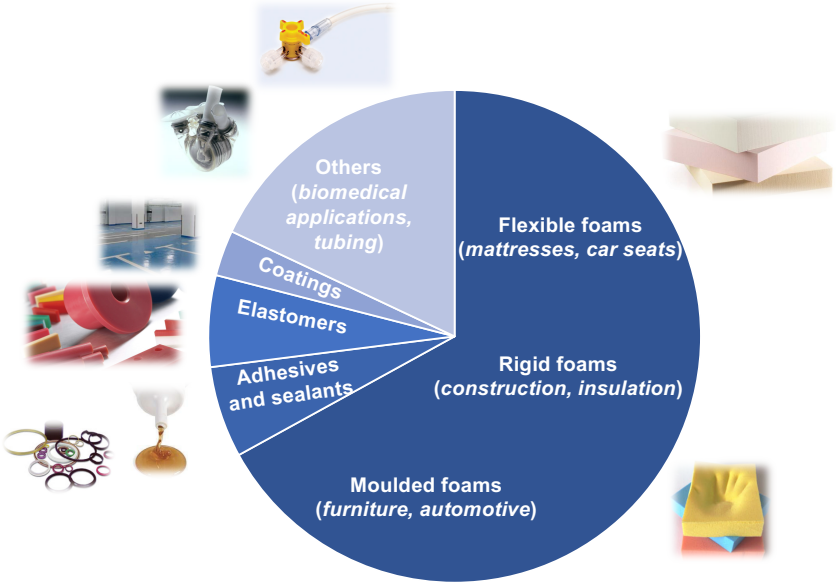

Figure 1. Main applications of polyurethanes synthesized by step-growth polymerization of polyisocyanates and polyols.

Use of isocyanate-based monomers in PU synthesis indeed raises severe health concerns.[6] One of the deadliest industrial events, which took thousands of lives after a methyl isocyanate leakage, demonstrating the hazardous nature of isocyanates, happened in December 1984 in Bhopal, India.[7] Regular isocyanates are actually synthesized using phosgene, a highly reactive and toxic gas, used during World War I as chemical weapon.[8]

Moreover, PU synthesis most often requires the use of a catalyst, typically organotin compounds, such as dibutyltin dilaurate.[9] The success of this catalyst is related to its high activity at low loading. However, it can be hardly removed from the final polymers. The presence of residual catalyst in PUs causes detrimental effects on their aging. In addition, some studies suggested the possibility of tissue function endangerment through slow penetration of the catalyst into the blood

circulation system, which questions the usage of tin-derived PUs in biomedical and food contact applications.[10–16]

Finally, as PUs are usually synthesized in organic solvents, for a use in applications such as coatings, paints, inks and adhesives, this necessitates the evaporation of a large amount of volatile organic compounds (VOCs) and hazardous air pollutants (HAPs) in the atmosphere. Exposure to VOCs are known to provoke health effects, such as headaches, dizziness, irritation, cancer, etc.[17]

All these concerns about users' safety have led to the implementation of regulations by the European Union and the United States Environmental Protection Agency (EPA) to restrict the use of both organotin compounds and substances containing more than 0.1 wt. % of free diisocyanate, and reduce the amount VOCs releasable to the atmosphere. Thus, researchers in industry and in academia have put significant efforts in the past years to find synthetic alternatives to PUs, involving non-toxic reagents.[12,18]

1.1. Organocatalyzed step-growth polyaddition of cyclic dicarbonates and diamines

One of these alternatives consists in the synthesis of non-isocyanate polyurethanes, referred to as NIPUs (**Figure 2**). One can distinguish four synthetic pathways to NIPUs, including (1) the step-growth polymerization of bis-cyclic carbonates and amines, (2) the step-growth polymerization of linear activated dicarbonates and diamines, (3) the step-growth polymerization of linear activated dicarbamates and diols, and (4) the ring-opening polymerization of cyclic carbamates.[19]

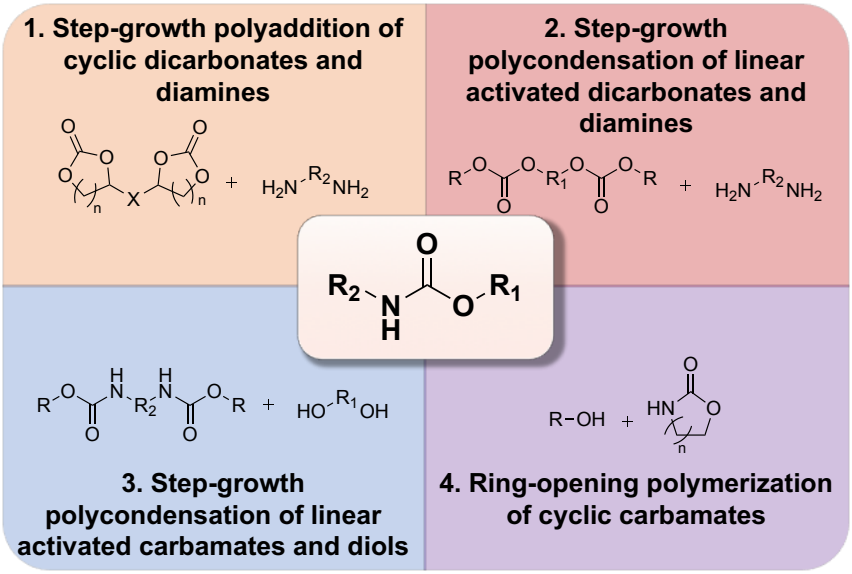

Figure 2. Main synthetic routes toward non-isocyanate polyurethanes (NIPUs); adapted from ref. 19

Amongst them, polymerization involving cyclic dicarbonates and diamines has been extensively studied. In this context, 5-, 6-, 7 and 8-membered dicyclic carbonate monomers have been the most employed.[20–31] While 6-, 7- and 8-membered carbonates prove more reactive than their 5-membered counterparts, and facilitate catalyst-free polymerization, their synthesis generally requires the use of toxic chlorinated carbonylating agents, such as phosgene or alkyl chloroformates.[29] In contrast, synthesis of 5-membered cyclic carbonates can be readily achieved by coupling CO_2 onto epoxides.[32] The step-growth polyaddition of five-membered cyclic carbonates and diamines for the formation of polyhydroxyurethanes (PHU)s was reported as early as 1957.[33] It is important to note that PHUs structurally differ from conventional PUs by the presence of primary and/or secondary alcohols adjacent to the β-position of the urethane bond, which impart them specific features (**Scheme 1**).[34] PHUs are thus generally amorphous due to the primary and secondary hydroxy-containing units randomly distributed along the polymer chain.[35] These hydroxyl groups can participate into intra- and

intermolecular hydrogen bond interactions, which generally leads to single-phase PHUs with poor mechanical properties, especially, when combined with polyether-based diamines. However, as demonstrated by Torkelson *et al*., these hydrogen bonds can be tuned by adequate choice of soft segments to provide PHUs with segmented morphologies.[36,37] Moreover, the reactive pendant hydroxyl groups enable further post-functionalization of the PHUs with chemical functionalities, such as ether, ester and carbonates moieties.[38,39]

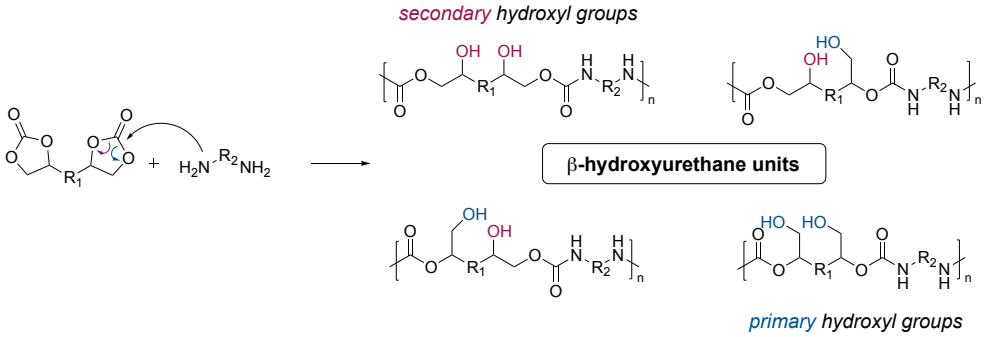

Scheme 1. Synthesis of polyhydroxyurethane from 5-membered cyclic carbonates and diamines; adapted from ref. 34

Two reaction mechanisms have been proposed for the formation of urethanes by the aminolysis of cyclic carbonates (**Figure 3**). Tomita *et al.* and Garipov *et al.* have suggested a mechanism involving an amphoteric tetrahedral intermediate.[40,41] With the aid of density functional theory (DFT) calculations, Zabalov and Sardon *et al.* have established that hydroxyurethane formation may progress notably through a six-center ring intermediate based on the 5-membered cyclic carbonate and two amine molecules, one acting as catalyst and the other performing the nucleophilic attack.[31,42] In any of the two pathways, the ring-opening reaction of cyclic carbonates may be accelerated through monomer activation.

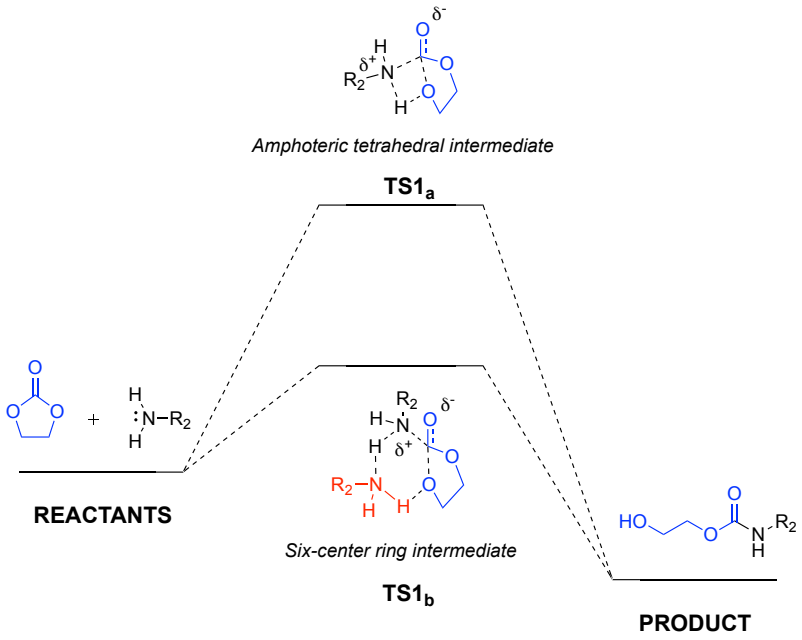

Figure 3. Proposed mechanism of the activation of cyclic carbonates with amines *via* an amphoteric tetrahedral intermediate ($TS1_a$) or *via* a six-center ring intermediate ($TS1_b$); adapted from ref. 42

Metal catalysis is essential to synthesize step-growth polymers, and nowadays, most of industrial polymers produced by step-growth polymerization utilize metallic catalysts, based for instance on tin, antimony, titanium or ruthenium.[43] More recently, several classes of organic compounds, including strong and weak Brønsted/Lewis acid or bases, phosphazenes, amines and ammonium derivatives, guanidines and amidines, and thiourea derivatives have demonstrated high catalytic activity towards the preparation of step-growth polymers, including NIPUs.[18,20,44–55]

There are eventually three ways to activate the reaction and facilitate the polymerization, namely, by a) increasing the electrophilicity of the carbonate center; b) increasing the nucleophilicity of the amine and c) through a nucleophilic activation of the carbonate (**Scheme 2**).[56]

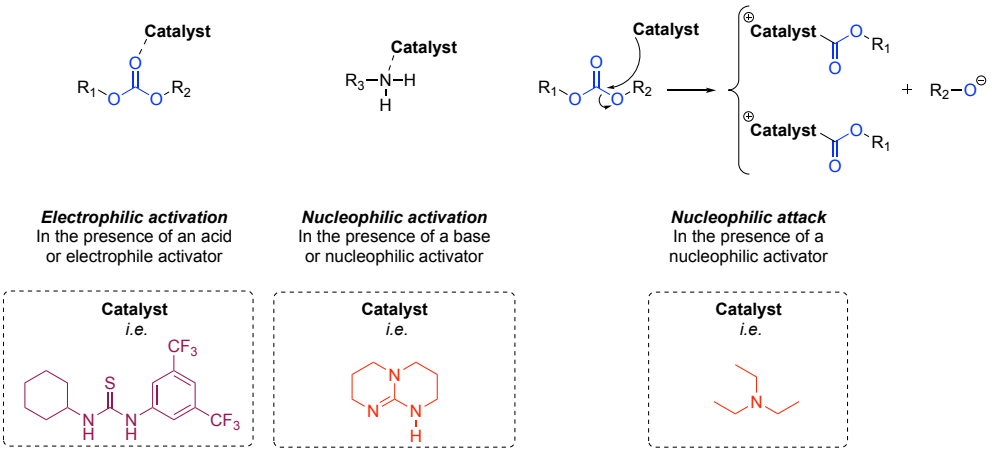

Scheme 2. General activation mechanism for the organocatalyzed isocyanate-free synthesis of polyurethanes from 5-membered cyclic carbonates and diamines; adapted from ref. 56

As discussed in more detailed in **Chapter 2**, reactions triggered by ureas and thioureas rest on the first activation mechanism, *i.e.* through an electrophilic monomer activation. This involves activation of the carbonyl either by protonation or by interaction by hydrogen bonding, facilitating nucleophilic attack of the amino-group (RNH_2) of the co-monomer or the chain-end.[57,58]

Strong bases, such as amidines and guanidines derivatives, *e.g.* 1,8-diazabicyclo[5.4.0]undec-7-ene (DBU) and 1,5,7-triazabicyclo[4.4.0]dec-5-ene (TBD), phosphine and phosphazene derivatives, such as triphenylphosphine and *t*-BuP_2, enable activation through a nucleophilic monomer activation mechanism, also referred to as a basic mechanism. In the latter case, activation of the amine or the chain-end occurs by deprotonation or H-bonding, which increases the nucleophilicity of the amine. The latter further attacks the carbonyl moiety by a ring-opening reaction to form a carbamate.[59]

Finally, nucleophilic attack of the electrophile moiety by an amino-containing organocatalyst, *e.g.* triethylamine (TEA), has also been proposed. This involves attack by the catalyst onto the carbonyl carbon of the monomer, resulting in ring-opening and formation of a zwitterionic intermediate species.[44]

Although intensive research has been devoted to the use of organic catalysts to enhance the kinetics of NIPU synthesis derived from 5-membered cyclic carbonates, a comprehensive study is still lacking.

1.2. Aqueous non-isocyanate polyurethane dispersions

Polymerization utilizing organic solvents refrain potential industrialization, for obvious reasons of cost and environmental concerns, and regulation. In this sense, the utilization of water as a reaction medium is of high scientific and industrial interest. The past decade has witnessed a progressive evolution of waterborne processes for the synthesis of PUs. Waterborne polyurethanes (WPUs) are environmentally friendlier materials used in coatings and adhesives for numerous substrates such as wood or textiles. However, due to the inherent incompatibility between water and isocyanates, it is highly challenging to achieve WPUs by conventional water processes, such as emulsion or suspension polymerization. Therefore, several alternative strategies have been developed. The most common referred to as the acetone process (see further).[60–65] Other strategies include the solvent-free prepolymer mixing process, the melt dispersion process and the bis-ketimine/bis-ketazine process.[60,66,67] All of these techniques share in common the use of low molecular weight prepolymers that are functionalized by an isocyanate terminal function and that are dispersed in water. Such pre-PUs further undergo chain-extension with diamines/polyamines to achieve poly(urethane-urea).

The acetone process consists into a three-steps procedure as depicted in **Figure 4**.[62,66]

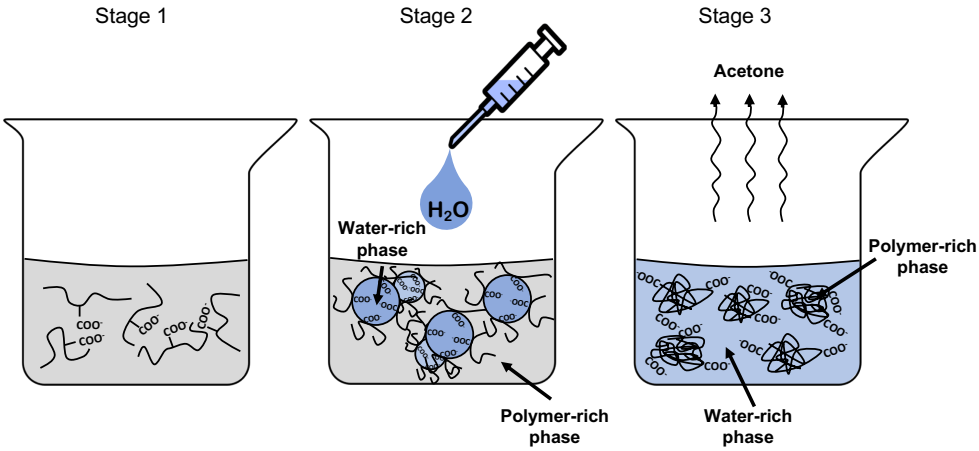

Figure 4. Schematic representation of the "acetone process" utilizing a component containing carboxylate groups in its backbone; adapted from ref. 62

A pre-PU is synthesized first, using a low boiling point water-miscible solvent, typically acetone. In this stage, hydrophilic and potentially charged groups are incorporated into the polymer backbone (**Figure 4.1**). These groups act further as internal emulsifiers, enabling the formation of stable PU dispersions. These hydrophilic groups are either of anionic-type, *e.g.* carboxylic acid groups arising from (2,2-bis(hydroxymethyl) propionic acid (DMPA), or of cationic-type, for instance resulting from alkylation of tertiary amino groups, and contribute to the PU electrostatic stabilization.

In the second step, water is added to the PU/acetone solution (**Figure 4.2**). Thanks to the hydrophilic groups previously incorporated into the polymer, stable dispersions can be achieved. The particle formation mechanism can be divided in three stages. In the first one, when water is initially added, the hydrophilic groups allow the PU/acetone mixture to absorb a certain amount of water. At this stage, the viscosity of the mixture slightly decreases. Once the system cannot absorb more water, the solution becomes turbid, which corresponds to the formation of polymer particles. PU particles can thus be form either *via* a precipitation or *via* a phase inversion.

Finally, once PU particles are formed, the viscosity of the solution drops as the addition of more water has only a dilution effect. Removal of acetone under vacuum yields the WPU (**Figure 4.3**).

Only one example can be found in the literature on the preparation of isocyanate-free poly(urethane-urea) aqueous dispersions. This was realized using the acetone process for the transurethanization reaction of the protected dicarbamate *N*-*N*′-di-*t*-butyloxycarbonyl isophorone diamine with poly(propylene glycol) diol (M_w = 2 kDa) (**Scheme 3**).[68] In their study, Ma *et al*. used 30 mol. % of 3,3′-diamino-*N*-methyldipropylamine as internal dispersing agent and methanol as low boiling point solvent. The authors thus obtained NIPUs with M_n = 35 kDa, and stable NIPU aqueous dispersions with an average particle size of 120 nm.

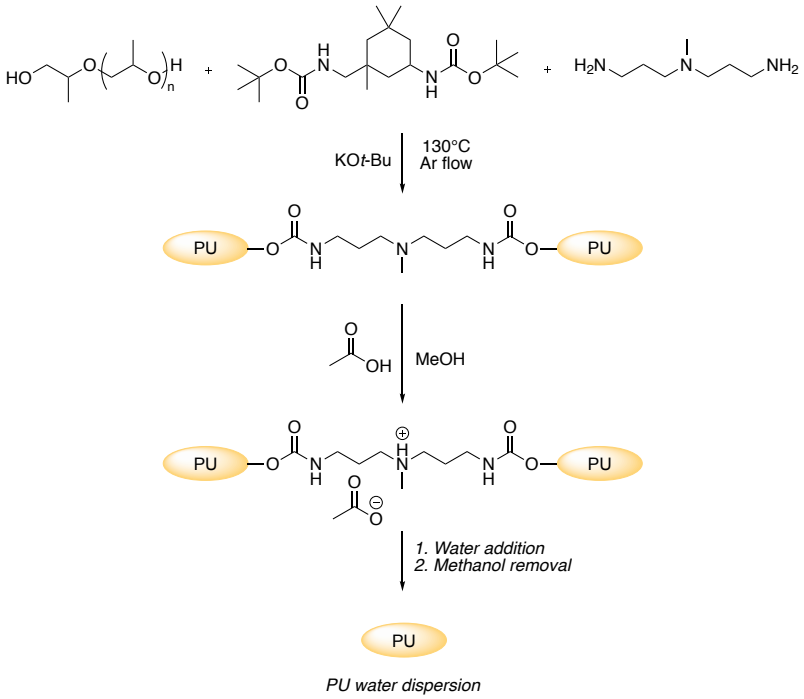

Scheme 3. Preparation of aqueous NIPU dispersions from *N*-*N*′-di-*t*-butyloxycarbonyl isophorone diamine, 3,3′-diamino-*N*-methyldipropylamine and poly(propylene glycol) diol using the acetone process; adapted from ref. 68

Despite being attractive, this system does not really fulfill criteria of a “green strategy” for the preparation of non-isocyanate WPU, as the reaction is performed using activated linear carbamates synthesized from phosgene-derived di-*t*-butyl dicarbonate and amines. Moreover, it suffers from side-reactions occurring during the polymerization, as confirmed by model reactions. Similarly to the amidation of esters, carbamates are indeed subjected to *N*-alkylation with amines during aminolysis reaction, which consequently leads to an off-stoichiometry of the monomers (**Scheme 4**). Thus, the resulting PUs exhibit lower molecular weights than expected and the materials obtained possess lesser physical properties.[69]

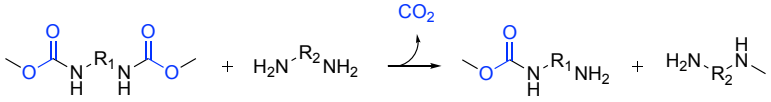

Scheme 4. *N*-Methylation of a diamine by a dicarbamate; adapted from ref. 69

Although the acetone process has attracted an increasing interest to prepare WPUs materials with very low VOC content, both the particle size and particle stability are difficult to control. While this process can be considered when designing PU dispersions for large scale industrial applications, such as coatings – where good control over the particle’s morphology is not crucial – other processes should be considered to obtain well defined structures; for instance, when targeting applications in nanomedicine, where the particle size and polydispersity index are critical parameters for *in vivo* applications. In these cases, other techniques that could be directly performed in aqueous media, such as mini-emulsion or interfacial polymerization, are highly desired to obtain well-defined PU nanoparticles.[70–73] In general, these techniques lead to high yields, can be conducted at moderate temperature, and employs less catalyst due to the existence of a large interfacial area, in comparison to bulk polymerization.[74]

While WPUs have been extensively studied, despite their environmental benefits, only one example concerning the preparation of aqueous NIPU dispersion

has been reported, starting from 5-membered cyclic carbonates and diamines. Cramail *et al.* have synthesized waterborne NIPUs latexes by mini-emulsion polymerization with up to 30 wt. % solid content (**Figure 5**).[75] For that purpose, three fatty acid-based 5-membered cyclic carbonates were designed and polymerized with Priamine 1075, a fatty acid diamine, in a mini-emulsion process at 60 °C for 24 h. Different surfactants, such as Tween 80 (non-ionic), sodium dodecylsulfate (SDS, anionic) and cetyltrimethylammonium bromide (CTAB, cationic), and hydrophobic agents have been tested in order to obtain stable emulsions and polymer particles. For example, the authors have found that while 10 wt. % of Tween 80 enabled to obtain stable NIPU dispersions with particle sizes around 100 nm, use of 5-membered cyclic carbonate derived from 1,4-butanedithiol in presence of SDS and CTAB led to sedimentation. However, NIPUs thus prepared in mini-emulsion exhibited lower molar masses (M_w = 7 kDa, $Đ$ = 1.6) than compounds formed in bulk (M_w = 14 kDa, $Đ$ = 2), due to the partial hydrolysis of cyclic carbonates.

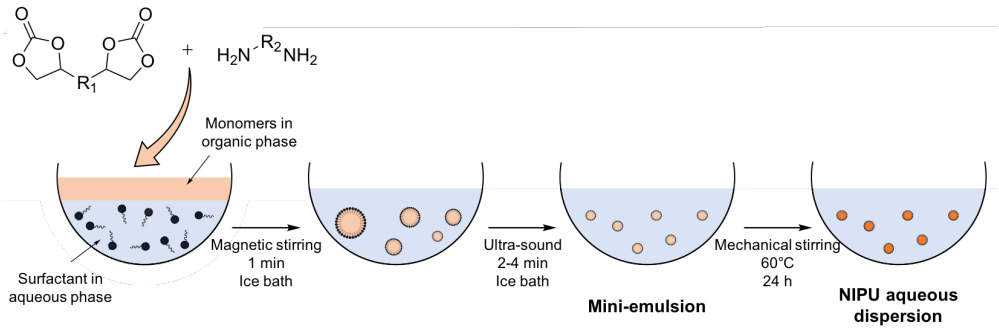

Figure 5. Preparation of aqueous NIPU dispersions starting from 5-membered cyclic carbonates and diamines through mini-emulsion process.

As an alternative to avoid decomposition of the carbonate in water, Sardon *et al*. have developed, the direct synthesis of PEG-based NIPU in aqueous solution, from the step-growth polycondensation of linear activated dicarbonates and diamines (**Scheme 5**).[46] The main advantage of this process lies in the utilization of

linear dicarbonates synthesized from the condensation reaction of diols with bis(pentafluorophenyl)carbonate. Indeed, these dicarbonates prove water-soluble and are not subjected to hydrolysis within 24 h. The polymerization was carried out at room temperature for 1 h in presence of TEA catalyst, achieving NIPUs with molecular weight in the range of M_n = 15-16.5 kDa ($Đ$ = 1.9). However, pentafluorophenol generated as side-product had to be removed before any potential applications. Moreover, this synthetic route does not lead to aqueous PU dispersions, as NIPUs obtained are water-soluble.

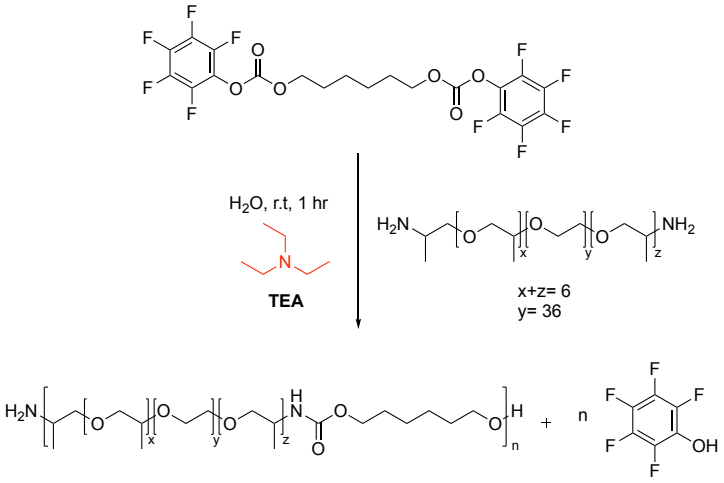

Scheme 5. Synthesis of a linear pentafluorophenyl dicarbonate and *Jeffamine* based polyurethane utilizing TEA; adapted from ref. 46

1.3. Concluding remarks and aims of the thesis

Considering the reduction of fossil resources and the subsequent environmental impact linked to the use of fossil fuel, synthesis of isocyanate-free PUs holds great promise as a cost-effective alternative for the production of PUs. In this context, miscellaneous isocyanate-free synthetic pathways to PUs have been

developed by an organocatalytic (metal-free) pathway. These greener and environmentally friendlier approaches employ mainly diols, diamines, carbon dioxide to achieve NIPUs. Regarding the literature, and in our opinion, the step-growth polyaddition of 5-membered cyclic carbonates with diamines represent the most promising route to NIPUs. However, this strategy is limited by the low reactivity of the cyclic carbonates, which requires harsh polymerization conditions, such as high temperatures, bulk conditions, long reaction times and the use of organocatalysts, to push the reaction to completion and obtain high molecular weight polymers. These conditions imply the formation of side reactions, including transamidations inter- or intra-molecular, leading to urea. Surprisingly, very few reports have addressed these side reactions, and there is still a lot to be done to fully understand how these side-reactions impact the PU physico-chemical properties. This prompted us to conduct a detailed investigation into the effect of the organocatalysts and reaction conditions, on the final properties of the resulting PHUs, as will be discussed in **Chapter 2**.

It is worth pointing out that, not only the synthesis of PUs using renewable reagents is important, but also to perform the polymerization under sustainable conditions, ideally under solvent-free conditions or using waterborne processes. In this regard, waterborne PUs have attracted a lot of attention in the last decade, owing to severe restrictions on the use of VOCs. Due to the inherent incompatibility of isocyanate-containing monomers and water, direct synthesis of PUs in water cannot be carried out using emulsions or microemulsions techniques. Several strategies have thus been developed to produce WPUs, among them the “acetone process” represents the most common employed in industry. *A contrario*, processes aimed at preparing well-defined isocyanate-free PU nanoparticles in aqueous media are scarce. Moreover, the aqueous dispersions prepared from 5-membered cyclic carbonates suffer from a side reaction, the partial hydrolysis of the cyclic carbonates. Thus, alternative strategies would be needed to obtain well-defined NIPU nanoparticles in water and with limited extent of side-reactions.

In **Chapter 3** is described the design of stable NIPU dispersions through an adaptation of the “acetone process” in the step-growth polyaddition of 5- and 8-membered cyclic carbonates and diamines. As for **Chapter 4,** it focuses on the synthesis of well-defined NIPU nanoparticles in water by a one-pot interfacial polymerization of linear activated carbonates and diamines/triamines. Overall, these new developments in PU synthesis should broaden the scope of functional isocyanate-free PU materials for a potential use in coating and drug delivery applications, respectively.

The objectives of this thesis are twofold, including (1) a thorough investigation of the effect of organocatalysts on the step-growth polymerization of bio-based 5-membered cyclic carbonate and diamines, and (2) synthesis of novel water-based NIPU materials by adapting established techniques, such as the acetone process or the interfacial polymerization.

With these challenges in mind, and as shown in **Figure 6**, the manuscript is organized as follows:

- **Chapter 2** focuses on the investigation of the effect of both structural variation of organocatalysts and experimental conditions on the bulk polymerization of bio-based 5-membered cyclic carbonates with diamines. A comprehensive study is first carried out to probe the underlying urea formation mechanisms occurring during the reaction and a novel synthetic approach to non-isocyanate poly(hydroxyurea−urethane)s (PHUUs) that are characterized by a tunable urethane-to-urea ratio was proposed for the first time.

- **Chapter 3** is devoted to the synthesis of supramolecular water-dispersible non-isocyanate polyurethanes (WNIPUs) featuring ionic moieties. These WNIPUs have been prepared from aminoalkyl-terminated

poly(dimethylsiloxane), diglycerol dicarbonate and 8-membered cyclic carbonate *via* phase inversion using the so-called acetone process. Novel NIPUs supramolecular materials showing excellent mechanical properties and self-healing abilities have been elaborated by incorporating multifunctional carboxylic acids into the dispersions.

- **Chapter 4** describes the preparation of well-defined soft NIPU nanoparticles following a one-pot process using interfacial polymerization. Linear activated dicarbonates have been polymerized with diamines and/or triamines by interfacial polymerization, in presence of an anionic emulsifier, affording NIPU nanoparticles with a potential use in drug delivery applications.

- **Chapter 5** summarizes the accomplishments and main results of this PhD thesis work.

This thesis was part of the European Joint Doctorate (EJD) funded by the European Union's Horizon 2020, in "Organocatalysis and Sustainable Polymers" (SUSPOL). It has been conducted within two distinctive polymer groups, namely, POLYMAT in San Sebastián (Spain) and LCPO in Bordeaux (France) under the supervision of Dr. Haritz Sardon and Prof. Daniel Taton. These groups have a wide experience in the field of organocatalysis, the synthesis and characterization of bio-based non-isocyanate polyurethanes, as well as the preparation of polyurethane aqueous dispersions.

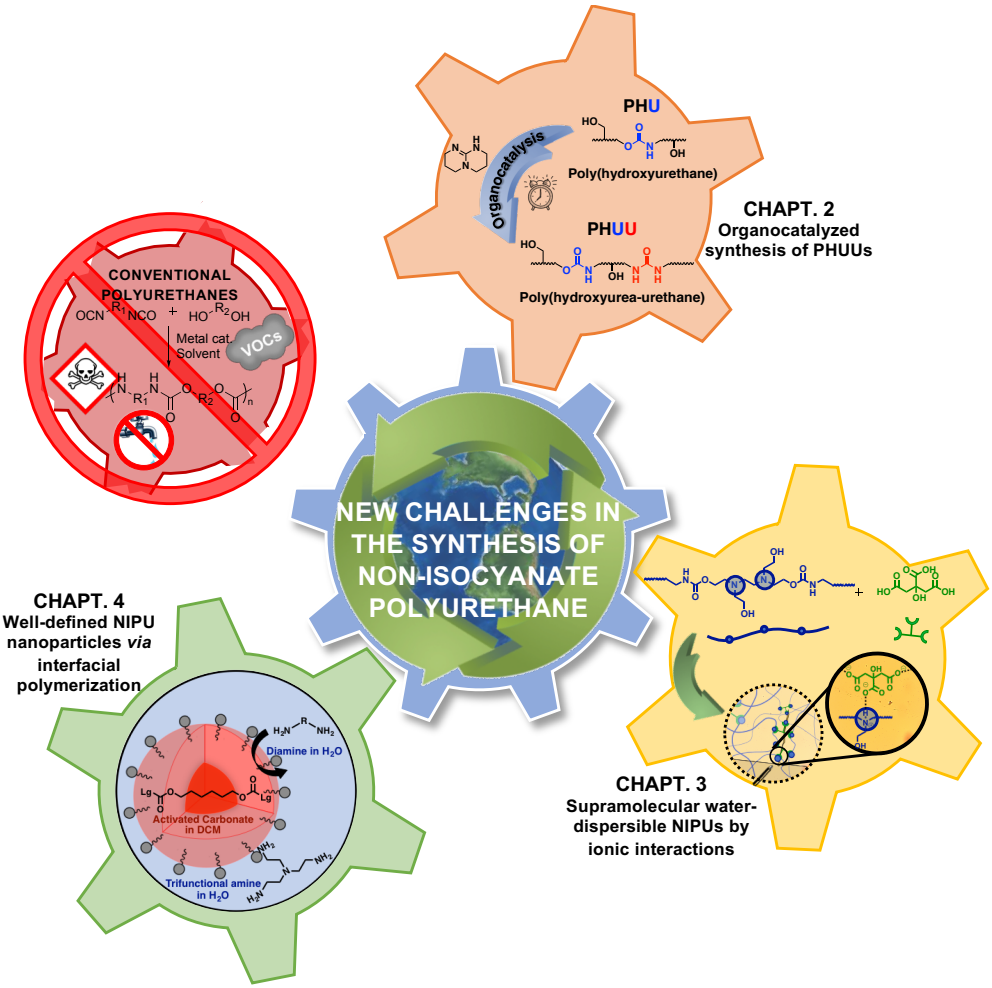

Figure 6. Aims of the thesis.

Chapter 2

Organocatalyzed Synthesis of Poly(hydroxyurea-urethane)s from Diglycerol Dicarbonate and Diamines

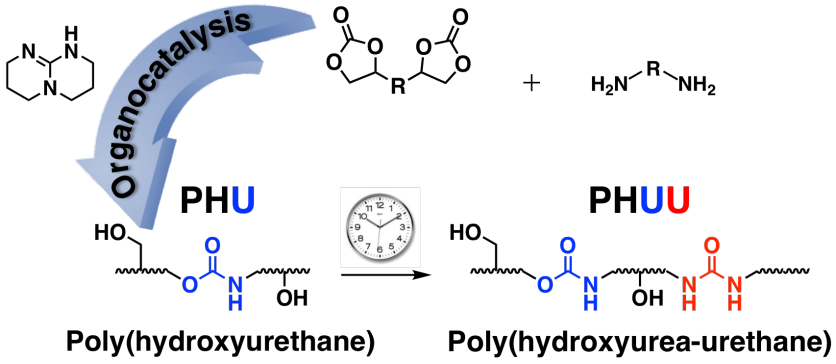

Bossion A., Aguirresarobe R.H., Irusta L., Taton D., Cramail H., Grau E., Mecerreyes D., Su C., Liu G., Müller A.J., Sardon H. *Macromolecules*, **2018**, 51 (15), 5556–5566.

CHAPTER 2. ORGANOCATALYZED SYNTHESIS OF POLY(HYDROXYUREA-URETHANE)S FROM DIGLYCEROL DICARBONATE AND DIAMINES

2.1. Introduction

Issues regarding the use of isocyanates as monomeric building blocks have prompted the necessity for alternative and greener routes towards industrially relevant polymers, such as PUs and poly(urethane-urea)s (PUU)s, based on non-toxic reagents. As discussed in **Chapter 1**, among these approaches, the step-growth polyaddition of bifunctional cyclic carbonates with diamines, which leads to the formation of PHUs represent the most promising one. In this context, 5- and 6-membered dicyclic carbonate monomers have been the most studied.[3,20–25,27,29,76–79] While 6-membered carbonates prove more reactive than 5-membered ones, their synthesis generally requires the use of chlorinated carbonylating agents, such as phosgene or alkyl chloroformates.[80–82] On the other hand, 5-membered cyclic carbonates can be produced in a sustainable way from the chemical insertion of CO_2 into naturally abundant epoxides.[83–90] NIPU synthesis from 5-membered cyclic carbonates often requires high reaction temperatures, bulk conditions, long reaction times and, last but not least, the use of a catalyst to achieve high molecular weights. Yet, some authors have recently reported the synthesis of high molecular weights NIPUs from activated 5-membered cyclic carbonate with limited side reactions at room temperature.[56,91]

In 2004, Diakoumakos and Kotzev presented the first examples of organocatalyzed step-growth polymerization of cyclic carbonates and diamines.[44] Piperazine and TEA were employed as organocatalysts, and polymerizations were performed using aromatic and aliphatic diamines in conjunction with a

cyclocarbonate resin, reacted in bulk at 25 and 60 °C. Addition of TEA (1 wt. %) to the reaction mixture led to a decrease in the activation energy by 17.5 % (5.23 kJ/mol), in comparison with the non-catalyzed reaction (6.33 kJ/mol), and the reactions reached full conversion faster at both temperatures. According to the authors, activation mechanism by TEA involves the nucleophilic activation of the carbonate moiety prior to nucleophilic addition of the monomeric amine (**Scheme 6**).

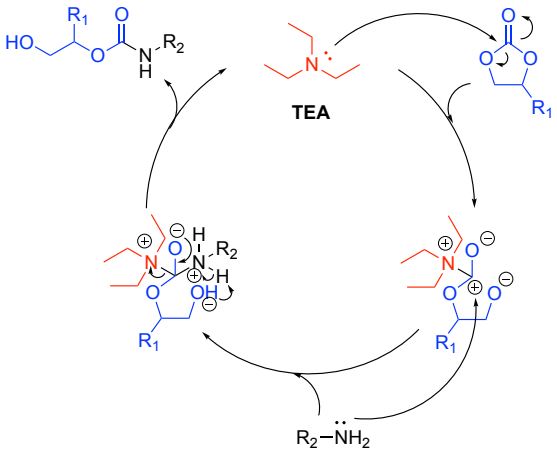

Scheme 6. Proposed catalytic activation of cyclic carbonates utilizing triethylamine; adapted from ref. 44

Similarly, some authors reported the synthesis of PHUs in presence of amidines and cyclic guanidines as organocatalysts. In particular, TBD proved efficient for the aminolysis reaction of cyclic carbonates with amines.[47] Lambeth and Henderson conducted the aminolysis model using TEA, TBD and DBU.[20] Carrying out the reactions in DMSO at room temperature, DBU and TBD improved the reaction rate in comparison to TEA. When applied to difunctional monomer precursors, these conditions enabled to achieve PHUs with molecular weights up to M_n = 53.4 kDa ($Đ$ = 1.38). In comparison, the non-catalyzed polyaddition yielded PHUs of much lower molecular weight (M_n = 5.43 kDa, $Đ$ = 1.39).

Caillol *et al.* further exploited TBD as catalyst to prepare NIPU-type foams. Their study focused on the step-growth polymerization of diamines (Priamine1073 or *Jeffamine*-EDR148) with 5-membered cyclic carbonates (trimethylolpropane tris-carbonate or polypropyleneoxide bis-carbonate).[49] Poly(methylhydrogenosiloxane) was used as blowing agent, which reacted with the diamines releasing dihydrogen that expanded the NIPU materials in the presence of 5 mol.% catalyst.

A H-bonding mechanism for catalytic activation using TBD was hypothesized, based on background literature about ring-opening polymerization (ROP) of cyclic carbonates (**Scheme 7**). However, recent studies indicated that a nucleophilic activation mechanism might operate.[59]

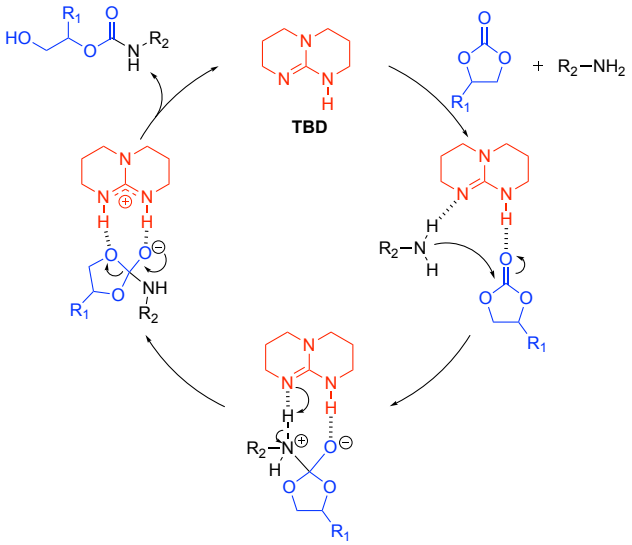

Scheme 7. Proposed hydrogen bonding activation mechanism of TBD-catalyzed step-growth polymerization of cyclic carbonates.

Andrioletti *et al.* investigated the use of stronger bases, such as phosphine and phosphazene derivatives (triphenylphosphine and *t*-BuP_2), for the aminolysis of propylene carbonate with cyclohexylamine at room temperature.[47] While these organo-compounds could effectively activate the conventional reaction between diisocyanate and diols, they appeared ineffective in the specific context of NIPU

synthesis. For example, 5 mol. % of 2-*tert*-butylimino-2-diethylamino-1,3-dimethylperhydro-1,3,2-diazaphosphorine (BEMP) catalyst, only achieved a maximum conversion of 24 % within 1 h.

Urea and thiourea derivatives represent another popular class of hydrogen-bonding catalysts that have been utilized successfully in NIPU preparation. In particular, ureas and thioureas bearing 3,5-bis(trifluoromethyl)phenyl rings were extensively studied due to the high acidity resulting from the strong σ-electron withdrawing properties. Overall, the urea derivatives exhibit lower acidity relative to the thioureas, as indicated by the pKa values in **Figure 7**.[92]

In 2014, Blain *et al.* examined the catalysis of aminolysis reactions between a range of amines and different cyclic carbonates with thioureas. They reported the use of two different thioureas as organocatalysts, namely, 1-(3,5-bis(trifluoromethyl)phenyl)-3-butylthiourea and 1-(3,5-bis(trifluoromethyl)phenyl)-3-cyclohexylthiourea.[47] Interestingly, the cyclohexylphenyl-based thiourea outperformed TBD at low catalyst loading.

Even though numerous studies have been dedicated to the enhancement of the reactivity of the 5-membered cyclic carbonate/amine aminolysis reaction by organocatalysis, molecular weights of the resulting PHUs remain relatively low. These limitations likely prevent the industrial development of isocyanate-free PHUs from 5-membered cyclic carbonates. On the other hand, Clement *et al.* reported the occurrence of intra- or intermolecular side reactions, such as the formation of oxazolidinones or urea derivatives, involving the hydroxyurethane moiety in absence of catalyst (**Scheme 8**).[93]

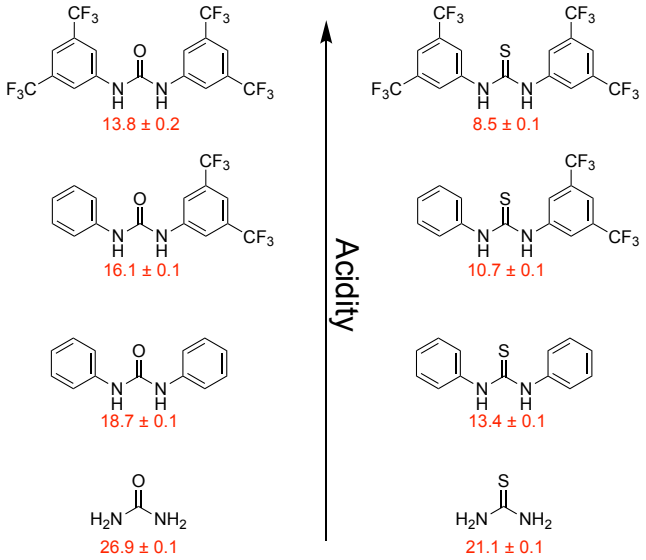

Figure 7. The effect of the 3,5-bis(trifluoromethyl)phenyl rings on the acidity of various ureas and thioureas. pKa values determined in DMSO; adapted from ref. 92

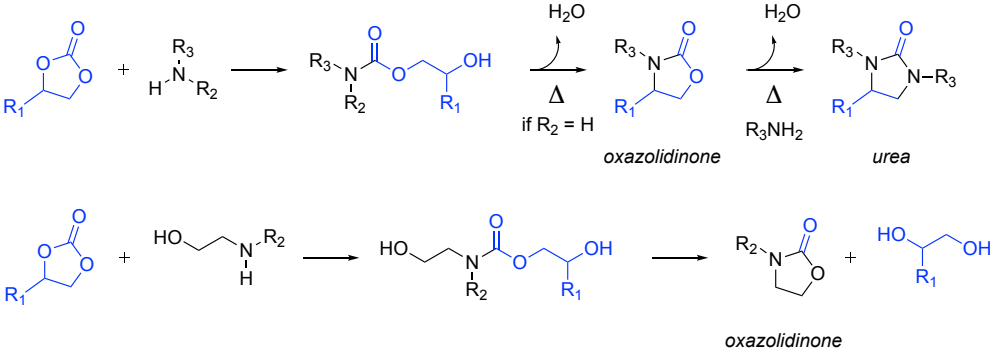

Scheme 8. Side reactions described by Clements *et al.*; adapted from ref. 93

Similarly, Macosko *et al.* showed that formation of urea by-products occurred by fast reaction of amines with urethanes in the melt at 180 °C.[94] More recently, Besse *et al.* and Lamarzelle *et al.,* observed that the use of harsh polymerization conditions aimed at enhancing the reactivity of 5-membered cyclic carbonates brought about side reactions, for instance, urea formation (**Scheme 9**).[26,35]

In spite of several studies related to the use of catalysts for the step-growth polymerization of cyclic carbonates and amines, a detailed investigation into the effect of the (organo)catalysts on the final properties of the resulting PHUs is lacking. This prompted us to rationalize the effect of both structural variations of organocatalysts and experimental conditions on the reaction outcomes, and to probe the underlying reaction mechanisms.

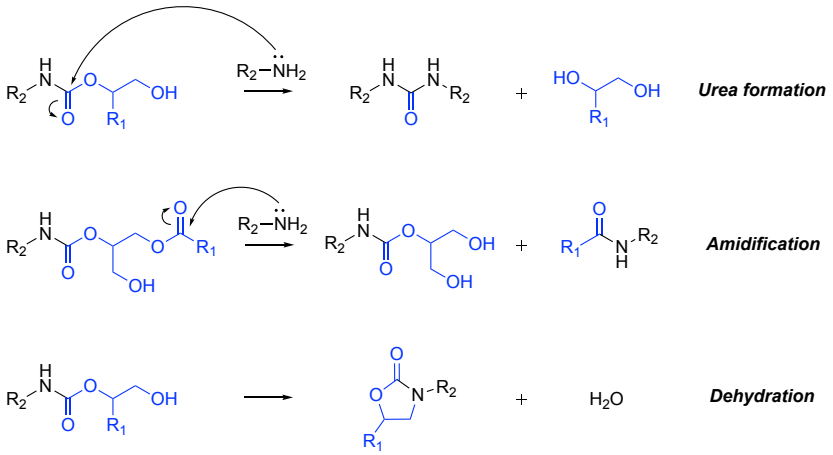

Scheme 9. Possible side reactions between 5-membered cyclic carbonate and amine: a) urea formation, b) amidification and c) dehydration; adapted from ref. 26

In this chapter, we have thus explored a novel synthetic approach to non-isocyanate poly(hydroxyurea-urethane)s (PHUUs) that are characterized by a tunable urethane-to-urea ratio. For this purpose, industrially scalable 5-membered dicyclic carbonates have been used as key monomer building blocks with a diamine, in presence of various organocatalysts, *i.e.* following a metal-free route. We have indeed discovered that PHUUs can be effectively achieved *via* a two-step process, involving the prior formation of hydroxyurethane linkages and their partial post-chemical modification into urea moieties. The final urethane-to-urea ratio is found to strongly depend on the organocatalyst and the overall reaction conditions. These observations are supported by results obtained from model reactions utilizing monofunctional substrates, which allow us to propose a reaction mechanism

pertaining to this unexpected chemical transformation in presence of peculiar organocatalysts. To the best of our knowledge, this is the first report on PHUU synthesis *via* an organocatalyzed step-growth polyaddition of diamines with 5-membered dicyclic carbonates.

2.2. Results and discussion

2.2.1. Effect of organocatalysts on the polymerization kinetics during polyhydroxyurethane synthesis

In order to evaluate the most suitable catalyst for the step growth polyaddition of 5-membered cyclic carbonates with diamines, polymerization studies were performed using renewable diglycerol dicarbonate (DGC) and *Jeffamine* ED-2003 (M_n = 1900 Da) (**Scheme 10.a**). On one hand, DGC was selected because it can be easily prepared from bio-based diglycerol and dimethyl carbonate and usually does not undergo side-reactions. On the other hand, a low molecular weight propylene oxide capped polyethylene glycol-based diamine (*Jeffamine* ED-2003) was selected as a diamine, because of its commercial availability and because it allowed the formation of soft polyurethanes that can be analyzed by ^{1}H NMR. In addition, this polyetheramine is analogous to the conventionally used poly(ethylene glycol)s (PEGs) in the polymerization of segmented isocyanate-based polyurethanes.[95]

Commercial organic acid, *p*-toluenesulfonic acid (PTSA), commercial organic bases of different pKa values such as DBU, TBD, and the phosphazene base 1-*tert*-butyl-4,4,4-tris(dimethylamino)-2,2-bis[tris(dimethylamino)-phosphoranylidenamino]-2λ^5,4λ^5-catenadi(phosphazene) (P_4), and H-bonding donors 1-(3,5-bis(trifluoromethyl)phenyl)-3-butylthiourea (TU) and potassium thioimidate based on 1-(3,5-bis(trifluoromethyl)phenyl)-3-butylthiourea (TU anion) were screened as catalysts for the polymerization of DGC with *Jeffamine* ED-2003 (**Scheme 10.b**).

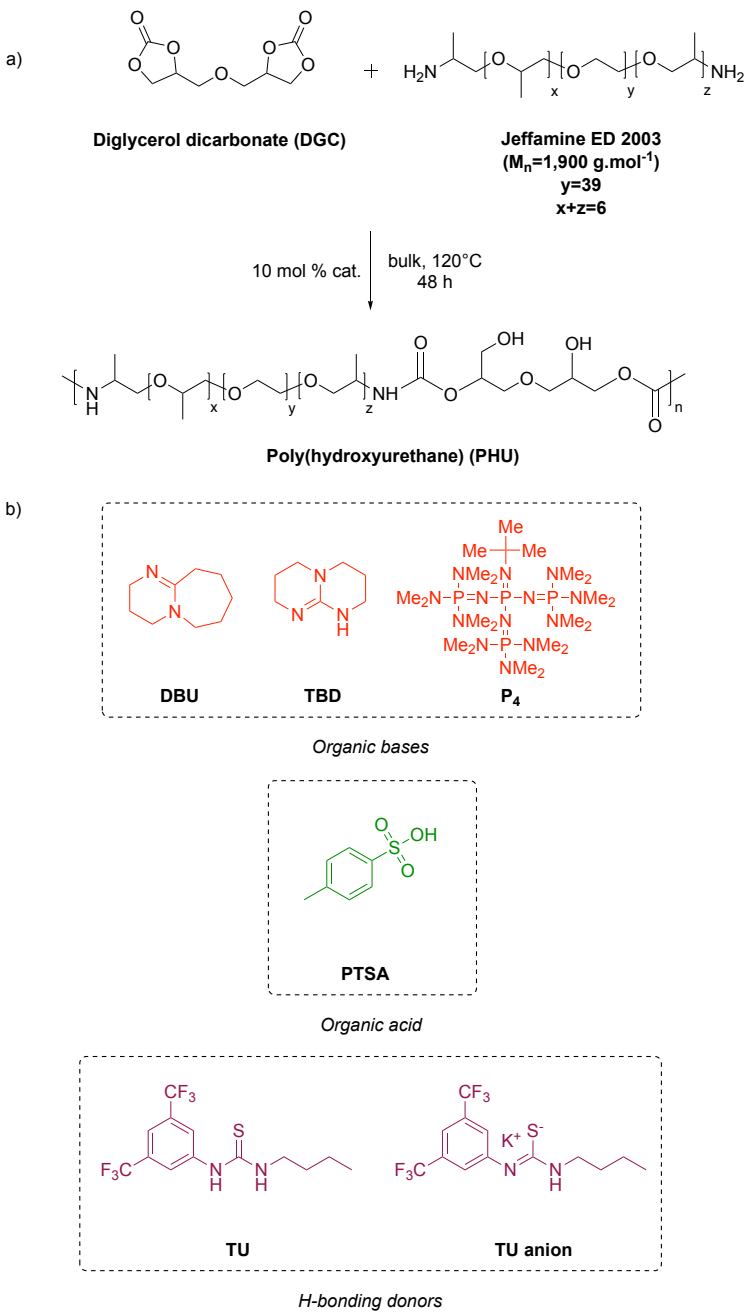

Scheme 10. a) Step-growth polyaddition of DGC with *Jeffamine* ED-2003; b) catalysts used in this study.

These different catalysts are rather well-established and are known to operate through several different activating mechanisms that can enhance the polymerization rate and/or selectivity.[47,96–99]

Polymerization studies were performed in bulk at 120 °C by mixing equimolar amounts of DGC and *Jeffamine* ED-2003 followed by the addition of 10 mol. % of a given catalyst. The reaction conversion was monitored by Fourier transform infrared spectroscopy (FTIR), by following the decrease of the relative area integration value of the carbonate moiety showing a characteristic band at 1780 cm^{-1}. According to the Beer-Lambert law, the absorbance of a material is directly proportional to its thickness.[100] To compensate for thickness changes in the analysis of the samples, the obtained absorbance values were normalized against an internal standard, *i.e.* a band whose intensity is unaltered during the polymerization reaction. For that purpose, we selected the total C—H stretching band in the range between 3000 and 2850 cm^{-1} as internal standard of normalization.

As can be seen in **Figure 8**, the polymerization rate was found to be highly catalyst-dependent. In absence of any catalyst, monomer conversion reached barely 70 % after 48 h, and full conversion could not be achieved. The TU anion appeared the most efficient catalyst in this series, as monomer conversion reached > 98 % within 5 min, while only 83 and 45 % monomer conversion was observed with P_4 and TBD respectively. While differences in the reaction rates were observed at the early stage of the polymerization, the three organocatalysts all gave a conversion exceeding 98 % within 10 h. DBU, and TU, however, did not provide any significant effect, as the reaction did not reach completion even after 48 h (86 and 90 % conversion, respectively). As for PTSA, it did not enable to reach a higher conversion than that obtained for the non-catalyzed reaction after 48 h.

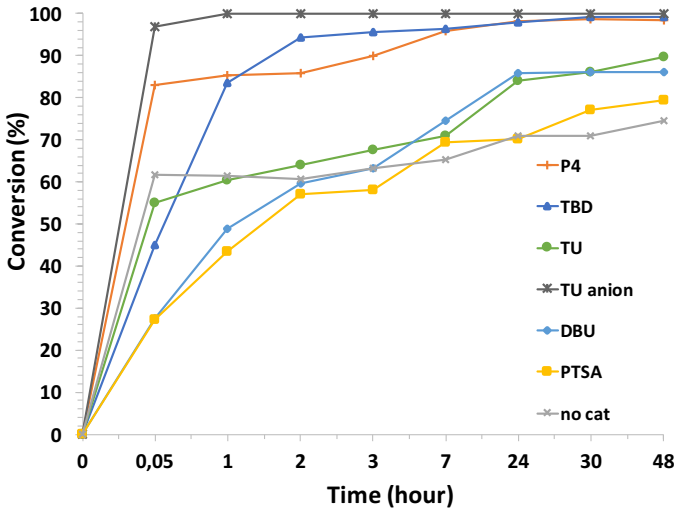

Figure 8. Kinetic plot of the step growth polymerization of DGC with *Jeffamine* ED-2003 at 120 °C using different organocatalysts.

Analysis of the carbonyl region of FTIR spectra run at different reaction times for polymers obtained in presence of the most active catalysts, *i.e.* P_4, TBD and TU anion (**Figure 9**), revealed an intriguing phenomenon. The signal at 1795 cm^{-1} of the carbonyl group of the starting DGC decreased after 1 h, as expected, while signals attributed to the newly formed urethane bond could be observed at 1715 (C=O stretching vibration) and 1530 cm^{-1} (N—H bending vibration). Surprisingly, a new signal appeared at 1670 cm^{-1} as the reaction proceeded (10 h) that was attributed to the C=O stretching vibration of urea groups.

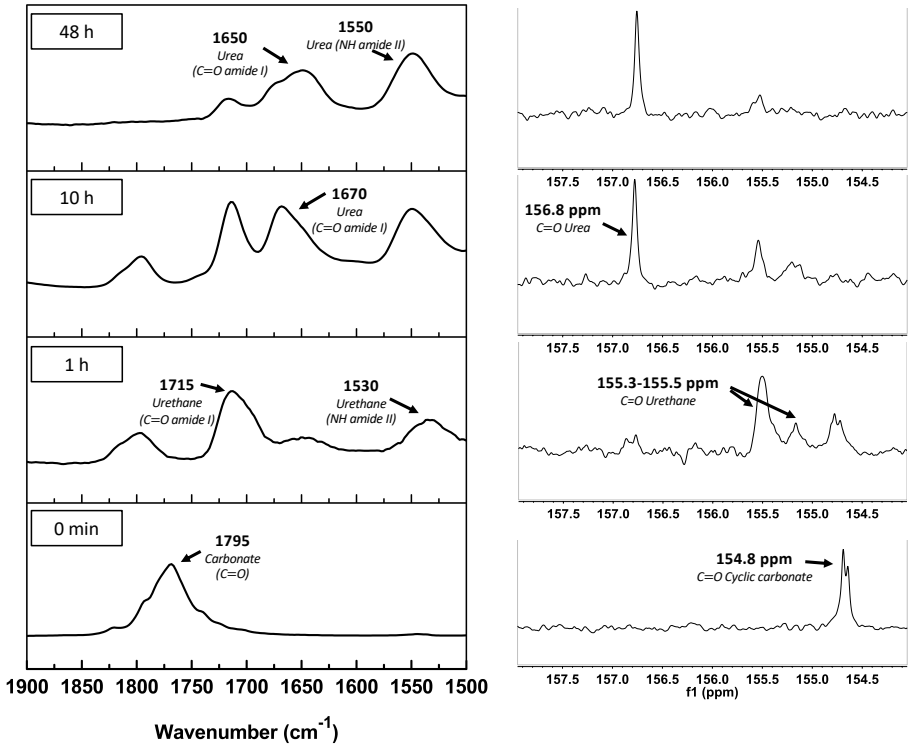

Figure 9. FTIR (left side) and ^{13}C NMR (DMSO-d_6, right side) spectra of products obtained at different times from the step-growth polymerization of DGC with *Jeffamine* ED-2003 performed at 120 °C using TBD as catalyst.

After 48 h of reaction, the urethane band continued to decrease in intensity and the signal of the urea groups became predominant in the carbonyl region. In addition, the latter signal evolved to lower wavenumbers (1650 cm^{-1}) and the N—H deformation vibration was recorded at higher wavenumbers (1550 cm^{-1}). In our opinion, this could be explained by the formation of strong hydrogen bonding interaction between the urea groups. It has been shown in poly(urethane−urea) blends with poly(ethylene glycol), that the band near 1670 cm^{-1} is due to a hydrogen-bonded urea/ urea carbonyl where the N-H atoms are hydrogen bonded to an ether oxygen, while the lower frequency band at 1650 cm^{-1} can be attributed to hydrogen-bonded urea carbonyls with N-H groups hydrogen-bonded to other

urea carbonyls.[101] With DBU, PTSA, TU, as well as without catalyst, this behavior was not observed at this temperature.

To further confirm the progressive transformation of the PHU precursors to PHUUs, quantitative ^{13}C NMR analysis was performed in the carbonyl region for higher resolution (**Figure 9**). Polymers were analyzed at different reaction times (1, 10 and 48 h). After 1 h, three different signals were observed at 154.8, 155.3 and 155.5 ppm, respectively. While the first one was assigned to the DGC C=O group, the second one might correspond to the newly formed (–NH–(C=O)–O–) urethane linkages (containing primary and secondary hydroxyls).[102,103] After 10 h, the area of the signal attributed to the cyclic carbonate decreased and the new signal appearing at 156.8 ppm could be attributed to the urea (–NH–(C=O)–NH–) carbonyl group. The reaction was confirmed by the complete disappearance of the carbonyl band associated to the 5-member cyclic carbonate monomer. Moreover, the formation of urea bond was evidenced by ^{1}H NMR, with the disappearance of the urethane NH signal over time at 6.94 ppm, and the formation of a new peak at 5.67 ppm corresponding to the urea labile NH proton (**Figure 10**).[104]

In order to speed up the urea formation, polymerization was performed at higher temperature (*i.e.* 150 °C) using TBD as organocatalyst. Overall, we found that urea formation proceeded faster at 150 °C than at 120 °C (**Figure 11**). For example, 77 % urea was achieved in 2 h at 150 °C while 24 h were required to attain similar urea ratio at 120 °C.

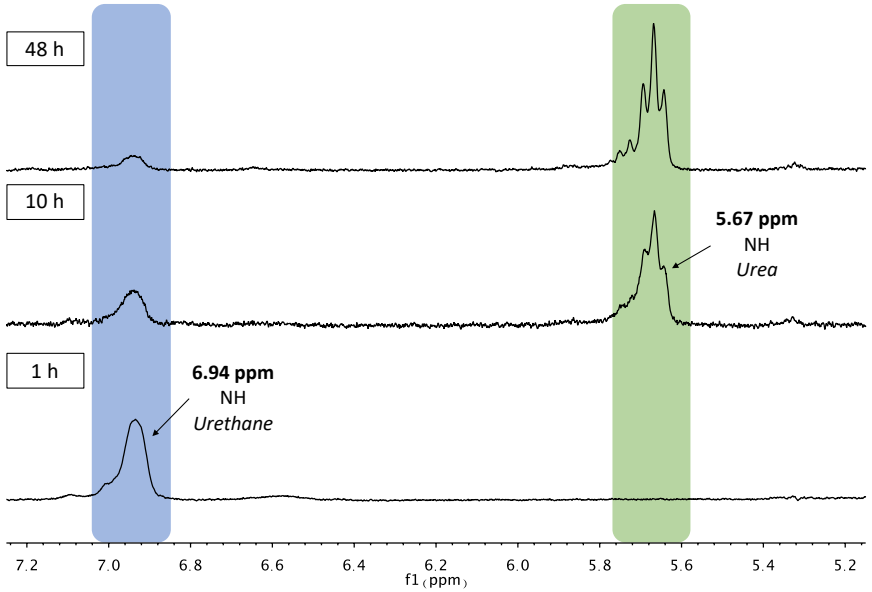

Figure 10. ^{1}H NMR (300 MHz, DMSO-d_6) in the area 5-7 ppm of the products obtained at different times from the step-growth polymerization of DGC with *Jeffamine* ED-2003 performed at 120 °C using TBD as catalyst showing the change in the shifts of the NH protons.

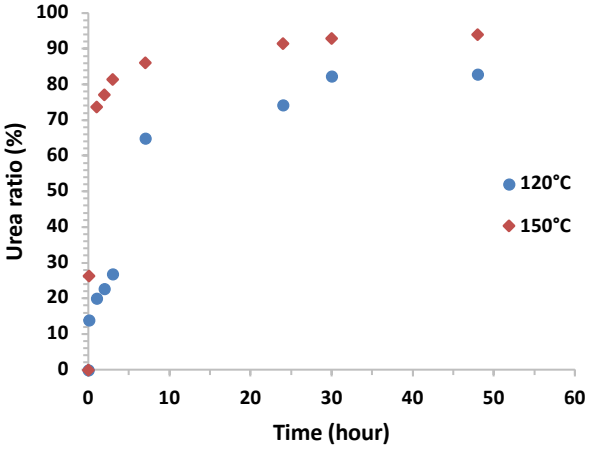

Figure 11. Kinetic of urea formation followed by FTIR over 48 h at 120 and 150 °C from the reaction of DGC with *Jeffamine* ED-2003 in the presence of 10 mol. % of TBD catalyst.

In summary, the effect of various organocatalysts on outcomes of the bulk step-growth polyaddition of diglycerol dicarbonate and a poly(ethylene glycol)-based diamine performed at 120 °C was thoroughly studied. The reaction was found to be dramatically catalyst dependent, higher rates being observed in presence of strong bases, such as P_4 or TBD. Unexpectedly, the as-formed urethane linkages entirely vanished with time, as evidenced by FTIR and ^{13}C NMR spectroscopies, while signals due to urea bond formation progressively appeared. To gain a better insight into this observation, a model reaction involving propylene carbonate and dodecylamine as monofunctional reagents was carried out in presence of TBD.

2.2.3. Model reaction

In light of the previous results and in order to get a better understanding on the urea formation, a model reaction was implemented between propylene carbonate and dodecylamine, in presence of 10 mol. % of TBD as organocatalyst (**Figure 12**).

As propylene carbonate reacted with dodecylamine, ^1H NMR signals of the methylene protons of the cyclic carbonate at 4.96-4.91, 4.52 and 4.27-4.20 ppm progressively vanished (**Figure 12.a**). Meanwhile, new signals attributed to the urethane moieties were detected at 4.92-4.84 ppm (C*H*–OCONH compound 1), 4.76 ppm (C*H*–OH compound 1'), 3.90-4.12 ppm (CH_2–OCONH compound 1'), 3.55-3.70 ppm (CH_2–OH compound 1) and 3.16 ppm (CH_2–NHCOO) (**Figure 12.b**). As the reaction proceeded, a clear evolution of the signals of the urethane groups was noted. These signals decreased in intensity and a new signal due to the methylene protons linked to the urea groups appeared at 3.16 ppm (CH_2–NH). In addition, a new peak was observed at 4.30 ppm, which was assigned to protons of the urea moiety. To our surprise, signals of the methylene protons of the cyclic carbonate reappeared, as a sign of the partial reversion of the process, thus regenerating free amines (**Figure 12.c**).

Similar findings have actually been reported by Torkelson *et al*.[105] These authors have indeed found that PHU-based networks are able to dissociate to cyclic carbonates and amine groups, under specific reprocessing conditions. Moreover, we noted that substantial amounts of a condensate formed at the early stages of the reaction. Analysis by ^{1}H NMR of this condensate revealed that it was propane-1,2-diol as side product, with characteristic peaks at 3.94-3.84 ppm (C*H*–OH), 3.63-3.58 and 3.41-3.35(CH_2–OH), 2.99 (O*H*) and 1.15 (CH_3) (**Figure 13**).[106] After 24 h (**Figure 12.c**), peaks of the urethane group completely vanished and peaks assigned to urea moieties were mainly detected in the corresponding ^{1}H NMR spectrum.

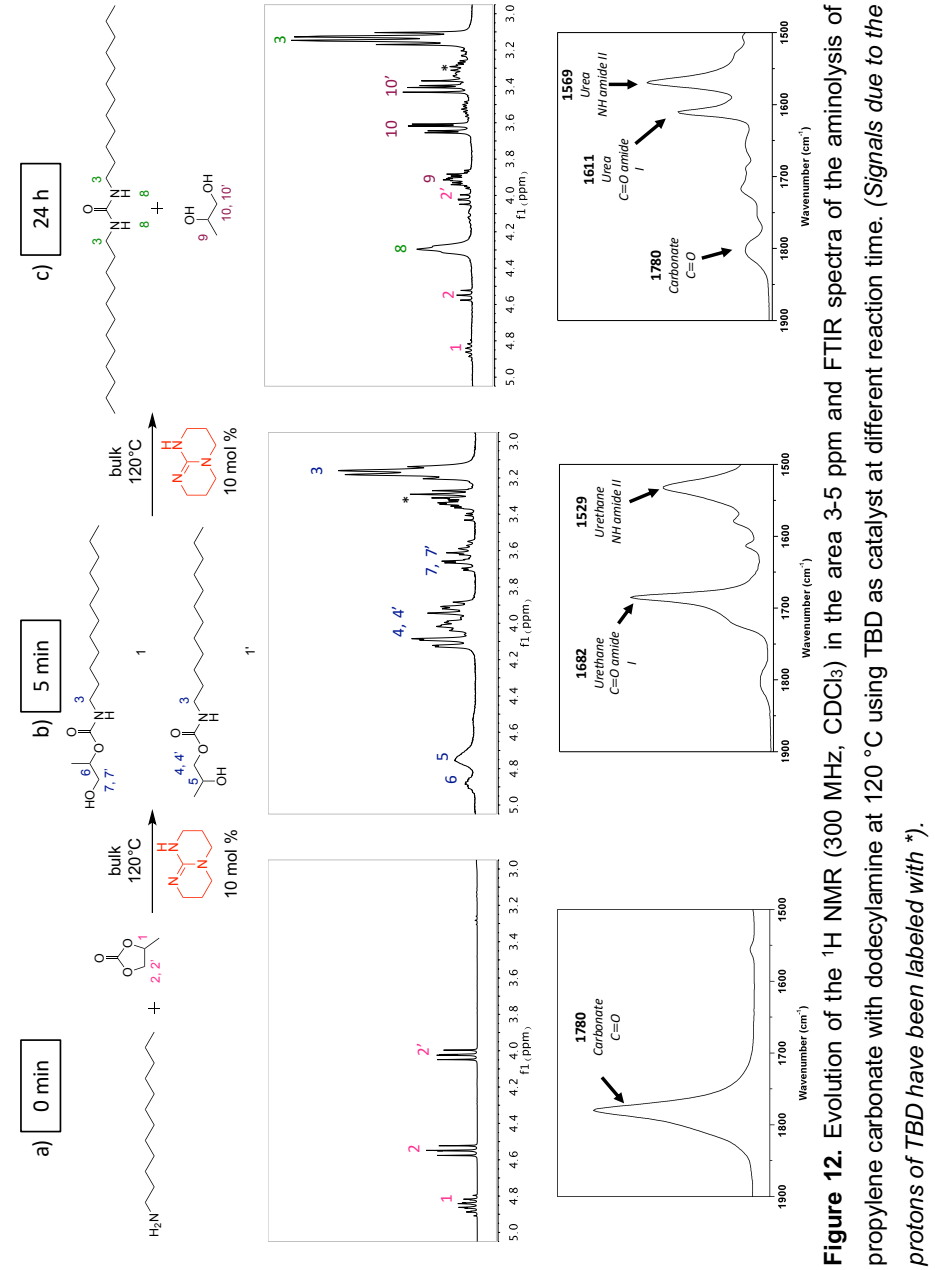

Figure 12. Evolution of the ^{1}H NMR (300 MHz, $CDCl_3$) in the area 3-5 ppm and FTIR spectra of the aminolysis of propylene carbonate with dodecylamine at 120 °C using TBD as catalyst at different reaction time. *(Signals due to the protons of TBD have been labeled with *).*

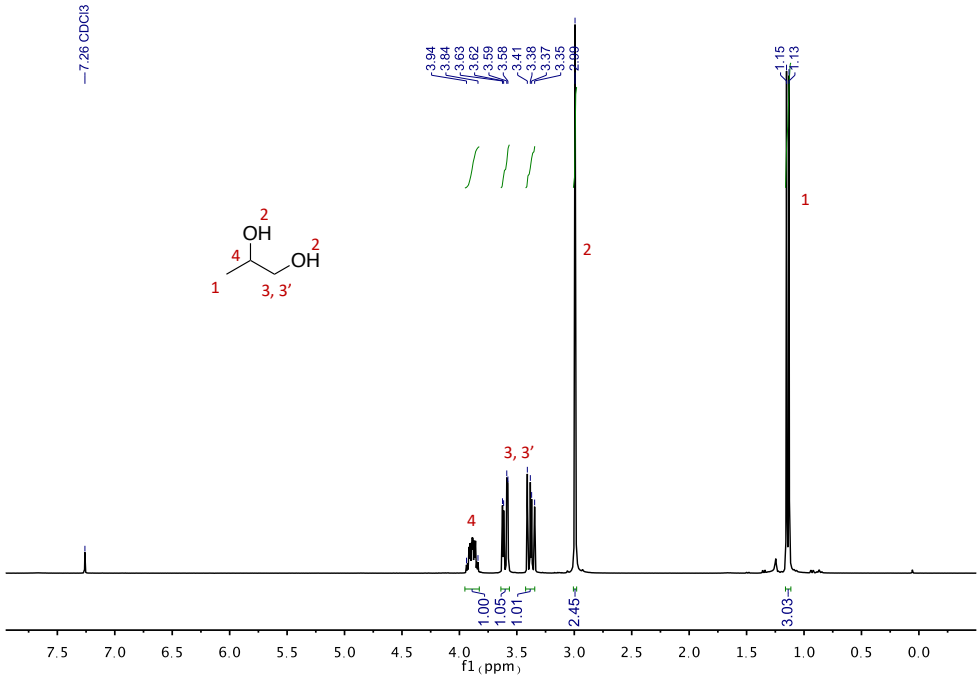

Figure 13. ^{1}H NMR (300 MHz, $CDCl_3$) of the condensate, propane-1,2-diol, that appeared during the aminolysis of propylene carbonate with dodecylamine at 120 °C using TBD as catalyst.

Urea formation was further analyzed by FTIR. Similar results to those of the polymerization were observed, *i.e.* disappearance of urethane moieties and appearance of highly intense signals attributed to urea groups (**Figure 12**). In addition, analysis of the FTIR spectra at different reaction times showed that full urea formation was achieved in 24 h, confirming the results obtained by NMR spectroscopy (**Figure 12.c**).

Elemental and LC-TOF-MS analyses of the reaction between propylene carbonate and dodecylamine after 24 h were conducted to characterize the final compound, after its recrystallization in cold chloroform. One main compound was detected at m/Z = 397.42. The empirical formula proposed for this protonated molecule was: $C_{25}H_{53}N_2O$ [$M+H^+$], eventually corresponding to the structure of 1,3-

didodecylurea (**Figure 14**). In addition, elemental analysis gave experimental values that fitted well with this chemical formula (**Table 1**). These results thus confirmed that organocatalysts such as TBD or P_4, mainly generated urea groups starting from a cyclic carbonate and a primary amine.

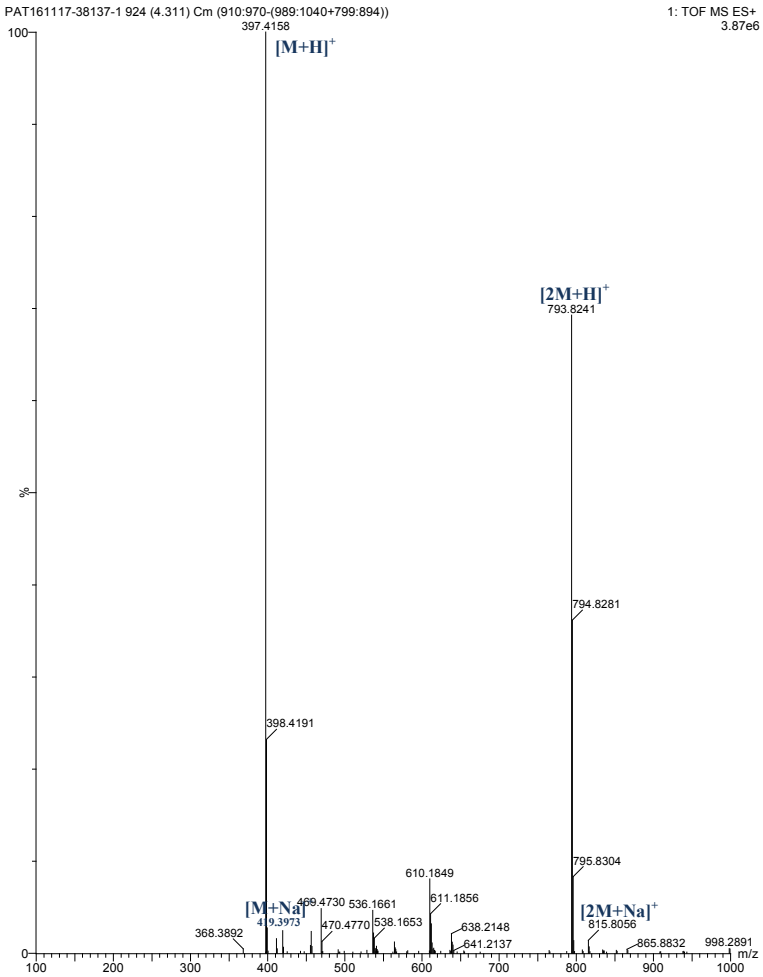

Figure 14. Mass spectra of the molecule obtained from the aminolysis of propylene carbonate with dodecylamine at 120 °C using TBD as catalyst after 24 h eluted after 4.3 min.

Nevertheless, the nearly complete conversion of the cyclic carbonate into urethane, followed by urea formation suggested that the reaction mechanism followed a different pathway than the well-established amidation side reaction of hydroxyurethane with primary amine (**Scheme 11**).[77]

Table 1. Elemental analysis results from the aminolysis of propylene carbonate with dodecylamine at 120 °C using TBD as catalyst after 24 h. Experimental values are matching with the chemical formulas of 1,3-didodecylurea.

Elemental composition	C	H	N
Experimental value (%)	75.1	13.4	6.9
Theoretical value (%)	75.7	13.2	7.1

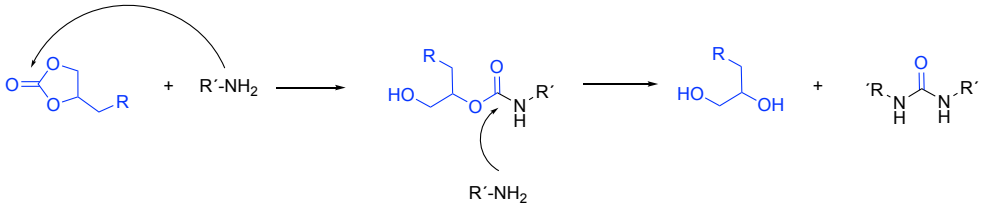

Scheme 11. Mechanism for urea formation as proposed by Lamarzelle *et al*.; adapted from ref. 77

Recent studies have reported the dissociative reversible aminolysis reaction in PHU reprocessability process; however, no detailed mechanism has been proposed.[105,107] Our study suggests that urea formation is favored in presence of basic organocatalysts. Therefore, a possible mechanism for such an aminolysis is illustrated in **Scheme 12**.

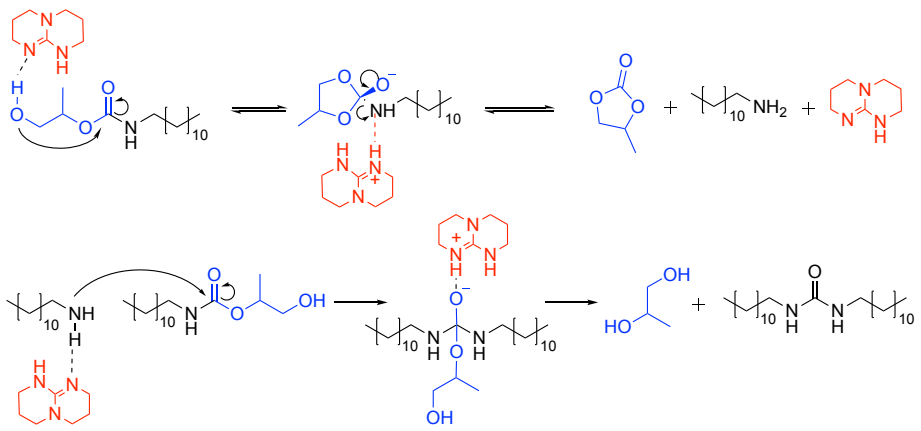

Scheme 12. Proposed mechanism for the formation of urea from urethane with TBD as example of base catalyst.

It was apparent that urethane groups initially formed from cyclic carbonate and primary amine, and further evolved into urea moieties. In presence of TBD, the hydroxyl group created upon aminolysis might be deprotonated. The newly formed alkoxide might react with the carbonyl electrophilic center of the urethane group. We hypothesized that the mechanism further involved a proton transfer from the catalyst to the urethane amine concomitantly, followed by cleavage of the bond between the amine and the carbonyl carbon, leading to the formation of the cyclic carbonate and the free amine. This mechanism was supported by ^{1}H NMR data with the appearance of characteristic signals assigned to the cyclic carbonate monomer (**Figure 12.c**). In a second step, the newly formed dodecylamine could either react with the cyclic carbonate to regenerate the urethane compound, or react with another urethane group to form a linear urea along with propane-1,2-diol. In the latter case, the strong base could deprotonate the amine making it more nucleophilic for an attack onto another urethane linkage and/or facilitate the proton transfer from the amine to the propane-1,2-diol side-product after the cleavage of the urethane bond, yielding the urea. The presence of both compounds was confirmed by ^{1}H NMR (**Figure 12**).

To further ascertain the base-promoted formation of linear ureas, the as-formed hydroxyurethane synthesized from propylene carbonate and dodecylamine was placed at 120 °C with 10 mol. % of TBD. As expected, 1,3-didodecylurea and propylene glycol were thus generated, supporting our hypothesis (**Figure 15** and **Figure 16**).

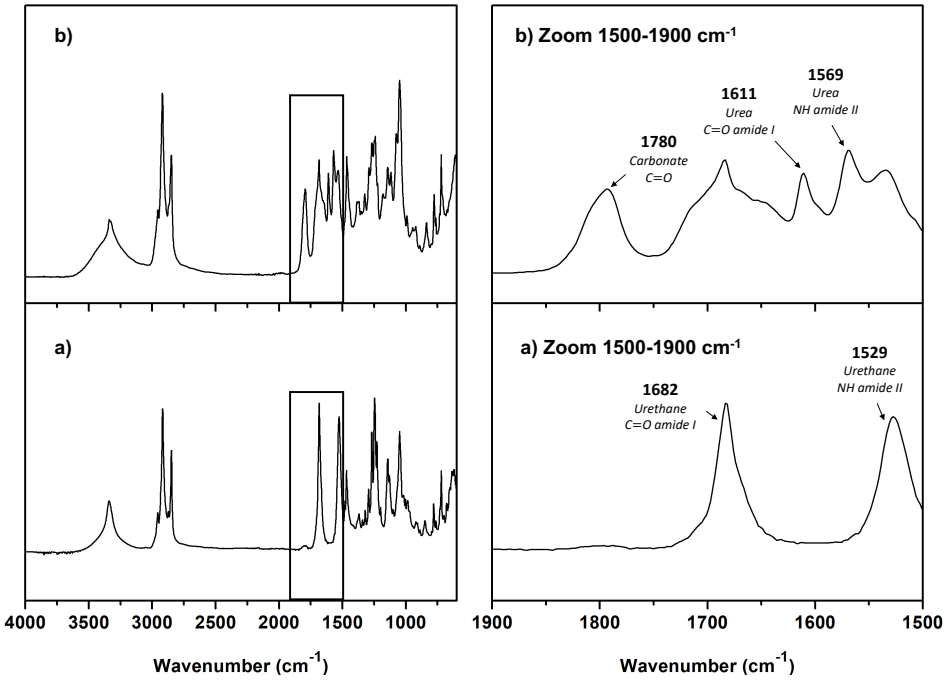

Figure 15. FTIR spectra of the control model reaction between propylene carbonate and dodecylamine at 120 °C after: a) 5 h without catalyst (until complete conversion of propylene carbonate into urethane); b) 48 h after incorporation of TBD as catalyst.

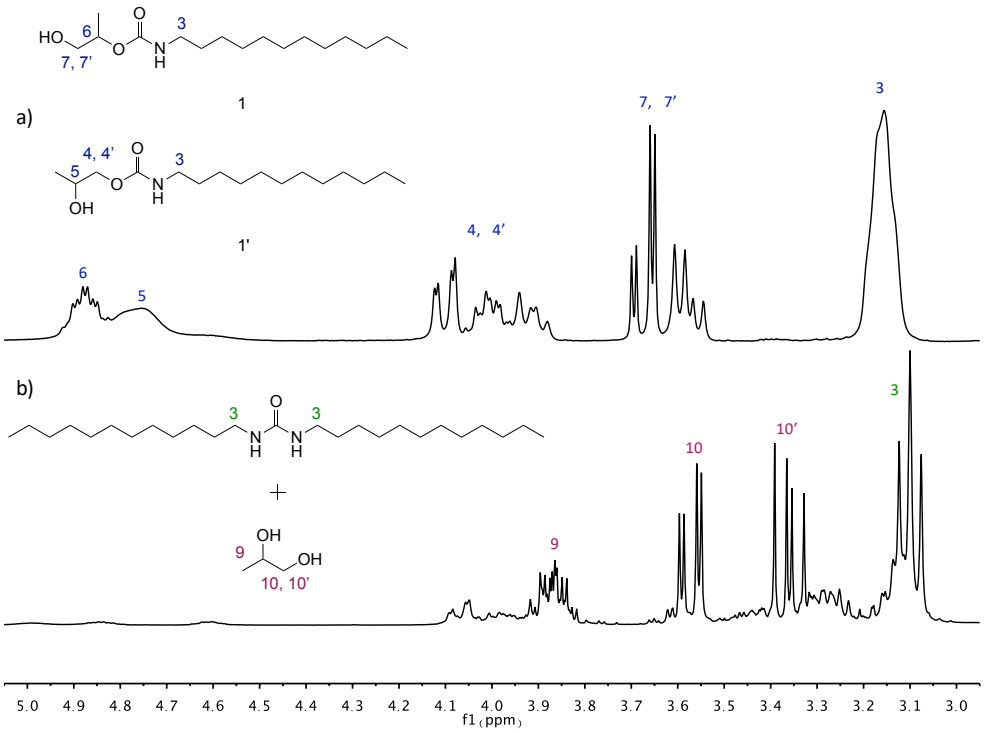

Figure 16. ^{1}H NMR (300 MHz, $CDCl_3$) in the area 3-5 ppm of the control model reaction between propylene carbonate and dodecylamine at 120 °C after: a) 5 h without catalyst (until complete conversion of propylene carbonate into urethane); b) 48 h after incorporation of TBD as catalyst. The b) NMR shows mainly proton shifts of propane-1,2-diol due to partial solubility of urea in $CDCl_3$.

Similarly, the pre-formed polyhydroxyurethane underwent urea formation after 48 h in the presence of 10 mol. % TBD, which further strengthens the proposed mechanism (**Figure 17**).

In summary, urea formation was clearly evidenced from the aminolysis of propylene carbonate with hexylamine, using combined analyses, including FTIR and NMR spectroscopies, and elemental analysis. Advantage of the chemical transformation occurring from urethane to urea linkages was further taken, by

optimizing the polymerization conditions to access a range of poly(hydroxyurea-urethane)s with precise urethane-to-urea ratio in a one pot process.

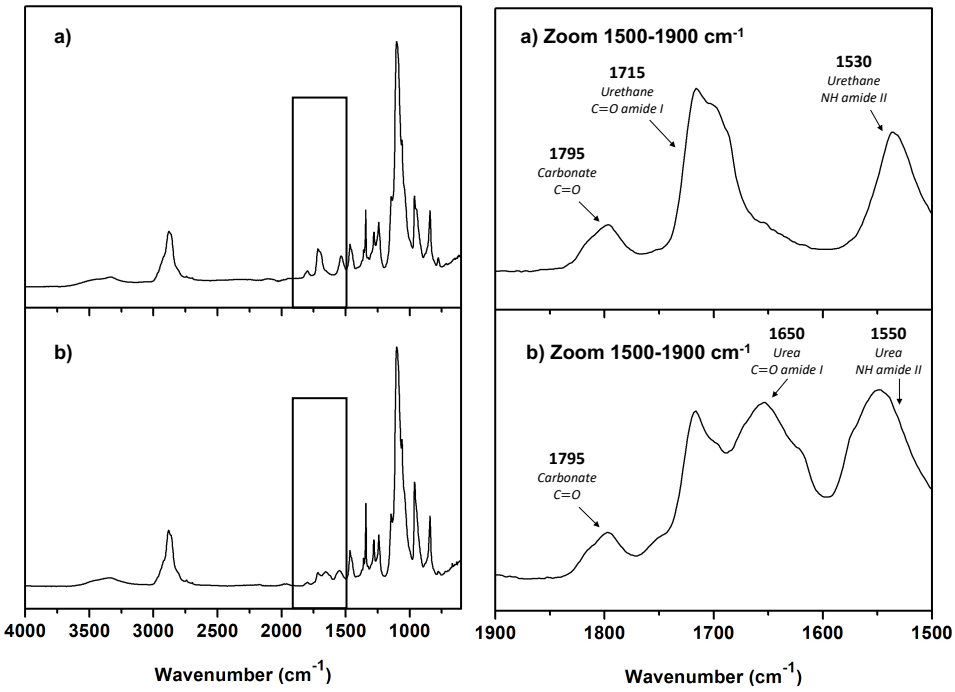

Figure 17. FTIR spectra of the control polymerization between DGC and *Jeffamine* ED-2003 at 120 °C after: a) 7 days without catalyst (88% urethane conversion); b) 48 h after incorporation of TBD as catalyst. (Urea/urethane ratio 69/31).

2.2.4. Synthesis of poly(hydroxyurea-urethane)s based on DGC and diamines

On the basis of the findings discussed above, the scope of urea formation was expanded to the synthesis of various PHUUs with different urea-urethane ratios in a one pot-process, from dicyclic carbonates. Poly(urea-urethane)s (PUUs) are important polymeric materials generally exhibiting high toughness and extensibility; they are extensively used in the textile industry (Lycra™ DuPont de Nemours and Co.), in foams and for medical prostheses.[108,109] PUUs combine the processability of

polyurethanes with the superior mechanical and thermal properties of polyureas that are imparted primarily by the stronger hydrogen bonding ability of urea moieties relatively to urethanes.[110] Whereas PUUs can be readily synthesized from isocyanate precursors with polyamines, there is only one report dealing with the synthesis of a PUU following a non-isocyanate route, namely, by melt transurethane polycondensation reaction.[111] In addition, the few works having reported the preparation of isocyanate-free ureas have not employed cyclic carbonates.[112,113]

Three different PHUUs with different urethane/urea ratios were thus prepared, by polymerizing *Jeffamine* ED-2003 with DGC at 120 °C, in presence of 10 mol. % of TBD as catalyst (PHUU1, PHUU2 and PHUU3), by simply discontinuing the reaction at different reaction times (**Scheme 10**). The urethane/urea ratio was determined by FTIR and ^{1}H NMR (**Table 2**, **Figure 19**, **Figure 18** and **Figure S1**, **Figure S2**, **Figure S14** and **Figure S15** in appendix section).

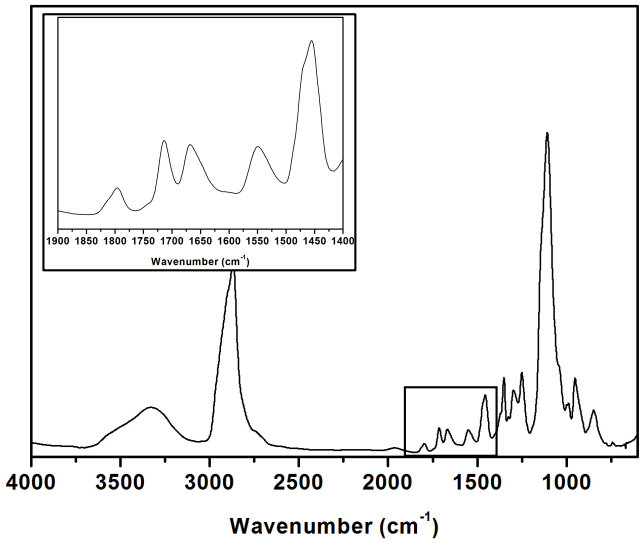

Figure 18. Representative FTIR spectra of the PHUU obtained; the ratio urethane/urea for PHUU2 calculated from the FTIR is 45/55.

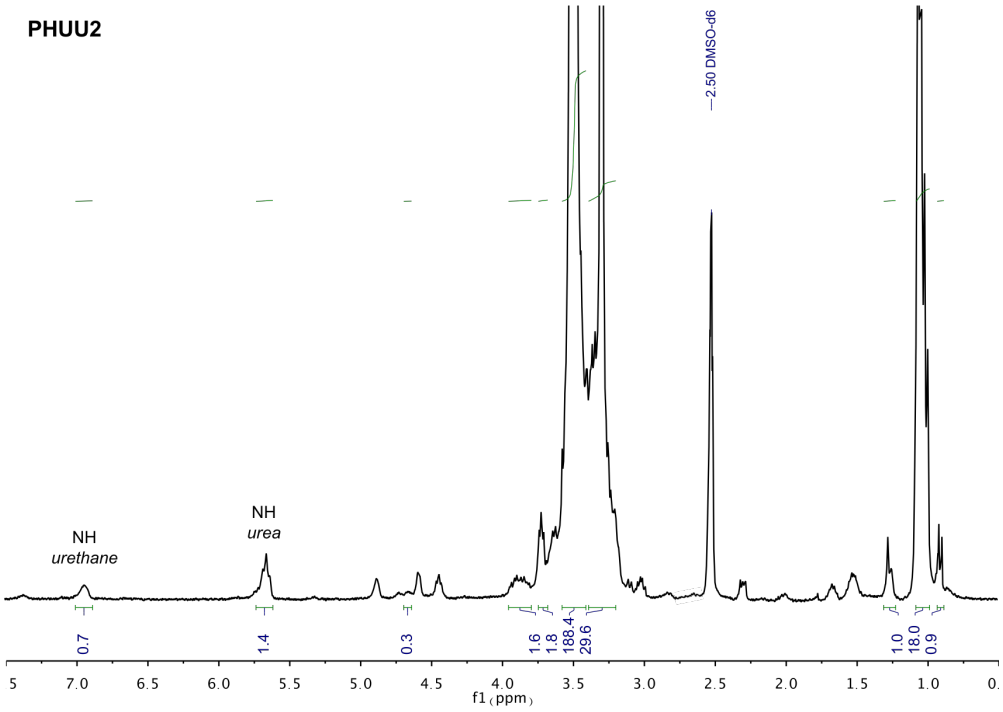

Figure 19. Representative ^{1}H NMR of the PHUU obtained. PHUU2 (300 MHz, DMSO-d_6) δ (ppm) = 6.93 (bs, 0.7H, N*H*(CO)O), 5.67 (m, 1.4H, N*H*(CO)N*H*), 4.90 (bs, O*H*), 4.74 (bs, O*H*), 4.68 (m, 0.3H, C*H*O(CO)N), 3.95-3.82 (m, 1.6H, CH_2OCH_2), 3.74 (m, 1.8H, C*H*OH), 3.64-2.80 (m, 218H, CH_2O and CH_2NH), 1.27 (s, 1H, CH_3), 1.03 (m, 18H, CH_3), 0.91-0.89 (m, 0.9H, CH_3). The ratio urethane/urea calculated from the ^{1}H NMR is 50/50.

The thermal properties of the PHUU compounds were then evaluated by differential scanning calorimetry after purification (DSC, **Table 2** and **Figure 20**). Low T_g values were observed for PHUU1, PHUU2 and PHUU3 (-31, -37 and -40 °C respectively), which was related to the presence of the soft *Jeffamine* segment. Moreover, as the urea content increased, the T_g of the final polymers decreased. This might be related to a more pronounced phase separation due to two phenomena. Firstly, the presence of urea bonds which could form stronger hydrogen bond interaction than urethane groups. Secondly, because whilst urea groups were formed, the extent in hydroxyl pending groups was lower, reducing the

ability of the hard segment to interact with the polyether based soft segment *via* hydrogen bonding.

Table 2. PHUUs synthesized from DGC and diamines at 120 °C using 10 mol. % of TBD as catalyst.

						DSC			SEC		SAXS
PHUU	*Jeffamine* ED-2003 (mol. %)[a]	1,12 diaminododecane (mol. %)[a]	PEG content (wt. %)	time (h)	Ratio urethane/urea (%)[b]	T_g (°C)[c]	T_m (°C)[c]	ΔH_m (J/g)[d]	M_n (g/mol)[e]	$Đ$[e]	Long period (nm)
1	100	0	90	1	100/0	-31	33	86	4000	1.8	-
2	100	0	95	10	45/55	-37	32	77	6200	1.6	-
3	100	0	98	48	17/83	-40	32	72	11200	1.8	-
4	60	40	83	3	100/0	-33	32	93	5700	1.4	11.2
5	60	40	85	10	59/41	-38	30	90	7700	1.7	12.5
6	60	40	87	18	43/57	-39	31	80	8700	1.6	12.5
7	60	40	88	24	32/68	-54	29	76	8400[f]	1.7[f]	10.8
8	60	40	90	48	16/84	-57	28	74	8100[f]	1.6[f]	9.6

[a]Calculated according to the mol. % of diglycerol dicarbonate. [b]Conversions were calculated by FTIR using the carbonyl characteristic bands of urethane at 1715 cm^{-1} and urea at 1670 cm^{-1}. [c]Data calculated from the second heating run of the DSC analysis. [d]Data normalized to the weight fraction of PEG. [e]M_n values were obtained by SEC in THF, the reported numbers are in reference to polystyrene standards. [f]The polymers were partially soluble in THF. Analyses were performed after purification of the polymers, performed by dissolving and precipitating in methanol and cold ether, respectively.

Despite their intriguing properties, one limitation of PHUs based on polyether soft segments, with respect to conventional polyurethanes, is their poor mechanical

properties at high temperature. This is due to their lower ability to phase separate as strong hydrogen bonding interaction develop between pending hydroxyl groups and the polyether-based soft segments.[36]

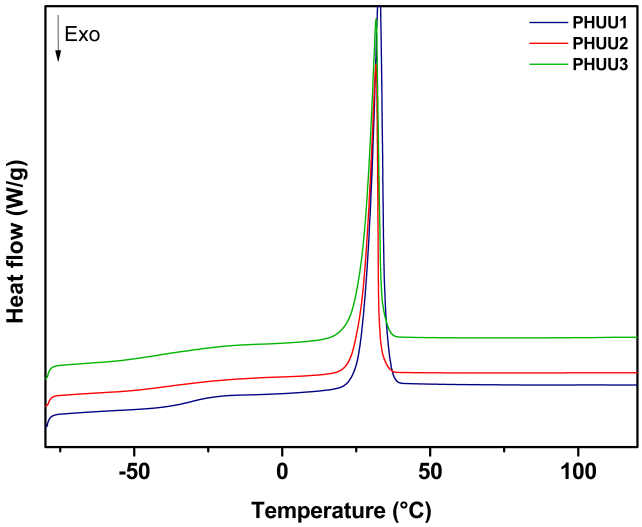

Figure 20. DSC curves of PHUU1, PHUU2 and PHUU3.

As Torkelson *et al.* have reported, PHUs consisting of oxygen-free soft segments, *i.e.* made of polybutadiene-co-acrylonitrile, exhibit sharper domain interphases, which is explained by a lack of hydrogen bonding between hard and soft segments.[37] Likewise, we expected phase-separation to occur with our PHUUs, due to the lesser probability for forming hydrogen bonding. The effect of the urea content on the thermomechanical properties was thus investigated with samples prepared from a mixture of two primary amines, namely, the same *Jeffamine* ED-2003 and 1,12-diaminododecane with a molar ratio = 60/40 (**Table 2**). Five PHUUs were thus synthesized at 120 °C in presence of 10 mol. % of TBD as catalyst, with different urea/urethane ratios (PHUU4, PHUU5, PHUU6, PHUU7 and PHUU8) (**Scheme 13**).

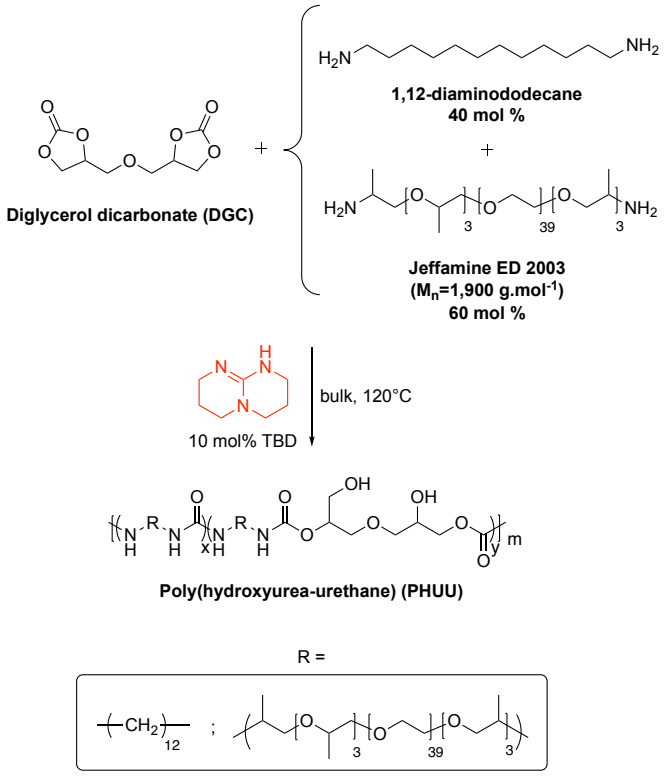

Scheme 13. Synthesis of poly(hydroxyurea-urethane)s (PHUUs) from DGC and diamines at 120 °C using 10 mol. % of TBD as catalyst.

The urethane content was varied from 100 % to 16 % as determined by FTIR, ^{1}H and ^{13}C NMR (**Figure S3** to **Figure S13** and **Figure S16** to **Figure S20** in the appendix section).

Analysis by ^{13}C NMR of the carbonyl region showed the presence of two types of urethane groups, namely, one due to *Jeffamine* ED-2003 (155.6 and 155.3 ppm) and the other one due to 1,12-diaminododecane (156.3 and 155.9 ppm), confirming the successful polymerization. Moreover, three different urea-type (–NH–(C=O)–NH–) carbonyl groups could be observed at 158.1, 157.5 and 156.9 ppm. As the urea content increased, peaks due to the urethane carbonyls progressively disappeared (**Figure 21**).

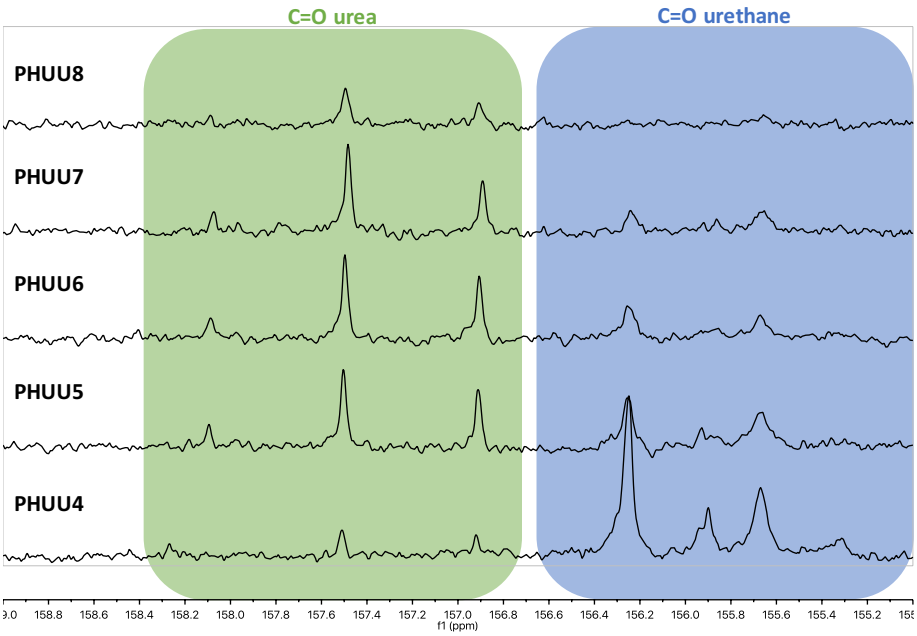

Figure 21. Evolution of the ^{13}C NMR in the carbonyl region from PHUU4 to PHUU8.

The molecular weight of the as-synthesized PHUUs were estimated by size exclusion chromatography (SEC, **Table 2** and **Figure 22**). Values varied between 4,000 and 11,200 Da with dispersities ranging from 1.6 to 1.8, typical of a step-growth polyaddition reaction.

DSC measurements of the PHUUs showed soft segment glass transition temperatures (T_g) ranging from -33 to -57 °C due to the soft segments (**Table 2** and **Figure 23**). Increasing the urea content resulted in a decrease of the T_g of the soft segment of the polymer, likely due to a higher phase separation. This effect was more pronounced for samples containing the short diamine, indicating that the introduction of this compound allowed for a reorganization of the hard and soft segments, giving rise to a segmented phase separated structure. Regarding the semi-crystalline PEG chains, we observed a small drop in the enthalpy of melting, as urea groups were formed during the polymerization, which was explained considering a change of PEG segments distribution in the polymer matrix.

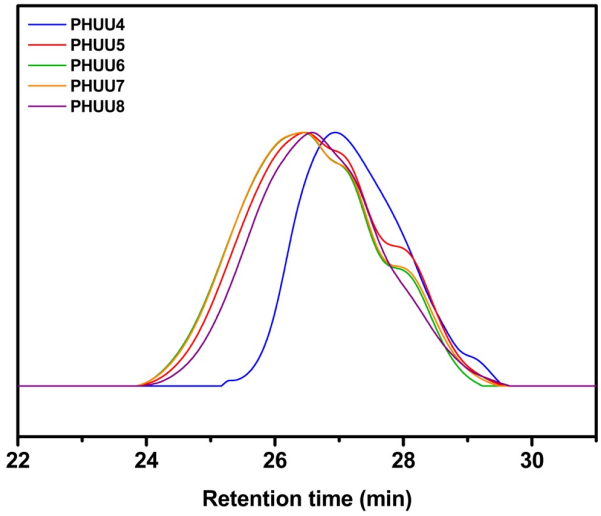

Figure 22. SEC traces of PHUU4, PHUU5, PHUU6, PHUU7 and PHUU8.

The thermo-mechanical properties of the five synthesized PHUUs containing the short diamine were analyzed by rheological measurements in parallel plates geometry. **Figure 24** shows the temperature dependence of the storage modulus (G') of the PHUUs. Consistent with the DSC measurements, all polymers showed a drop in elastic modulus at around 32 °C, corresponding to the melting temperature of the aliphatic polyether chain (PEG) of *Jeffamine* ED-2003. As expected for PHUU4, without any urea domain in the hard segment, the material exhibits a direct transition from the solid state to the liquid state without a significant rubbery plateau, after the melting temperature of the polyether chain is reached. As described by Torkelson *et al.* this might be explained by the stronger ability of PHUs relative to PUs to form hydrogen bonding between the soft and the hard phases, which could limit the phase separation and thus leads to a total loss of rubbery plateau domain.[36]

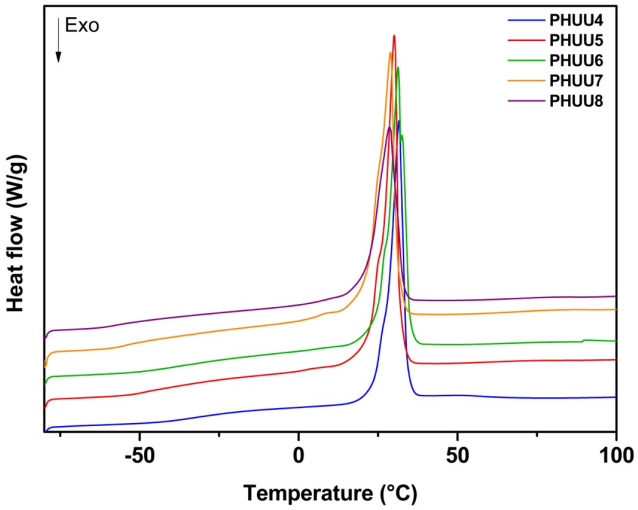

Figure 23. DSC curves of PHUU4, PHUU5, PHUU6, PHUU7 and PHUU8.

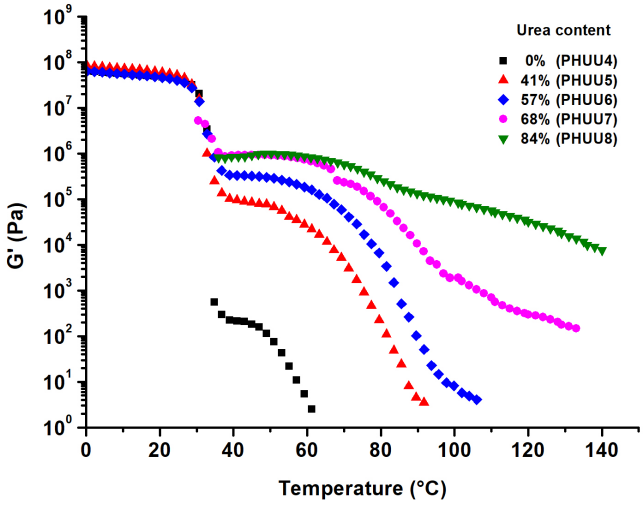

Figure 24. Temperature dependence of storage modulus (G') of the synthesized PHUUs.

Looking at PHUU5, PHUU6, PHUU7 and PHUU8, polymers with urea domains ranging from 41 to 84 %, respectively, we also observed a drop on G' upon heating near the melting temperature of *Jeffamine* ED-2003. However, in all these

cases a rubbery plateau region can be observed, which extends to higher temperatures as the urea content is increased.

Figure 25 shows the small angle X-ray scattering (SAXS) curves of the PHUU samples at room temperature and at 60 °C (above the melting temperature of PEG segments). A peak was observed for all the samples at room temperature which vanished at 60 °C. Therefore, these peaks correspond to the long period of the lamellar structure of the matrix phase (PEG), which can be estimated according to $d = 2\pi/q_{max}$ and listed in **Table 2**. The values of long period obtained correspond to the average distance between the crystalline lamellar centers of PEG. When the samples were heated to 60 °C, the long period peaks vanished as PEG melts. For PHUU4, a broad peak was observed at intermediate q range and a power law at low q. For all of the other samples, only a power law was observed. The general SAXS features proved very different from the self-assembly morphology of block copolymers with microphase separation. For this reason, the phase behavior was examined by phase contrast optical microscopy.

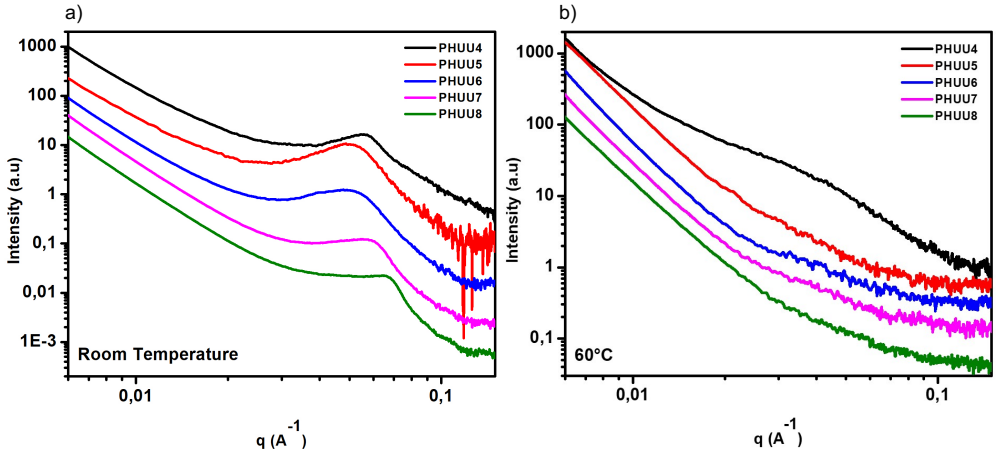

Figure 25. SAXS patterns of the synthesized PHUUs at: a) room temperature; b) at 60°C.

Phase contrast optical microscopy images are shown in **Figure 26**. All PHUU samples exhibit macroscopic phase separation at 40 °C. These results explain the lack of structure detected by SAXS at temperatures above the melting point of the

PEG crystals, as the scale of phase segregation is beyond the resolution of the SAXS. The amount of phase segregated domains increased from PHUU4 to PHUU8. Phase segregation was thus favored by the presence of urea groups. At 80 °C, a uniform phase was obtained for PHUU4. On the other hand, at 200 °C, PHUU6 exhibited a single phase while PHUU8 still showed some phase separated morphology. The miscibility temperatures shown in optical microscopy followed the same trend, as the transition temperature shown by rheology, although the former ones were higher.

Thus, results obtained by rheometry, SAXS and phase contrast microscopy results indicated that our poly(hydroxyurea-urethane)s were subjected to an order-disorder transition at temperatures well above the glass transition temperature of the hard segments. Upon cooling from a single-phase melt, the materials are able to phase segregate as the hard segments vitrified, and further cooling leads to the crystallization of the PEG phase.

Finally, increasing the urea content in the hard segment up to 84 % (PHUU8) promoted an elastomeric behavior of the material well above the melting temperature of the *Jeffamine* polyether chain, as confirmed in the rheology measurement by a rubbery plateau regime up to 140 °C. This effect was attributed to the improved phase separation of soft and hard segments probably due to the presence of lower amounts of pending hydroxyl groups in the hard segment which substantially reduced the ability of PHUUs to form hydrogen bonding with the oxygen of the ether groups of the soft segment. Furthermore, structure-property-relationship studies which consider the influence of the hydroxyl group in the phase separation, are still underway in order to achieve segmented PHUUs with improved properties.

In summary, we accessed a series of poly(hydroxyurea-urethane)s with precise urethane to urea ratio following a one-pot process. Characterization of the as-obtained polymers by rheological measurements showed that the storage modulus reached a plateau at high temperatures at high urea contents. The usage

temperature of poly(hydroxyurea-urethane)s could thus be increased from 30 °C to 140 °C, as for regular polyurethanes. Furthermore, SAXS and phase-contrast microscopy images demonstrated that increasing the urea content improved the phase separation between soft and hard segments of these poly(hydroxyurea-urethanes).

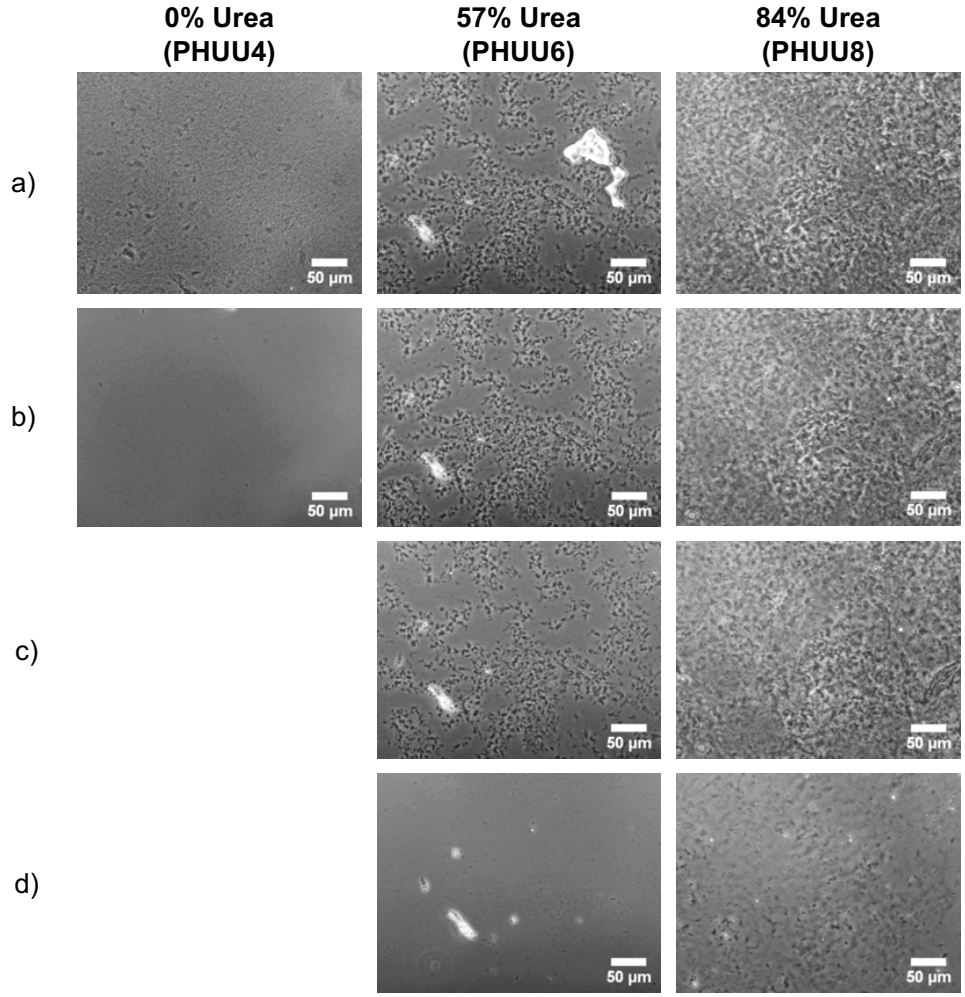

Figure 26. Phase-contrast microscopy images of PHUU4, PHUU6 and PHUU8 at: a) 40 °C; b) 80 °C; c) 120 °C; d) 200 °C. *Note: the phase-contrast microscopy images of PHUU4 at 120 and 200 °C did not show any differences with the one obtained at 80 °C.*

2.3. Conclusion

In this chapter, we developed a novel synthetic approach to solvent-free poly(hydroxyurethane-urea)s following one-pot organocatalytic pathway, starting from a 5-membered dicyclic carbonate and a diamine. The polymerization reaction outcomes proved highly catalyst dependent. Monitoring of the reaction revealed the formation of side urea groups at the completion of the polymerization. The occurrence of this side reaction was particularly noticeable upon using strong basic catalysts, such as TBD or P_4. In order to get a better understanding of the urea formation, a model reaction between propylene carbonate and dodecylamine was implemented, showing that with TBD and by increasing the temperature, the urea could selectively and quantitatively form from cyclic carbonates, which had never been reported before. A mechanism was proposed to account for the transformation of the urethane into urea. We then took more benefit of this reaction by synthesizing various PHUUs with a controlled urethane to urea ratio. Increasing the urea content induced a phase separation of the corresponding poly(hydroxyurea-urethane), even in the presence of polyether-based soft segments. All these results confirmed that use of base organocatalysts enabled the relatively facile synthesis of isocyanate-free poly(hydroxyurea-urethane) one-pot, with a possibility to achieve phase-separated compounds upon using conventional polyether-based soft segments and by a proper selection of the experimental conditions.

2.4. Experimental part

Instrumentation

Nuclear Magnetic Resonance (NMR). ^{1}H and ^{13}C spectra were recorded with Bruker Avance DPX 300 or Bruker Avance 400 spectrometers. The NMR chemical shifts were reported as δ in parts per million (ppm) relative to the traces of non-deuterated solvent (*e.g.* δ = 2.50 ppm for DMSO-d_6 or δ = 7.26 ppm for $CDCl_3$).

Data were reported as: chemical shift, multiplicity (s = singlet, d = doublet, t = triplet, m = multiplet, br = broad), coupling constants (J) given in Hertz (Hz), and integration.

Size Exclusion Chromatography (SEC). SEC was performed in THF at 30 °C using a Waters chromatograph equipped with four 5 mm Waters columns (300 mm "x" 7.7 mm) connected in series with increasing pore sizes. Toluene was used as a marker. Polystyrenes of different molecular weights, ranging from 2,100 $g.mol^{-1}$ to 1,920,000 $g.mol^{-1}$, were used for the calibration.

Fourier Transform Infrared Spectroscopy. FT-IR spectra were obtained by FT-IR spectrophotometer (Nicolet 6700 FT-IR, Thermo Scientific Inc., USA) using attenuated total reflectance (ATR) technique (Golden Gate, spectra Tech). Spectra were recorded between 4000-525 cm^{-1} with a spectrum resolution of 4 cm^{-1}. All spectra were averaged over 10 scans.

Differential Scanning Calorimetry. A differential scanning calorimeter (DSC-Q2000, TA Instrument Inc., USA) was used to analyze the thermal behavior of the samples. A total of 6-8 mg of samples were first scanned from -80 °C to 150 °C at a heating rate of 20 $°C.min^{-1}$ to eliminate interferences due to moisture. The samples were then cooled to -80 °C to remove the thermal history and reheated to 150 °C at 20 $°C.min^{-1}$. The glass transition and melting temperatures were calculated from the second heating run.

Elemental analysis. The elemental analysis for carbon, hydrogen and nitrogen content was performed using a Leco TruSpec Micro instrument (Germany) at 1000 °C using helium as transport gas. The analysis was conducted twice for comparison using 1-2 mg of sample.

Mass Spectroscopy (LC-TOF-MS) The mass spectroscopy analysis consisted in a chromatographic separation in an ultrahigh performance liquid chromatograph (UPLC, Acquity system from Waters Cromatografia S.A., USA) coupled to a high-resolution mass spectrometer (Synapt G2 from Waters Cromatografia S.A., USA, time of flight analyzer (TOF)) by an electrospray ionization source in positive mode

(ESI). The chromatographic separation was achieved using an Acquity UPLC BEH C18 column (1.7 µm, 2.1×50 mm i.d.) with an Acquity UPLC BEH C18 1.7 µm VanGuard pre-column (2.1×5 mm) (Waters Cromatografia S.A., USA) and a binary A/B gradient (solvent A: water with 0.1 % formic acid and solvent B: methanol with 0.1 % formic acid). The gradient program was established as follows: initial conditions were 5 % B, raised to 100 % B over 2.5 min, held at 100 % B until 4 min, decreased to 5 % B over the next 0.1 min, and held at 5 % B until 5 min for re-equilibration of the system prior to the next injection. A flow rate of 0.25 $mL.min^{-1}$ was used, the column temperature was 30 °C, the autosampler temperature 4 °C and the injection volume 7.5 µL. High resolution mass data were acquired in SCAN mode, using a mass range 50–1200 u in resolution mode (FWHM ≈ 20,000) and a scan time of 0.1 s. The source temperature was set to 120 °C and the desolvation temperature to 300 °C. The capillary voltage was 0.5 kV and the cone voltage 15 V. Nitrogen was used as the desolvation and cone gas at flow rates of 800 L/h and 10 L/h, respectively. Before analysis, the mass spectrometer was calibrated with a sodium formate solution. A leucine-enkephalin solution was used for the lock mass correction, monitoring the ions at mass-to-charge ratio (m/z) 556.2771 and 278.1141. All of the acquired spectra were automatically corrected during acquisition based on the lock mass. The sample was dissolved in acetone at 65 °C and diluted in methanol for the analysis (around 20 $µg.mL^{-1}$).

Rheometry measurements. Small-amplitude oscillatory experiments were performed in a stress-controlled Anton Paar Physica MCR101 rheometer and the experiments were carried out using 25 mm parallel plate geometry. All the experiments were conducted in linear viscoelastic conditions for the studied temperature range (strain = 0.5 % and frequency 1 Hz).

Small Angle X-ray Scattering (SAXS). SAXS experiments were carried out on a Xeuss SAXS/WAXS system (Xenocs SA, France). A multilayer focused Cu-Kα X-ray source (GeniX3D Cu ULD), generated at 50 kV and 0.6 mA, was employed. The wavelength of the X-ray radiation was 0.15418 nm. A semiconductor detector (Pilatus 300K, DECTRIS, Swiss) with a resolution of 487 × 619 pixels (pixel size

172 × 172 μm^2) was applied to collect the scattering signals. The exposure time for each SAXS pattern was 30 minutes. The one-dimensional scattering intensity profiles were integrated after background correction from 2D SAXS patterns.

Optical Microscopy. The phase morphology of the samples was observed with a phase contrast microscope (Olympus BX51, Japan) equipped with a Linkam THMS600 hotstage (Linkam Scientific Instruments, UK).

Materials

1,5,7-Triazabicyclo[4.4.0]dec-5-ene (98 %) (TBD), 1,12-diaminododecane (98 %), *N*-butylamine (99.5 %), *O,O′*-bis(2-aminopropyl) polypropylene glycol-block-polyethylene glycol-block-polypropylene glycol (*Jeffamine* ED-2003) with a molecular weight around 1,900 Da, *p*-toluenesulfonic acid monohydrate (98.5 %) (PTSA), phosphazene base P_4-*t*-Bu solution (0.8M solution in hexane) (P_4) and sodium methoxide (95 %) were purchased from Sigma Aldrich. 1,8-Diazabicyclo[5.4.0]undec-7-ene (≥ 98 %) (DBU) and diglycerol (≥ 80 %) were purchased from TCI chemicals. 3,5-Bis(trifluoromethyl)phenyl isothiocyanate (99 %), hexane (laboratory reagent grade), methanol (analytical reagent grade) and tetrahydrofuran (analytical reagent grade) were purchased from Fisher. Dimethyl carbonate (extra dry, ≥ 99 %), dodecylamine (98 %) and propylene carbonate (99.5 %) were purchased from Acros Organics. Deuterated solvents such as $CDCl_3$, DMSO-d_6 was purchased from Euro-top. All materials were used without further purification.

Synthesis of diglycerol dicarbonate (DGC). Synthesis of DGC was carried out in an adapted version of Van Velthoven *et al.*[102] In a 500 mL round-bottom flask equipped with a magnetic stirrer and a condenser, diglycerol (1 equiv., 23.18 g, 0.14 mol) and sodium methoxide (0.05 equiv., 0.38 g, 7 mmol) were added to a solution of dimethyl carbonate (10 equiv., 125.6 g, 117.5 mL, 1.4 mol) under nitrogen atmosphere. The reaction mixture was heated under reflux for 48 h. After cooling down to room temperature, the reaction was filtrated and concentrated

under vacuum. After evaporation of dimethyl carbonate, the product was crystallized in methanol at -80 °C. DGC was obtained as a white powder after drying in the vacuum oven at 40 °C for 24 h (11.79 g, 39 % yield). The structure was confirmed by ^{1}H and ^{13}C NMR spectroscopy. ^{1}H NMR (300 MHz, DMSO-d_6, δ): 4.97–4.91 (m, 1H), 4.52 (t, J = 8.5 Hz, 1H), 4.27–4.21 (m, 1H), 3.78–3.75 (m, 1H), 3.74–3.66 (m, 1H). ^{13}C NMR (75 MHz, DMSO-d_6, δ) 154.84, 75.40, 75.34, 70.39, 70.35, 65.88. IR (ATR, cm^{-1}): 2998, 2927, 2888, 1765, 1546, 1481, 1371, 1340, 1259, 1168, 1112, 1058, 956, 845, 801, 769, 711. Characterization data is consistent with previous reports.[102,103,114]

Synthesis 1-(3,5-bis(trifluoromethyl)phenyl)-3-butylthiourea (TU). Synthesis of TU was carried out following procedure described elsewhere.[47] Butylamine (1.61 g, 22.1 mmol) was added dropwise at room temperature to a stirred solution of 3,5-bis(trifluoromethyl)phenyl isothiocyanate (5 g, 18.44 mmol) in dry THF (50 mL). The solution was left stirring for another 4 h at room temperature. The reaction mixture was concentrated under vacuum and the product was recrystallized from hexane. After drying under vacuum, TU was obtained as a slightly yellow powder (5.89 g, 92 % yield). The structure was confirmed by ^{1}H NMR spectroscopy. ^{1}H NMR (300 MHz, DMSO-d_6, δ): 9.88 (s, 1H), 8.23 (s, 2H), 7.72 (s, 1H), 3.49 (t, 2H), 1.55 (m, 2H), 1.33 (m, 2H), 0.91 (t, J = 7.3 Hz, 3H). Characterization data is consistent with previous report.[47]

General procedure for the synthesis of potassium thioimidate (TU anion) Synthesis of TU anion was carried out adapting procedure describe elsewhere.[99] TU (16.4 mg, 50 µmol) and potassium methoxide (3.5 mg, 50 µmol) were added in a dry Schlenk flask under argon. Dry THF (10 mL) was then added and the reaction mixture was stirred at room temperature for 2 h. THF was then removed in vacuum and TU anion was obtained as a viscous liquid. The structure was confirmed by ^{1}H NMR spectroscopy. ^{1}H NMR (300 MHz, DMSO-d_6, δ): 8.23 (s, 2H), 7.72 (s, 1H), 3.49 (t, 2H), 1.55 (m, 2H), 1.33 (m, 2H), 0.91 (t, J = 7.3 Hz, 3H).

General procedure for polymerization reactions. In a typical procedure, DGC (1 equiv.), diamine (1 equiv.) and catalyst (0.1 equiv.) were mixed together in a 25 mL vial equipped with a magnetic stirrer. The polymerization reaction was conducted at 120 °C under stirring and under ambient atmosphere. Aliquots were taken at regular intervals for FTIR, NMR, DSC and SEC analyses.

General procedure for model reaction. In a typical procedure, propylene carbonate (1 equiv., 7 mmol), dodecylamine (1 equiv., 7 mmol) and catalyst (0.1 equiv., 0.7 mmol) were mixed together in a 25 mL vial equipped with a magnetic stirrer. The reaction was conducted at 120 °C under stirring and ambient atmosphere for 24 h. Aliquots were taken at specific intervals of time for FTIR, NMR, elemental analysis and LC-TOF-MS.

General procedure for urea formation from hydroxyurethane. In this procedure, propylene carbonate (1 equiv., 7 mmol) and dodecylamine (1 equiv., 7 mmol) were mixed together in a 25 mL vial equipped with a magnetic stirrer. The reaction was conducted at 120 °C for 53 h in two parts. First, the reaction was let under stirring at 120 °C until complete conversion of propylene carbonate. Then, TBD (0.1 equiv., 0.7 mmol) was added in the medium and the reaction was let stirring at 120 °C for 48 h. Aliquots were taken after 5 h (without TBD) and 48 h (with TBD) for FTIR and ^{1}H NMR spectroscopy analysis

Chapter 3

Synthesis of Self-Healable Waterborne Isocyanate-Free Poly(hydroxyurethane)-Based Supramolecular Networks by Ionic Interactions

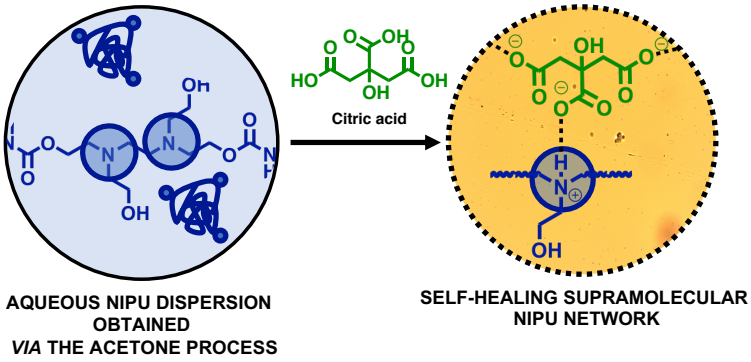

Bossion A., Olazabal I., Aguirresarobe R.H., Marina S., Irusta L., Taton D. and Sardon H. *To be submitted*, 2018.

CHAPTER 3. SYNTHESIS OF SELF-HEALABLE WATERBORNE ISOCYANATE-FREE POLY(HYDROXYURETHANE)-BASED SUPRAMOLECULAR NETWORKS BY IONIC INTERACTIONS

3.1. Introduction

As highlighted in the previous chapter, the search for sustainable approaches to polyurethanes is a developing field, in particular to address the toxicity issue of isocyanates used as co-monomers in traditional syntheses. In this context, the synthesis method resting on the step-growth polyaddition of 5-membered cyclic carbonates with diamines, resulting in poly(hydroxyurethane)s (PHUs), appears as very promising for large scale applications.[19,34] However, the low reactivity of conventional 5-membered cyclic carbonates limits the achievement of high molecular weight PHUs with good mechanical properties, owing to a limited diffusion at room temperature and the occurrence of side reactions during polymerization.[3,20,21,23–25,27,29,32,34,56,76,77,79,105,115–119] Although other cyclic carbonates have been studied to increase the reactivity of these monomers, Caillol *et al*. have shown that they could be activated in presence of protic solvents, such as methanol, at room temperature, rather than using harsh polymerization conditions or a catalyst.[31,91,120,121] The authors have evidenced formation of inter- and intramolecular hydrogen interactions between pendent hydroxyls of PHUs and urethane moieties. The observed limited monomer conversion was explained by a decrease of polymer chain diffusivity owing to these interactions. This could be alleviated using a protic solvent, such as methanol, which allowed reaching completion of the reaction within 24 h. In comparison, performing the reaction in

aprotic solvent, such as chloroform, conversion reached 85 % after 24 h and did not evolve after 7 days. This was explained by the existence of hydrogen bonds between the solvent and carbamate groups of PHUs, preventing the formation of inter- and intramolecular interactions thus increasing chain mobility (**Scheme 14**).

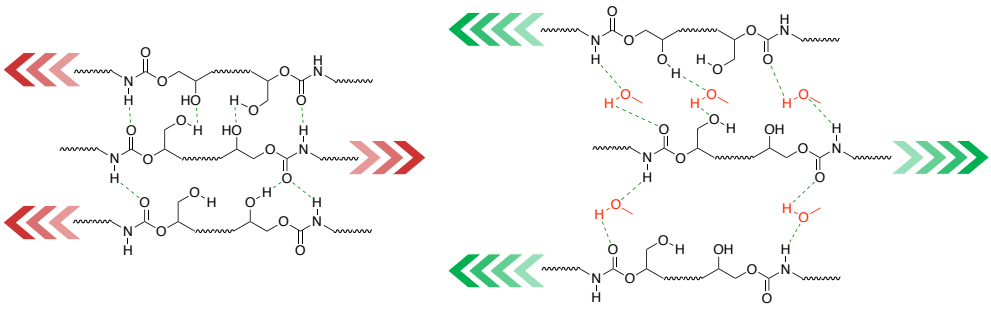

Scheme 14. Effect of protic solvent on the PHU hydrogen bonds and the chains mobility; adapted from ref. 121

Instead of solvent-borne processes, utilization of water as a medium of step-growth polymerization reactions is attracting an increasing interest, as related waterborne processes do not require VOCs and also allow the formation of stable crosslinked nanoparticles, which can be subsequently used in coating applications.[122,123] However, only a handful of studies have been dedicated to the preparation of waterborne NIPUs.[68,75,124] For example, Cramail *et al*. have reported the synthesis of waterborne NIPU-based latexes by mini-emulsion polymerization at up to 30 wt. % solid content. Hydrolysis of cyclic carbonates has yet been noted, leading to low molecular weights, as compared to NIPUs obtained in bulk polymerization.[75]

In the continuity of our efforts to achieve waterborne NIPUs, we turned to the so-called “acetone process”, which is commonly implemented at the industrial scale to prepare regular waterborne polyurethanes.[66,67] As explained in the introductive

chapter, this three-step procedure involves the prior synthesis of PU in a low boiling point solvent, *e.g.* acetone or THF (**Figure 27**).

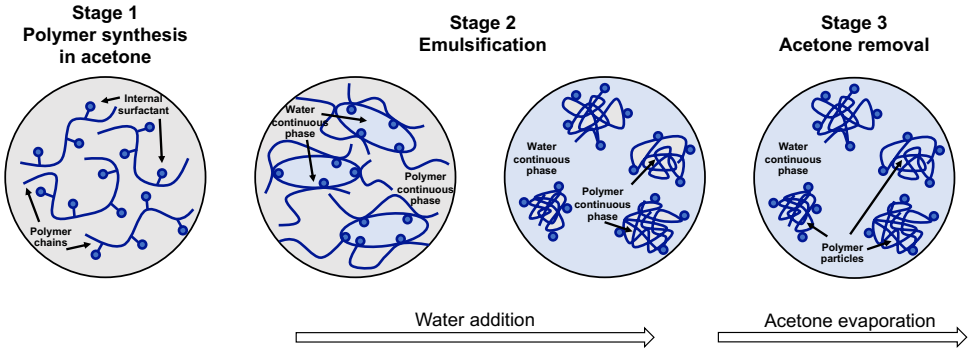

Figure 27. Waterborne polyurethane synthesis by means of the acetone process.

As regular PUs are usually immiscible with water, a modification step of the polymer structure is required before any dispersion into the aqueous medium. This is usually achieved by incorporating ionic or nonionic hydrophilic moieties acting as "internal emulsifiers" in the PU backbone and imparting water dispersibility. Non-ionic dispersions can thus be stabilized sterically thanks to the presence of hydrophilic soft segments, such as poly(ethylene oxide), while anionic or cationic moieties enable electrostatic stabilization of the dispersions. Ionic groups thus incorporated generally consist of either pendant sulfonic or carboxylic acid groups, *e.g.* deriving from 2,2-bis-(hydroxymethyl) propionic acid (DMPA), or of ammonium salts, for instance deriving from *N*-methyldiethanolamine (MDEA; **Figure 28**). PU thus-obtained can be readily dispersed in water under mild conditions.

In a second step, water is added dropwise into the polymeric solution, which causes the polymer phase to be dispersed in water. The transition from the one phase (PU/acetone mixture) to the two-phase dispersion (PU particles dispersed in water) occurs continuously. PU particles are thus directly generated *via* precipitation due to the change in polarity of the solvent mixture and stabilization is provided by the "internal emulsifier".

In a final step, *i.e.* after of PU particle formation, more water is added as a means to further dilute the dispersion, and, acetone is finally removed to lead to the aqueous PU dispersion.[61,64]

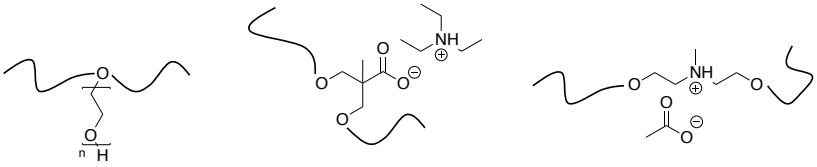

Figure 28. Different types of hydrophilic groups employed to stabilize PU water dispersions.

This method proves particularly attractive for the formation of PU waterborne dispersions (almost) free of any VOCs, and it also enables to introduce a wide variety of functional groups into the PU backbone. However, several parameters can dramatically impact the stability of the final dispersion, including the content in the internal emulsifier, the extent of neutralization, the initial solid content or the affinity of the organic solvent towards water. For example, Sardon *et al.* thoroughly studied the effect of molecular parameters, such as ionic group concentration, phase-inversion temperature or PU content in acetone, on the colloidal properties of the PU dispersions. For this purpose, WPUs were prepared from isophorone diisocyanate, DMPA, 1,4-butanediol and poly(propylene glycol) using dibutyltin dilaurate (DBTDL) as metallic catalyst.[64] It was found that stable PU dispersions with an average particle size around 30 nm (PDI = 0.14) could be obtained using DMPA, and by finely tuning the phase inversion temperature as well as the initial polymer/acetone concentration.

A potential method to access water-dispersible non-isocyanate polyurethanes (WNIPUs) through the acetone process is to employ the 8-membered bicyclic carbonate featuring tertiary amines in its structure (**Scheme 15**). Similarly to

conventional WPUs, these tertiary amines are expected to play further the role of "internal emulsifiers" in presence of carboxylic acids, thus allowing the facile preparation of stable aqueous NIPU dispersions. In addition, such tertiary amino-containing NIPUs can be further exploited when used as reactive polymer platforms for chemical post-modification. For instance, their post-treatment with simple multifunctional carboxylic acids could lead to a new family of supramolecular side-chain ionic NIPUs with improved mechanical properties compared to non-functionalized NIPUs.

Non-functionalized NIPUs, indeed, often suffer from low physical properties due to hydrogen bond interactions within the polymer chains, given by the numerous hydroxyl groups in their structures. One common method to increase the mechanical properties is through the synthesis of crosslinked material.[78,105,107,119] However, the formation of crosslinked networks in bulk often leads to non-reprocessable products. Moreover, as reported by Dichtel *et al*., PHU materials deriving from 5-membered cyclic carbonates can decompose at reprocessing temperatures (T = 180 °C) used for densely crosslinked thermosets, which also limits the application range of PHU-type thermosets.[107]

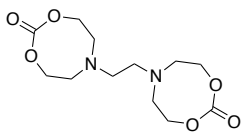

Scheme 15. Structure of the 8-membered cyclic carbonate bearing tertiary amines in its structure (bis-N-8-C).

In contrast to covalently crosslinked structures, and imparted by their dynamic nature, supramolecular materials can be easily reprocessed at mild temperatures. Supramolecular structures have emerged in material science for a potential use in high added value applications, ranging from biomaterials to energy transfer and storage. These materials are characterized by highly directional reversible non-covalent interactions, which differentiate them from conventional

covalently assembled polymers or networks. Different types of non-covalent reactions, such as hydrogen bonding, metal coordination, π−π (or arene−arene) interactions and ionic interactions, are known to form supramolecular networks with self-healing properties. This autonomous process can be triggered by an external stimulus, *e.g.* light, heat and pH variation, etc.[125–136] The use of ionic interactions in this context, as a means to tune the supramolecular assemblies in PUs, although very attractive and versatile as this can be easily achieved from a practical viewpoint, has been underexplored. These self-assembled PUs materials are easily prepared by proton transfer reactions between multifunctional carboxylic acids and amines.[137–139]

For example, in 2017, Cádiz *et al.* have reported the synthesis of self-healable PU elastomers *via* a post-synthetic process based on ionic interactions formed by tertiary side chain amino groups and multifunctional carboxylic acids, such as adipic and citric acid (**Scheme 16**).[138] This straightforward approach consisted in mixing equimolar amounts of carboxylic acids (with regards to the tertiary amine groups) and the PU in THF under stirring for 2 h. The resulting polymer films showed fast self-healing responses and were able in some cases to recover up to 90 % of the initial tension energy after 24 h. To the best of our knowledge, this "protic ionic liquid-type" method has never been applied to elaborate NIPU-based films with self-healing properties from water dispersions.

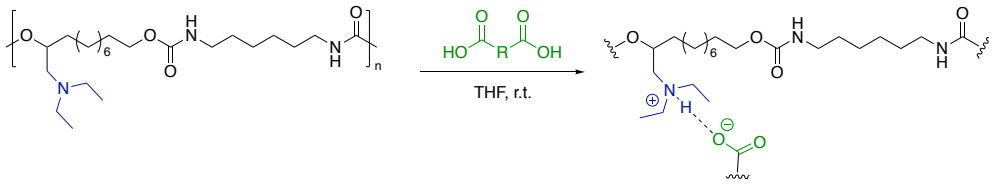

Scheme 16. Preparation of self-healable supramolecular PU elastomers *via* ionic interactions as proposed by Cádiz *et al.*; adapted from ref. 138

In this chapter, we describe a novel synthetic strategy to isocyanate-free water-dispersible PU (WNIPUs), by copolymerizing different ratios of 5-membered

cyclic carbonate, namely, diglycerol dicarbonate (DGC) and the 8-membered cyclic carbonate, bis-N-8-C, with a hydrophobic aminoalkyl-terminated polydimethylsiloxane (PDMS diamine) as co-monomer. NIPU-based dispersions could be obtained using the “acetone process”. The effect of different parameters, including the internal surfactant concentration, degree of neutralization and NIPU content, on the final particle size, particle morphology (TEM) and stability were studied. Last but not least, amino-containing films generated from such dispersions could be manipulated and exhibit self-healing supramolecular properties by post-chemical modification, using carboxylic acids. Rheology measurements of the corresponding films showed unique mechanical properties.

3.2. Results and discussion

3.2.1. Synthesis and characterization of poly(hydroxyurethane)s based on DGC and bis-N-8-C.

A series of dispersion experiments were first carried out in order to optimize the formulation and thus appreciate the effect of the degree of neutralization on the final polymer particle size. NIPUs were thus synthesized using different 5- to 8-membered cyclic carbonate ratios (**Scheme 17** and **Table 3**). Polymerizations were performed in bulk in absence of catalyst and under mechanical stirring at 80 °C for 48 h. The as-obtained polymers were characterized by FTIR, ^{1}H and ^{13}C NMR spectroscopy, thermogravimetric analysis (TGA), DSC and SEC.

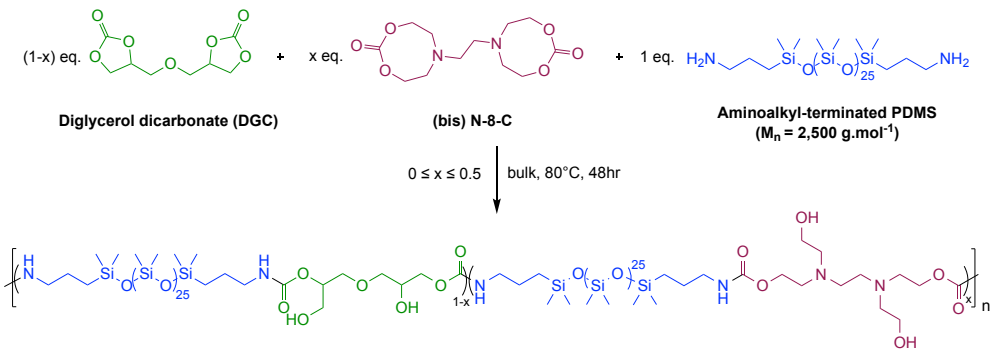

Scheme 17. Synthesis of poly(hydroxyurethanes) based on DGC, bis-N-8-C and PDMS diamine.

Completion of the reactions was first assessed by FTIR (**Figure 29** and **Figure S21** to **Figure S26** in the appendix section). As the reaction occurred, the band at 1795 (DGC) and 1725 cm^{-1} (bis-N-8-C) due to the cyclic carbonates disappeared, and signals attributed to the newly formed urethane group could be observed at 1702 (C=O stretching vibration) and 1532 cm^{-1} (N—H bending vibration). Characteristic siloxane bands of PDMS diamine were observed at 2962 cm^{-1} (C—H stretching of CH_3) and in the fingerprint region at 1257 cm^{-1} (CH_3 symmetric deformation of Si—CH_3), 1074 and 1010 cm^{-1} (Si—O—Si stretching vibration) and 785 cm^{-1} (Si—C stretching vibration and CH_3 rocking of Si—CH_3).

Formation of urethane moieties was confirmed by NMR spectroscopy (**Figure 30** and **Figure S27** to **Figure S31**). As the reaction occurred, characteristic ^{1}H NMR signals of the methylene protons of DGC centered at 4.88-4.79 (C*H*−OCO), 4.56-4.49 and 4.27-4.20 (CH_2−OCO) and 3.88-3.75 ppm (CH_2−OCH_2) gradually disappeared, while new signals attributed to the urethane group were observed at 4.87 (C*H*−OCONH), 4.13 (CH_2−OCONH), 3.97 (CH_2−OCH_2), 3.86 (C*H*−CH_2OCONH), 3.67 (CH_2−OCH_2) and 3.56 (CH_2−OH) ppm.

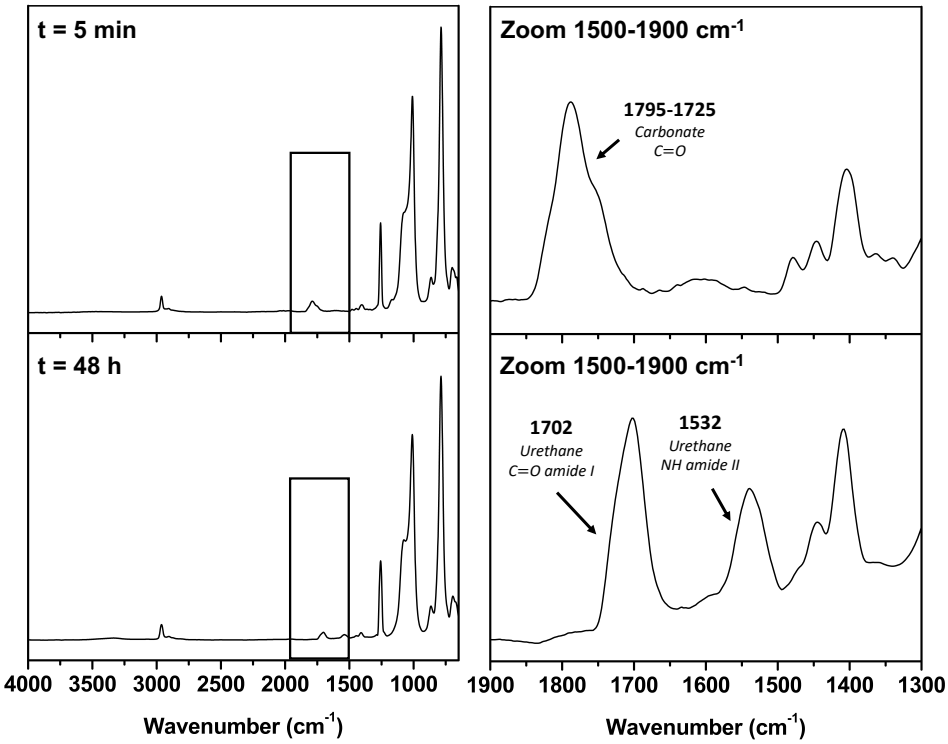

Figure 29. FTIR spectra of the poly(hydroxyurethane) based on DGC, bis-N-8-C and PDMS diamine after 5 min and 48 h. WNIPU4 (x = 0.3).

Similarly, protons due to the resonance bis-N-8-C at 4.19 (C*H*$_2$−OCO), 2.82 (C*H*$_2$−CH$_2$OCO) and 2.77 (C*H*$_2$−N) ppm shifted upfield to 4.13 (C*H*$_2$−OCONH), 3.56 (C*H*$_2$−OH) and 2.72-2.57 (C*H*$_2$−N) ppm, as the cyclic carbonate reacted with the PDMS diamine. Meanwhile, the methylene protons at 2.68 ppm (C*H*$_2$−NH$_2$) next to the amino groups in PDMS diamine shifted to 3.12 (C*H*$_2$−NHCOO) ppm as aminolysis occurred with the cyclic carbonates. A closer look at the carbonyl region of the ^{13}C NMR spectra showed the presence of a peak at 156.91 ppm, corresponding to the (–NH–(C=O)–O–) urethane carbonyl group as a result of the reaction between DGC and bis-N-8-C with PDMS diamine (**Figure S32** to **Figure S37**).

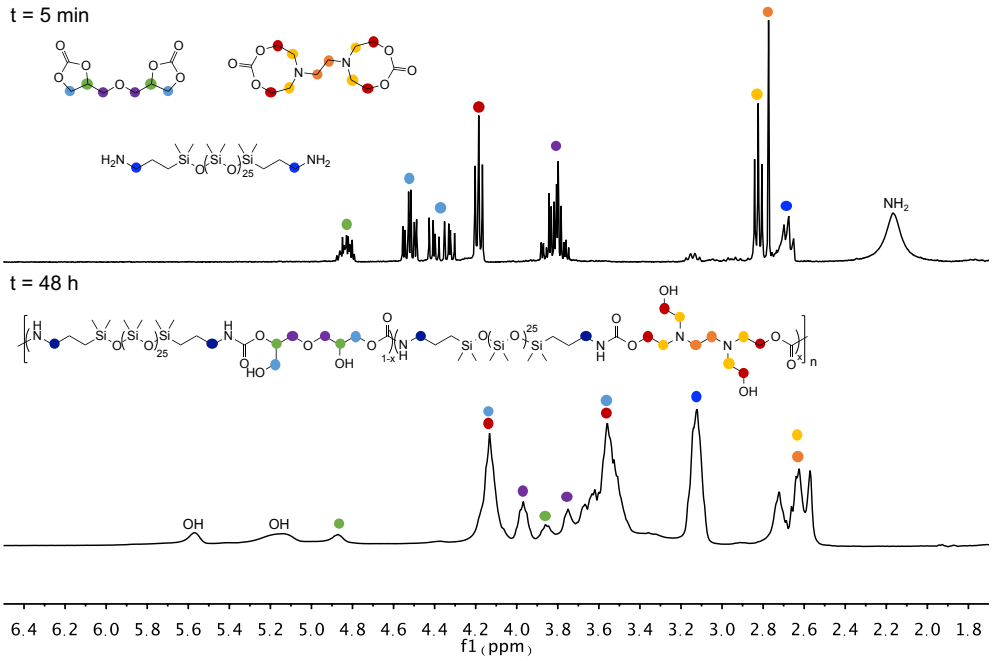

Figure 30. Expanded ^{1}H NMR (300 MHz, $CDCl_3$) of the poly(hydroxyurethane) based on DGC, bis-N-8-C and PDMS diamine after 5 min and 48 h. WNIPU4 (x = 0.3).

The NIPU molecular weight was determined by SEC in DMF. As illustrated in **Figure 31**, molecular weights ranged from 13.7 to 21 kDa while dispersities were found close to 2, which was typical of polymer synthesized by step-growth polymerization.

Thermal properties of these NIPUs were also evaluated by TGA and DSC (**Table 4**, **Figure 32** and **Figure S38**). The thermogravimetric curves obtained are shown in the appendix section. All NIPUs exhibit good thermal stability, with little weight losses up to 230 °C, which relate to degradation temperature range of previously reported linear PHUs.[75,77,140] DSC measurements of all NIPUs show one glass transition temperatures (T_g) well below room temperature, *i.e.* at -120 °C characteristic of the T_g of PDMS (**Table 3**).

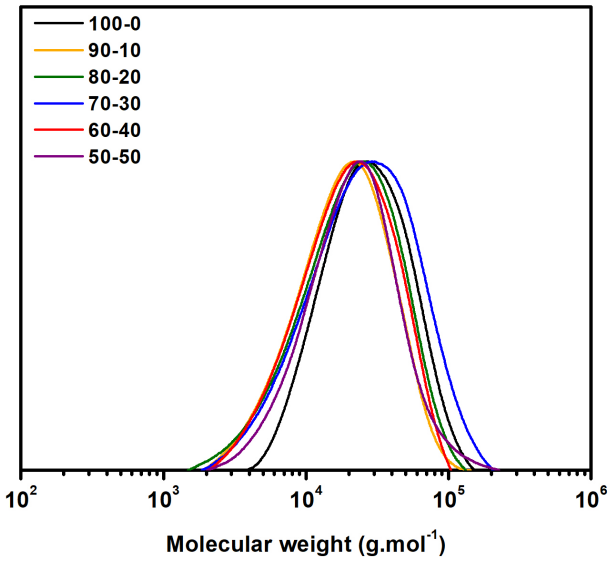

Figure 31. SEC traces of the synthesized poly(hydroxyurethanes).

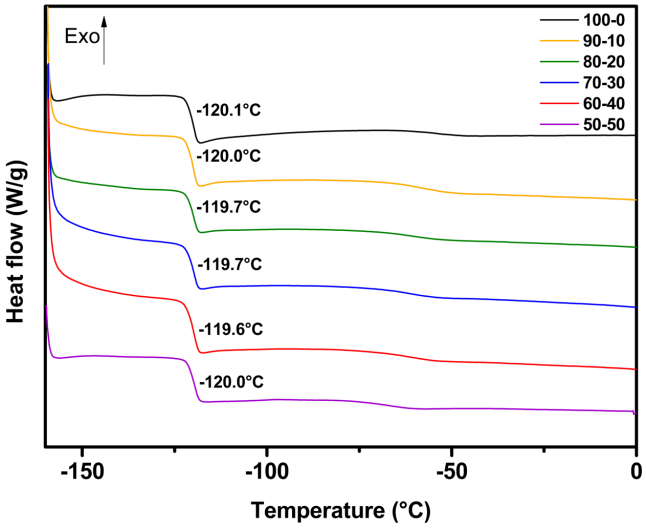

Figure 32. DSC curves of the synthesized poly(hydroxyurethanes).

Table 3. Summary of the water-dispersible poly(hydroxyurethane)s synthesized from DGC, bis-N-8-C and PDMS diamine and their properties.

WNIPU	DGC (mol. %)[a]	bis-N-8-C (mol. %)[a]	DSC	SEC	
			T_g (°C)[b]	M_n (g/mol)[c]	$Đ$[c]
1	100	0	-120.1	21,000	1.6
2	90	10	-120.0	13,700	1.7
3	80	20	-119.7	14,400	1.8
4	70	30	-119.7	17,200	2.0
5	60	40	-119.6	14,500	1.7
6	50	50	-120.0	16,000	1.7

[a]Calculated with regards to the mole of PDMS diamine. [b]Data calculated from the second heating run of the DSC analysis. [c]M_n values were obtained by SEC in DMF.

3.2.2. Effect of different parameters on the characteristics of the dispersions

It is well-established that particle size and particle size distribution of WPU are key features for subsequent film formation and film properties. These dimensions strongly depend on the amount of internal surfactant, and overall, on the initial conditions used (solid content, temperature, etc.).[61,64] Therefore, NIPUs described above were subjected to dispersion experiments.

3.2.2.1. Influence of the internal emulsifier (bis-N-8-C content)

To determine the effect of the 8-membered cyclic carbonate molar ratio, *i.e.* the internal surfactant concentration, six different dispersions were prepared by varying the amount of bis-N-8-C, from 0 to 50 mol. %, keeping constant the emulsification conditions. The amount of internal surfactant thus varied from 0 to 0.36 mmol/$g_{polymer}$ (**Table 4**). At first, an initial solid content of 50 wt. % was targeted, and excess of acetic acid was used to ensure full quaternization of tertiary amino

groups arising from, bis-N-8-C and forming ammonium carboxylates $–R_3NH^+\text{-}COO^-(CH_3)$.

For bis-N-8-C molar ratio lower than 20 mol. %, the resulting NIPUs were found to precipitate (WNIPU1 and WNIPU2) and were thus unstable. As reported by Keight *et al*., the lack of hydrophilic ionic groups along the polymer backbone might hamper the excess water to be absorbed by the polymer. Though emulsion can initially form, lack of stabilization led to the formation of, large aggregates, and finally to precipitation after phase inversion.[141] Increasing then the internal surfactant content to 0.15 $mmol/g_{polymer}$ (WNIPU3) yielded dispersions with an average particle size of 462 nm. However, a sharp increase of the particle size was then noted when acetone was removed, leading to the formation of particle sizes > 1 µm and resulting in rapid precipitation of the dispersion due to particle coalescence (**Figure 34**). At higher internal emulsifier concentration (WNIPU4), the mean particle size decreased to 200 nm. On the contrary to WNIPU3, the particle sizes of WNIPU4 did not significantly change during the whole acetone process, and the dispersions obtained were stable for more than one year (**Figure 34**). As observed on the TEM images of this WNIPU4 dispersion (see **Figure 33**), particles were in the nanometer size range. Further increasing the internal surfactant (WNIPU5 and WNIPU6) gave unstable dispersions, especially again after acetone removal. We hypothesized that this was due to the presence of large amounts of $–R_3NH^+\text{-}COO^-(CH_3)$ ions, with some ion pairs that might have come inside the particles pulling water in the polymer rich phase, while others remained at the surface stabilizing the particles.

Table 4. Effect of the internal surfactant concentration on the particle size.

WNIPU	DGC (mol. %)[a]	bis-N-8-C (mol. %)[a]	Internal surfactant ($mmol/g_{polymer}$)	DLS			
				$D_{pwater/acetone}$ (nm)[b]	PDI [b]	D_{pwater} (nm)[c]	PDI [c]
1	100	0	0	-[d]	-[d]	-[d]	-[d]
2	90	10	0.07	-[d]	-[d]	-[d]	-[d]
3	80	20	0.15	462 (± 15)	0.13 (± 0.04)	-[d]	-[d]
4	70	30	0.22	202 (± 25)	0.18 (± 0.06)	204 (± 24)	0,25 (± 0.13)
5	60	40	0.29	178 (± 46)	0.15 (± 0.15)	306 (± 131)	0.11 (± 0.08)
6	50	50	0.36	-[d]	-[d]	-[d]	-[d]

[a]Calculated regarding the mole of PDMS diamine. [b]Particle sizes and particle size distributions were calculated using dynamic light scattering (DLS) in water/acetone mixture over 3 experiments. The values in bracket are the standard deviation of the measurements. [c]Particle sizes and particle size distributions were calculated using DLS after acetone removal over 3 experiments. [d]Dispersions were unstable and resulted in precipitation. Dispersion experiments were carried out at room temperature with 50 wt. % initial solid content and excess acetic acid.

These results confirmed that an optimal amount of 30 mol. % of bis-N-8-C acting as internal surfactant was required to achieve stable NIPU dispersions.

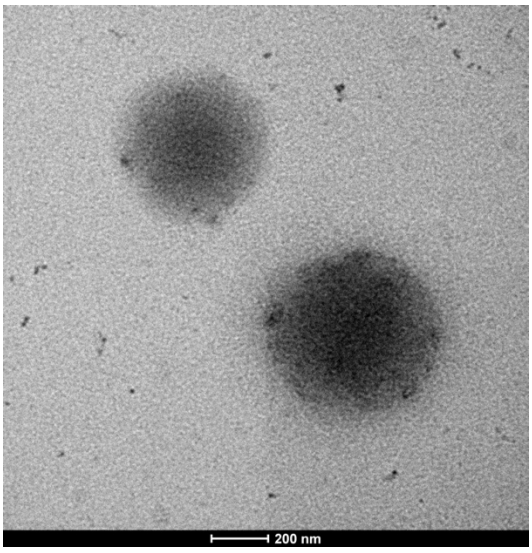

Figure 33. TEM image of the dispersion obtained from WNIPU4.

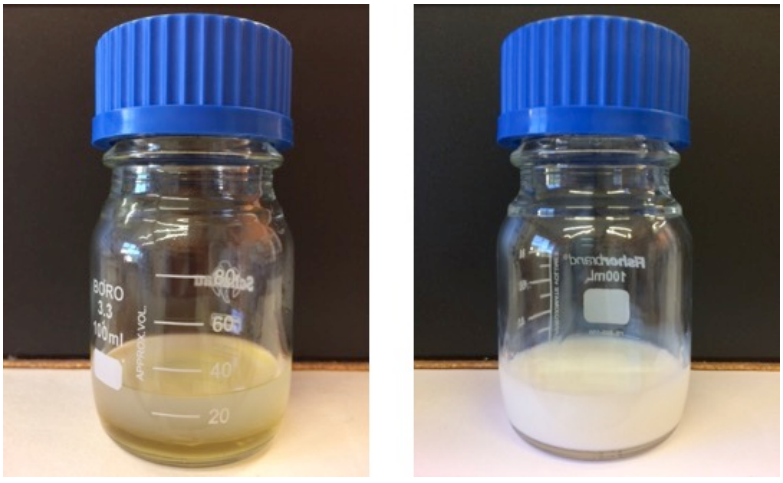

Figure 34. Photographs of the dispersion obtained from WNIPU3 after acetone removal (left) and WNIPU4 one year after acetone removal (right).

3.2.2.2. Influence of the degree of neutralization

The effect of the extent of neutralization on the particle size and dispersion stability was investigated through different experiments employing the base formulation of WNIPU4 with 60 wt. % initial solid content, and by varying the amount of acetic acid added into the polymer/acetone solution before addition of water.

As can be seen in **Table 5**, for the dispersion made with 25 and 50 % of neutralization, the particle sizes were found to be around 500 and 300 nm, respectively, with a broad dispersity. This can be explained by the lack of ionic groups to stabilize the particles at this extent of neutralization.

Table 5. Effect of the degree of neutralization on the particle size.

Degree of neutralization (%)[a]	$D_{pwater/acetone}$ (nm)[b]	PDI[b]	D_{pwater} (nm)[c]	PDI[c]
25	433 (± 2)	0.77 (± 0.003)	490 (± 17.5)	0.94 (± 0.07)
50	275 (± 23)	0.29 (± 0.2)	266 (± 22.0)	0.28 (± 0.03)
75	216 (± 1)	0.13 (± 0.07)	212 (± 0.9)	0.097 (± 0.002)
100	273 (± 7)	0.26 (± 0.04)	249 (± 0.7)	0.28 (± 0.04)
125	196 (± 23)	0.15 (± 0.008)	189 (± 15.8)	0.16 (± 0.02)

[a]Based on the concentration of internal surfactant in the polymer (0.22 $mmol/g_{polmymer}$). [b]Particle sizes and particle size distributions were calculated using DLS in water/acetone mixture over 3 experiments. [c]Particle sizes and particle size distributions were calculated using DLS after acetone removal over 3 experiments. Dispersion experiments were carried out at room temperature from WNIPU4 with 50 wt. % initial solid content.

As the amount of acetic acid was increased, the particles size decreased to 212 nm (75 % neutralization) were of low dispersity, thanks to the increase in concentration of $–R_3NH^+\text{-}COO^-(CH_3)$ hydrophilic groups. Full neutralization of the tertiary amino groups led to slightly bigger particles of higher dispersity. Finally, excess acetic acid yielded lower particle sizes. However, the dispersion made from

75 % neutralization was found to be the more reproducible, hence this degree of neutralization of 75 % was selected for the rest of the study.

3.2.2.3. Influence of the initial solid content

The initial PU content is another important parameter that can significantly affect the phase-inversion process, and thus the final particle size.[61,64] This parameter was studied here, *i.e.* by varying the initial NIPU contents (40, 50 and 60 wt. %) using the optimal dispersion (WNIPU4 at 75 % neutralization). As indicated in **Table 6** lower initial solid content in the dispersion led to slightly larger particle sizes with broader dispersity, before acetone removal. However, once the acetone was removed and on the range of initial solid content studied, no significant differences on the particle size was noted; though, dispersion produced with an initial solid content of 60 wt. % was the more reproducible, as characterized by a low standard deviation. The average particle size was essentially constant at 200 nm. This might be explained considering that, in the acetone process, the polymer particles were formed at the early stage in the phase inversion process, as addition of water could promote restructuration of the polymer-water interface. At this point the number of particles was likely fixed, and further addition of water had just a dilution effect.

Table 6. Effect of the initial solid content on the particle size.

Initial solid content (wt. %)[a]	$D_{pwater/acetone}$ (nm)[b]	PDI[b]	D_{pwater} (nm)[c]	PDI[c]
40	267 (± 31)	0.27 (± 0.2)	201 (± 25)	0.31 (± 0.2)
50	189 (± 16)	0.15 (± 0.02)	196 (± 23)	0.16 (± 0.01)
60	193 (± 5)	0.27 (± 0.06)	210 (± 4)	0.14 (± 0.02)

[a]Based on the total mass of polymer and acetone. [b]Particle sizes and particle size distributions were calculated using DLS in water/acetone mixture over 3 experiments. [c]Particle sizes and particle size distributions were calculated using DLS after acetone removal over 3 experiments. Dispersion experiments were carried out at room temperature from WNIPU4 and a degree of neutralization of 75 %.

In summary, first examples of waterborne poly(hydroxyurethane)-based dispersions using the acetone process have been described in this section. The presence of the tertiary amino groups emanating from the 8-membered cyclic bis-carbonate, enable to further manipulate these NIPU dispersions by imparting them hydrophilic properties *via* protonation using acetic acid, thus enhancing the polymer particle stabilization in water. The optimal dispersion was based on the WNIPU4 poly(hydroxyurethane) containing 0.22 mmol/$g_{polymer}$ of internal surfactant, with a degree of neutralization of 75 % and an initial solid content of 60 wt. %. NIPU nanoparticles with average size around 200 nm could thus be obtained. Unfortunately, films generated after casting such dispersions were not self-standing, likely owing due to the low T_g of PDMS. As a matter of fact, films thus prepared flowed, as evidenced by rheological measurements giving G" ≫ G' at a temperature as low as -10 °C in **Figure 35**.

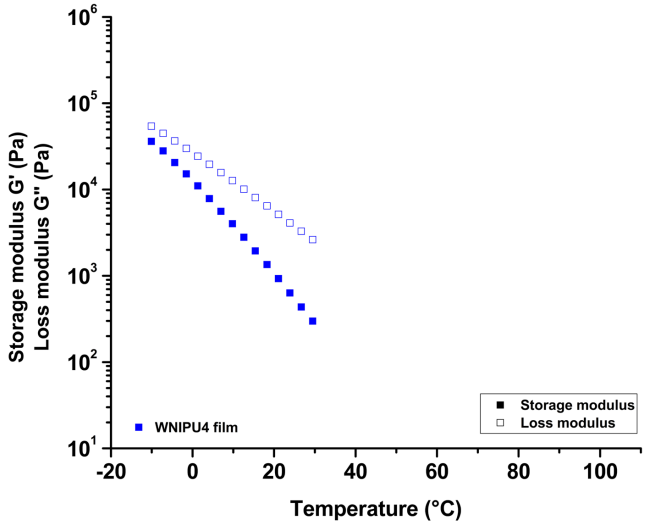

Figure 35. Evolution of the storage and loss modulus (G' and G") as a function of temperature for the film prepared from WNIPU4 dispersion.

3.2.3. Preparation of supramolecular NIPUs

As recently shown by Cádiz *et al.*, supramolecular polymers can be easily prepared by blending PU bearing tertiary amino groups with multifunctional carboxylic acids.[137,138] The resulting ionic interactions have been shown to enhance the overall mechanical properties of the final materials. Similarly, we investigated the possibility for crosslinking our NIPU dispersions in presence of citric acid (f = 3) as non-covalent crosslinker. By doing so, it was expected that supramolecular networks could be obtained through ionic interactions (**Scheme 18**). This synthetic method has the advantage of not requiring tedious synthetic steps, as a commercial multifunctional carboxylic acid is just added to the mother dispersion.

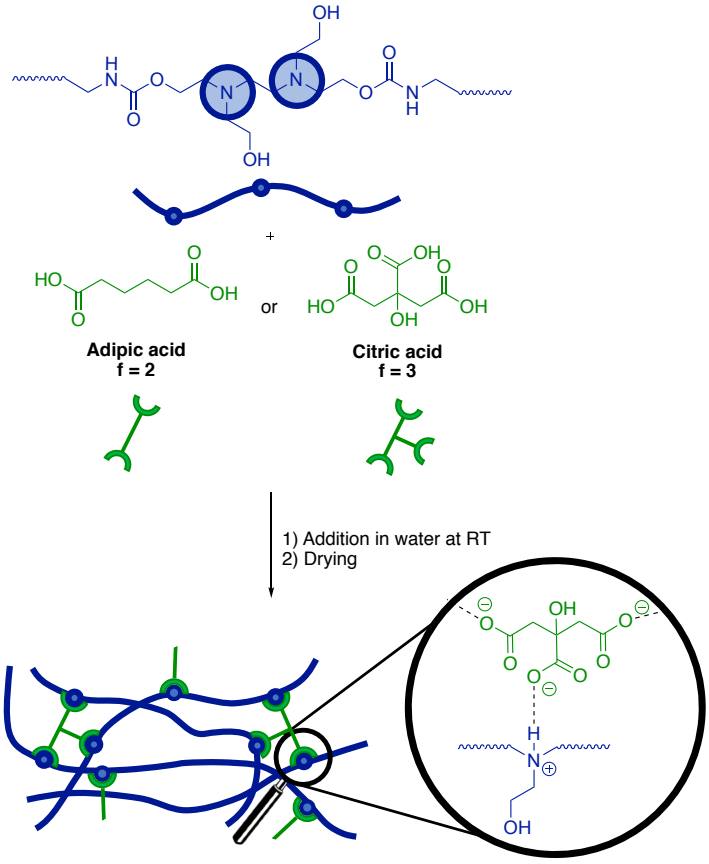

Scheme 18. Synthetic strategy to supramolecular ionic networks based on WNIPU4 and carboxylic acids.

Equimolar amounts of carboxylic acid relative to amino groups were first added to 4 mL of a PU dispersion at room temperature, before casting onto a silicon mold. After drying, the as-obtained film proved transparent, suggesting that carboxylic acid moieties were incorporated homogeneously. Immersion in water turned the films opaque (**Figure 36**).[138]

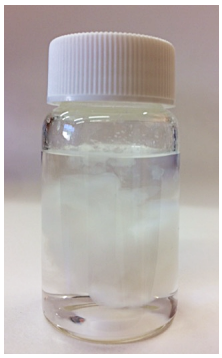

Figure 36. Photograph of the film obtained incorporating 100 mol. % of citric acid into the WNIPU4 dispersion after immersion in water.

The network structure was first analyzed by FTIR spectroscopy (**Figure 37**). As reported by Aboudzadeh *et al.,* the presence of bands associated to carboxylate anions are generally observed in the range of 1620-1550 cm^{-1}.[129,142] In our case, a broad band appeared at 1574 cm^{-1}, which corresponded to the asymmetric COO^- carboxylate groups overlapping with the N–H bending vibration, previously reported at 1532 cm^{-1}. Moreover, formation of a broad OH stretching vibration band at around 3400 cm^{-1} was observed, which distinguished from the band of free acids which possess well-defined bands at 3494, 3447 and 3289 cm^{-1}, due to the hydroxyl, carboxylic and terminal hydrogen-bonded carboxylic moieties, of free acids, respectively.[129] A complex broad band also appeared at 2800-2500 cm^{-1}, which was assigned to the absorption band of the quaternary ammonium groups. These results supported the successful protonation of the tertiary amino groups by the carboxylic acid groups of citric acid.

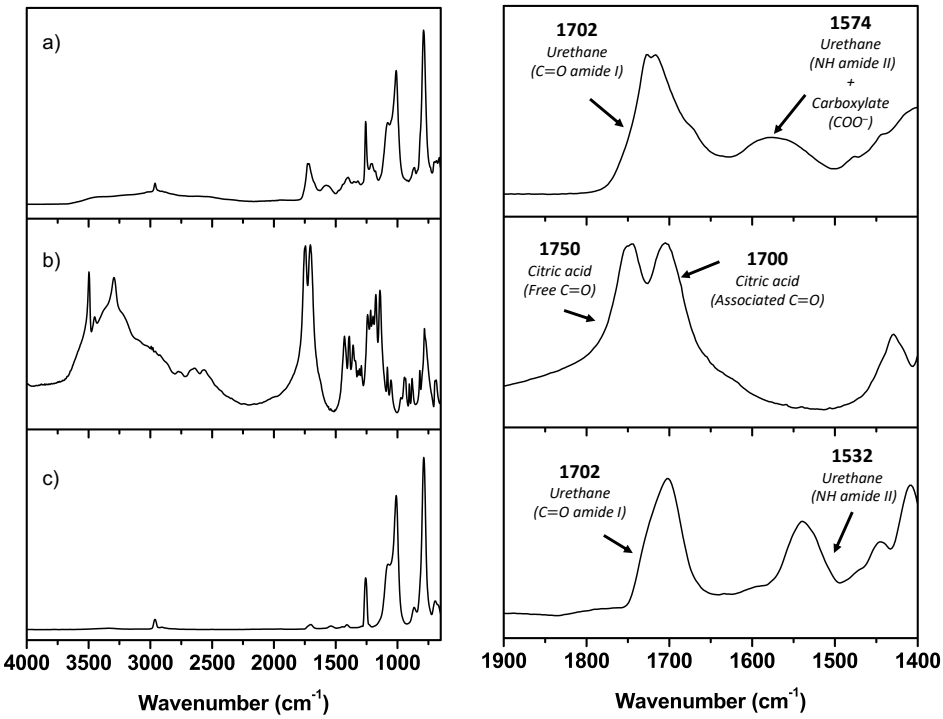

Figure 37. FTIR spectra of: a) WNIPU4/citric acid film; b) citric acid; c) WNIPU4.

The films were further characterized by ^{1}H NMR in d_6-acetone rather than $CDCl_3$ due to insolubility of carboxylic acids in the latter solvent. As can be seen in **Figure 38**, samples containing citric acid revealed characteristic signals due to the methylene protons (CH_2–NCH_2), initially present in the polymer at 2.64 and 2.75 ppm shifted to 3.30 and 3.81 ppm, as a result of the protonation of amino groups. Furthermore, the resonance at 2.91 ppm assigned to the methylene protons next to the carboxylic acid groups in citric acid (CH_2–COOH), appeared in the film at 2.84 ppm. Similar observations associated to ionic interactions have already been reported.[137,138] Moreover, the signal due to the urethane moiety (CH_2–OCONH) shifted from 4.10 to 4.32 ppm, while NH proton at 6.27 ppm completely vanished in the film. These data suggested that carboxylic acid groups of citric acid also developed ionic interactions with the urethane N-H moieties.

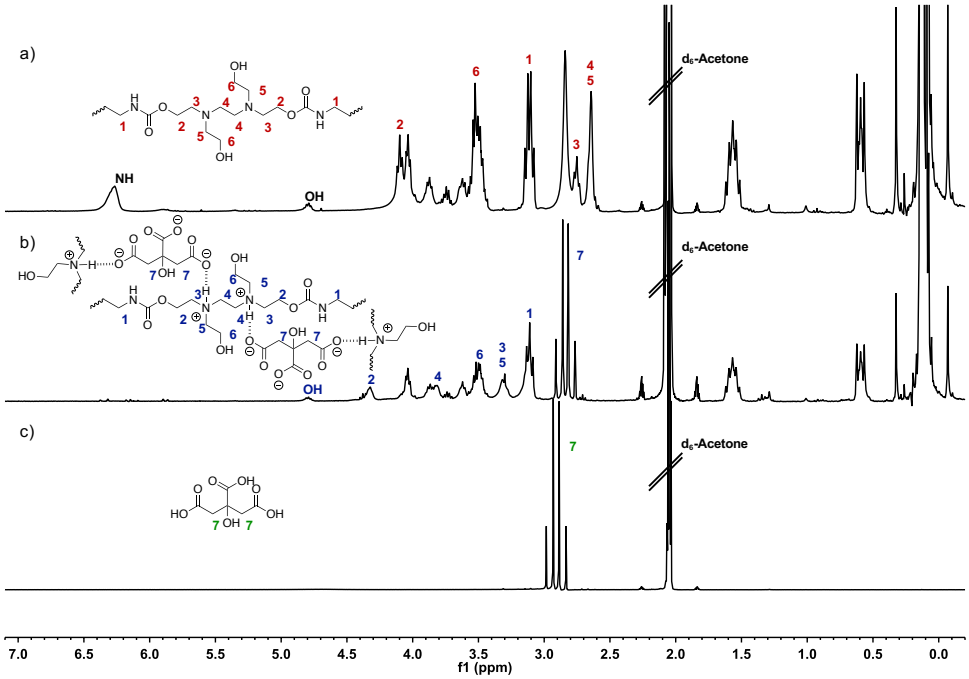

Figure 38. ^{1}H NMR (300 MHz, d_6-acetone) of: a) WNIPU4; b) WNIPU4/citric acid film; c) citric acid showing the proton shift associated with the formation of ionic bonds.

As with other materials consisting of supramolecular (ionic) interactions, properties of our crosslinked NIPU-based films were expected to be temperature dependent.[125,126,143] The rheological properties of these films were thus evaluated as a function of temperature and compared with films casted from a citric acid-free dispersion (control experiment). As shown in **Figure 39,** the presence of citric acid dramatically changed the film properties, as evidenced by the elastomeric region (G' > G") at temperature below 65 °C, supporting the formation of a supramolecular network. Crossover of the loss and the elastic moduli was observed at 65 °C, though the supramolecular network was not totally disrupted as our material was still able to flow. Additionally, reverse temperature sweep displayed similar values for both moduli, demonstrating the reversible formation of ionic interactions (**Figure 40**). Films were also prepared using a difunctional acid, namely, adipic acid (f = 2) for comparison purpose (**Figure S39** and **Figure S40**). In the latter case, however,

no significant change of the liquid behavior was noted in the temperature range tested, as characterized by G" > G' (**Figure 39)**; moduli were slightly higher though, in comparison to the control experiment.

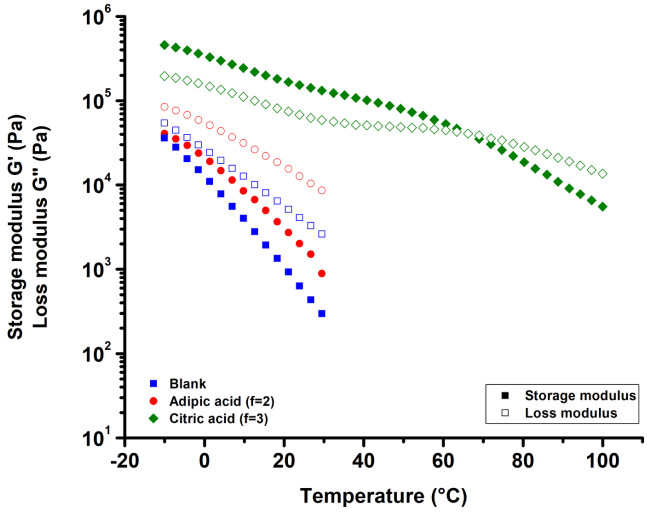

Figure 39. Evolution of the storage and loss modulus (G' and G") as a function of temperature for the films prepared from WNIPU4 and 100 mol. % of different functional carboxylic acids.

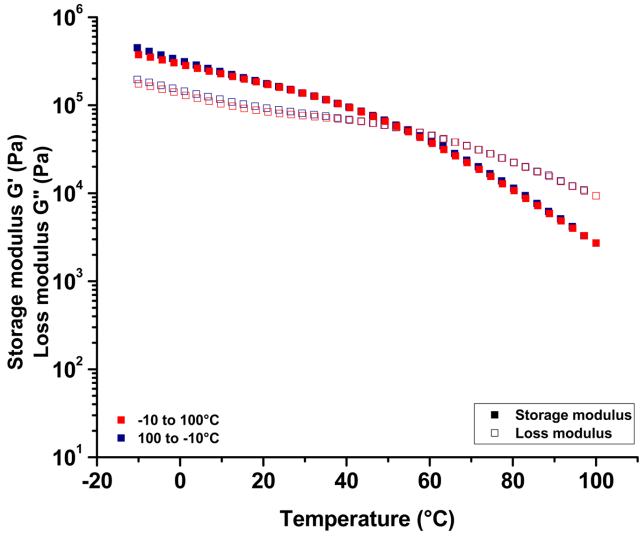

Figure 40. Evolution of the storage and the loss modulus (G' and G") in reverse temperature sweep between -10 and 100 °C of films prepared from WNIPU4 and citric acid.

These encouraging results prompted us to further investigate the effect of the concentration in citric acid on the rheological behavior of the films. Transparent to slightly white materials were thus obtained by increasing the content in citric acid. **Figure 41** shows the evolution of the storage modulus (G') and the loss modulus (G") with increasing temperature, at a constant frequency of 6.28 rad/s, of the different films. A network-liquid transition occurred from < -10 °C to 65 °C for 25 mol. and 100 mol. % of citric acid, respectively. Overall, both the storage and the loss moduli increased upon increasing the concentration in citric acid.

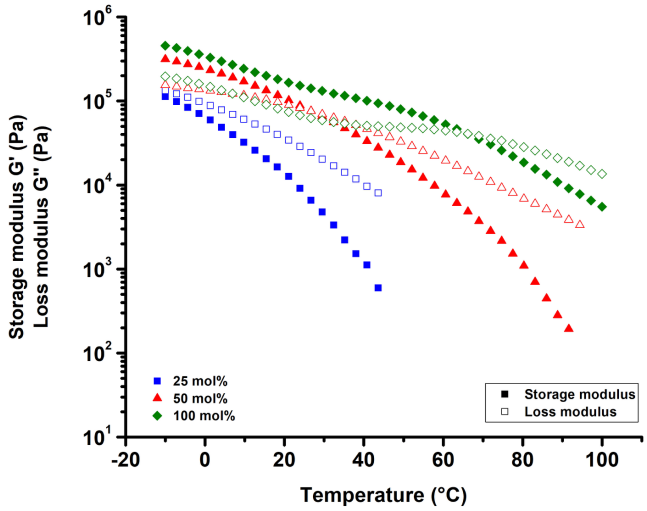

Figure 41. Evolution of the storage and loss modulus (G' and G") as a function of temperature for films prepared using different molar ratio of citric acid.

In summary, transparent WNIPU films can be obtained by incorporating carboxylic acids with different functionality, such as adipic acid or citric acid, into a mother dispersion. Formation of supramolecular networks based on ionic interactions can thus be achieved, in particular with citric acid, as evidenced by FTIR and NMR spectroscopies. Tuning the concentration in citric acid dramatically affects the mechanical properties of the resulting films, which is characterized by a solid/liquid transition from < -10 °C to > 60 °C. On this basis, we then thought that these intriguing materials could exhibit self-healing properties, which is examined in the next section.

3.2.4. Evaluation of the self-healing properties of WNIPUs

Many supramolecular polymers constituted of reversible bonds are well known to exhibit self-healing properties.[127] As films made from our WNIPU materials showed features of supramolecular networks, including well-defined temperature

transitions between the solid and the liquid state, the self-healing properties of these films were assessed. Frequency sweep experiments in linear viscoelastic conditions were thus conducted at different temperatures, from a film obtained with 100 mol. % of citric acid. The representation of G' and G" *vs.* frequency allowed us to elucidate the type of interactions taking place in these structures (**Figure 42**).[144]

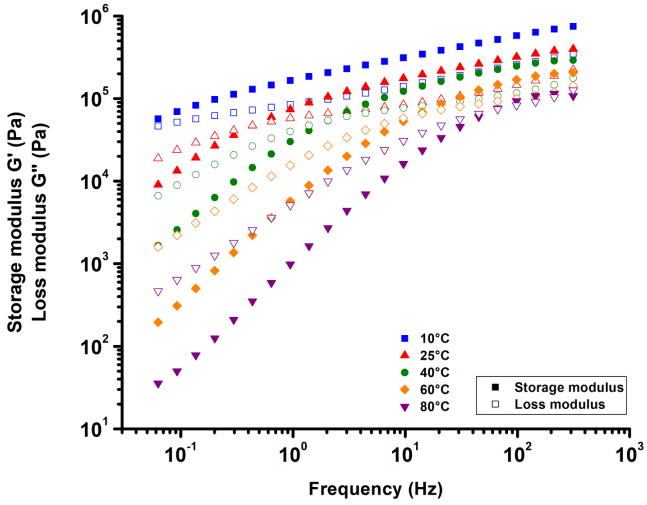

Figure 42. Storage and loss modulus (G' and G") as a function of frequency at different temperatures for supramolecular ionic film prepared from WNIPU4 and 100 mol. % of citric acid.

As can be seen, the rheological behavior of the film showed strong dependence on time. While the sample behaved as an elastic material at high frequencies (G' > G"), an inverted response was observed at low frequencies. Such a dynamic behavior is characteristic of a material constituted of temporary bonds.[145,146] Existence of supramolecular interactions was also supported by the terminal region of the curve, encompassing the lowest frequencies. While non-structured materials are generally characterized by -2 or -1 slopes for G' and G", respectively, a different behavior revealed was observed in our case, indicative of a structured polymer network preventing the film from flowing.[146] Increasing the

temperature resulted in a decrease of both storage and loss moduli, similarly to results obtained in temperature sweep experiments.

The ability of this material to fill cracks was then studied by optical microscopy (**Scheme 19** and **Figure 43**). Films were scratched with a disposable scalpel, and the filling process was monitored by optical microscopy at different temperatures (*i.e.* 10, 25, 40, 60 and 80 °C).

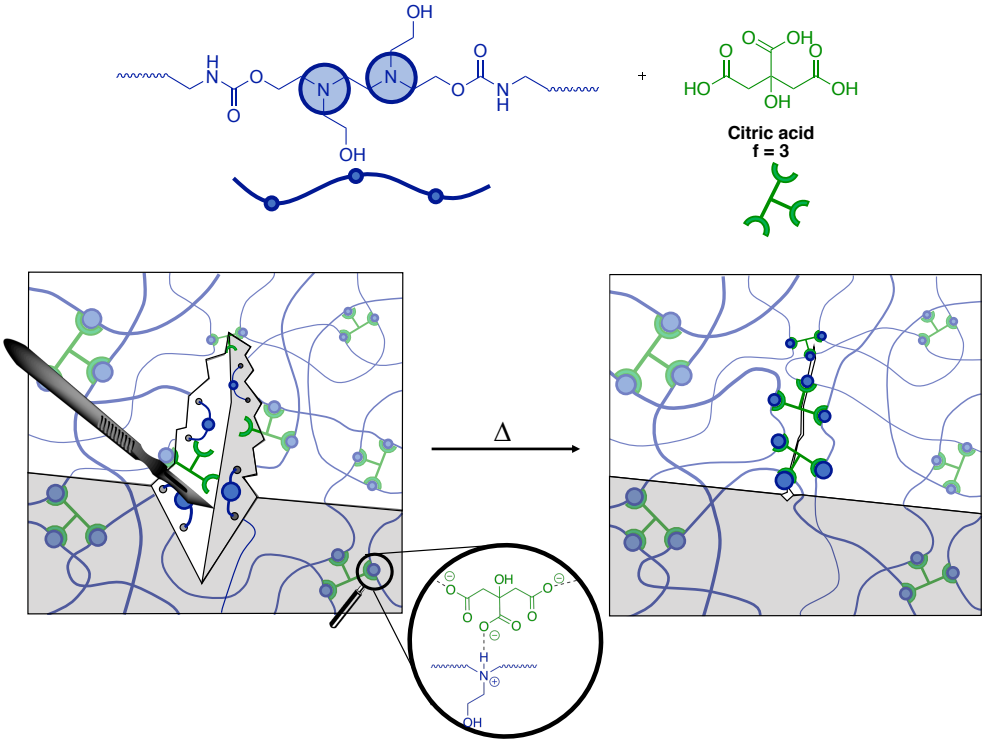

Scheme 19. Schematic representation of the healing mechanism of the WNIPU-based supramolecular network prepared using citric acid.

Very interestingly, damages could be mended at temperature as low as 10 °C, though the film could not recover entirely since the scratch was still perceptible after 72 h. As the temperature increased, the filling process proceeded faster and less than 6 min was needed for the film to recover at 60 °C. At 80 °C, *i.e.*

in the liquid state (**Figure 41**), the refilling process was even more efficient as it took place under 2 min. Although the scratch caused the rupture of ionic bonds, increasing the chain mobility in the impacted area, supramolecular interactions hindered the surface rearrangement. An increase of temperature, led to higher chain mobility thus promoting faster recovery.

Overall, their self-healing ability added to their mechanical properties, could make these films suitable for the preparation of flexible substrate; such as leather, in conventional waterborne polyurethane coating industries.

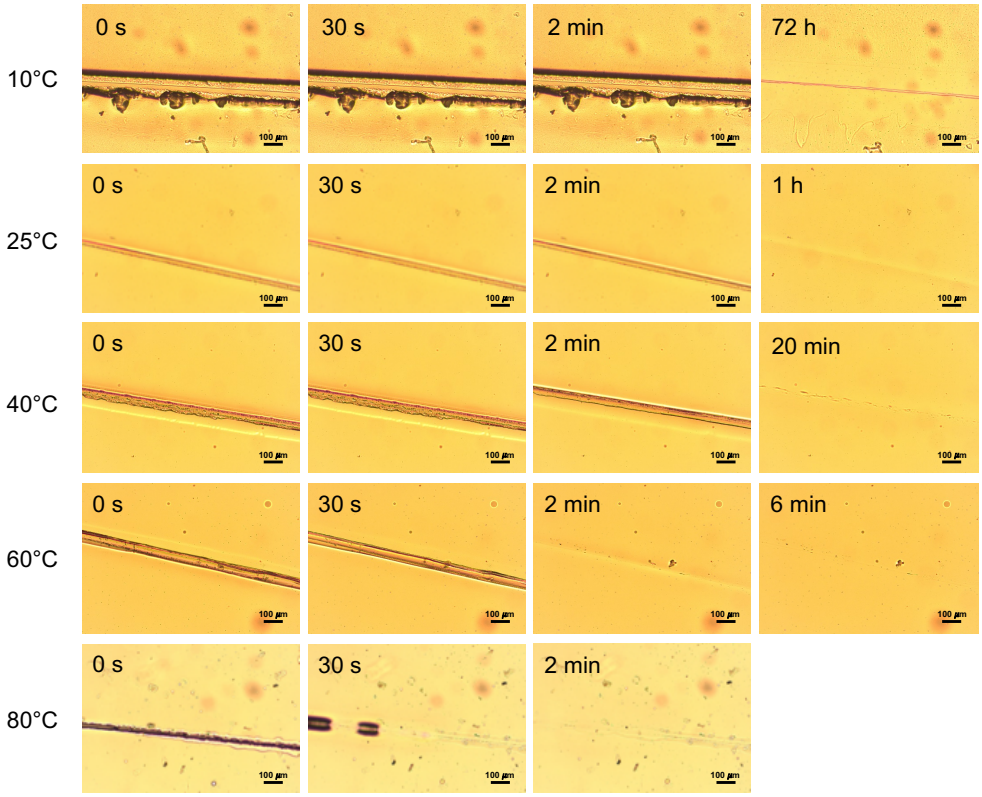

Figure 43. Evolution of the crack refilling process at different temperatures for supramolecular ionic film prepared from WNIPU4 and 100 mol. % of citric acid.

3.3. Conclusion

Altogether this study shows, for the first time, that waterborne non-isocyanate polyurethanes (WNIPUs) can be synthesized from 5- and 8-membered cyclic carbonates and amino PDMS telechelics. Stable WNIPU-based dispersions, with average particle size around 200 nm, could be obtained by means of the acetone process. A minimum of 0.22 mmol/$g_{polymer}$ is required to stabilize the WNIPU particles. Because of the low T_g of PDMS, films prepared from these dispersions showed poor mechanical strength. Yet, by taking advantage of ionic interactions generated after derivatization of tertiary amino groups using multifunctional carboxylic acids, supramolecular WNIPU-based films can be achieved. Specifically, in presence of citric acid, dynamic non-covalent 3D-structures can be manipulated thanks to the creation of ionic interactions between carboxylate and ammonium moieties. Formation of an elastic network can be evidenced by rheological measurements of the films at low temperatures/high frequencies, while at higher temperatures/lower frequencies, the network is disrupted. Importantly, this process of supramolecular assembling/disassembling is dynamic and reversible, which enables to impart films with self-healing properties. Overall, this versatile and straightforward strategy opens avenues for novel families of functional and self-healable supramolecular ionic WNIPUs, which could find applications in the coating industry.

3.4. Experimental part

Instrumentation

Nuclear Magnetic Resonance (NMR). ^{1}H and ^{13}C spectra were recorded with Bruker Avance DPX 300 or Bruker Avance 400 spectrometers. The NMR chemical shifts were reported as δ in parts per million (ppm) relative to the traces of non-deuterated solvent (*e.g.* δ = 2.50 ppm for DMSO-d_6 or δ = 7.26 ppm for $CDCl_3$). Data

were reported as: chemical shift, multiplicity (s = singlet, d = doublet, t = triplet, m = multiplet, br = broad), and integration.

Size Exclusion Chromatography (SEC). SEC was performed using a set of PSS GRAM columns with pore sizes of 10 µm (guard column) and 30 and 1000 Å calibrated with narrow polystyrene standards from Polymer Laboratories, using both refractometric and UV detectors (Varian). DMF was used as eluent (0.8 $mL.min^{-1}$) and toluene as a flow marker (300 µL toluene/100 mL DMF) at 50 °C, in the presence of LiBr (2.17 $g.L^{-1}$).

Fourier Transform Infrared Spectroscopy. FT-IR spectra were obtained by FT-IR spectrophotometer (Nicolet 6700 FT-IR, Thermo Scientific Inc., USA) using attenuated total reflectance (ATR) technique (Golden Gate, spectra Tech). Spectra were recorded between 4000-525 cm^{-1} with a spectrum resolution of 4 cm^{-1}. All spectra were averaged over 10 scans.

Thermogravimetric analysis. A thermogravimetric analyzer (TGA-Q500 V20, TA Instrument Inc., USA) was used to investigate the thermal stability of the samples. A total of 5-10 mg of samples was heated from 30 °C to 950 °C at a heating rate of 10 °C/min under N2 atmosphere (50 mL/min).

Differential Scanning Calorimetry. A differential scanning calorimeter (DSC-Q100, TA Instrument Inc., USA) was used to analyze the thermal behavior of the samples A total of 6-8 mg of samples were first scanned from -160 °C to 100 °C at a heating rate of 10 $°C.min^{-1}$ to eliminate interferences due to moisture. The samples were then cooled to -160 °C to remove the thermal history of the samples and reheated to 100 °C at 10 $°C.min^{-1}$. The glass transition and melting temperatures were calculated from the second heating run.

Dynamic Light Scattering. The particle size (Dp) and particle size distribution (PDI) of the PHU dispersions were measured by Dynamic Light Scattering (DLS) using a Zetasizer-Nano S from Malvern operating with a 4 mW He–Ne laser (633 nm wavelength) and a fixed detector angle of 173 (non-invasive backscattering geometry NIBSTM) and with the cell holder maintained at constant temperature by

means of a Peltier element. The samples were diluted with deionized water before the measurements to avoid multiple light scattering. The final value was an average of three measurements.

Transmission Electron Microscopy (TEM). TEM was performed using a Philips Tecnai 20 microscope working at accelerating voltage of 200 kV. Diluted samples of the dispersions (0.005-0.01 wt. %) were prepared.

Rheometry measurements. Small-amplitude oscillatory experiments were performed in a stress-controlled Anton Paar Physica MCR101 rheometer and the experiments were carried out using 25 mm parallel plate geometry. All the experiments were conducted in linear viscoelastic conditions for the studied temperature range (strain = 0.5 % and frequency 1 Hz).

Optical microscopy. Scratch-healing measurements were carried out at different temperatures using an optical microscope. The scratches were created using a feather disposable scalpel no. 21 (stainless steel). The microscopy glass slides were positioned in a microscope hot stage (Linkam Scientific Instruments, Ltd.). The system was then placed under the focus of a bright-field optical microscope (Zeiss Axio Scope A1 with 10X objective and tungsten-halogen bulb).

Materials

Diglycerol dicarbonate (DGC) and bis-N-8-C were synthesized according to literature procedures.[31,147] Acetic acid (≥ 99 %), citric acid (≥ 99.5 %), butyric acid (≥ 99 %), adipic acid (99 %) and poly(dimethylsiloxane), bis(3-aminopropyl) terminated (aminoalkyl-terminated PDMS) with a molecular weight around 2,500 Da were purchased from Sigma Aldrich. Acetone (technical grade) was purchased from Fisher. were purchased from Acros Organics. Deuterated solvents such as $CDCl_3$, DMSO-d_6 and $(CD_3)_2CO$ were purchased from Euro-top. All materials were used without further purification.

General procedure for the synthesis of poly(hydroxyurethane)s. In a typical procedure, diglycerol dicarbonate ((1-x) equiv.), bis-N-8-C (x equiv.) ($0 \leq x \leq 0.5$) and aminoalkyl-terminated PDMS (1 equiv., 0.015 mol, 37.5 g) were mixed together in a 250-mL flask equipped with a mechanical stirrer (200 rpm). The polymerization reaction was conducted at 80 °C for 48 h.

General procedure for the dispersion process. The dispersion process was carried out using several different experimental conditions (**Table 4**). In a typical procedure, the PHU was first fed into a 250-mL jacketed glass reactor equipped with a mechanical stirrer. The PHU was dissolved in acetone (to the desired solid content value), followed by the addition of a known amount of acetic acid. The mechanical stirrer was set at 400 rpm. The phase inversion was performed at 250 rpm at 25 °C, by adding 15 g of water at 1 mL.min^{-1} to 10 g of a NIPU solution in acetone. The particle size was measured by DLS before and after removal of acetone at 25 °C under vacuum. Samples were diluted with deionized water prior to the measurement to avoid multiple light scattering. The final value was an average of 3 measurements. Once the dispersion was achieved, acetone was removed by means of rotary evaporation at 25 °C.

General procedure for the film preparation. The films were prepared using the dispersion made with the poly(hydroxyurethane) composed of 70 mol. % of DGC and 30 mol. % of bis-N-8-C. First, a known amount of carboxylic acid was added to 4 mL of dispersion. The solution was stirred for 40 min until complete dissolution of the acid and then transferred into a Teflon mold. The films were dried for 2 days at room temperature and 48 h at 30 °C under vacuum.

Chapter 4

Non-Isocyanate Polyurethane Nanoparticles Obtained by Surfactant-Assisted Interfacial Polymerization

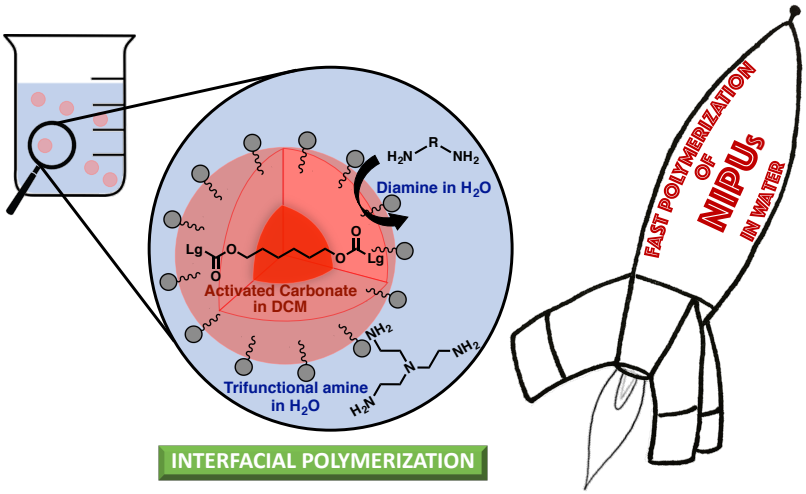

Bossion A., Jones G.O., Taton D., Mecerreyes D., Hedrick J.L., Ong Z.Y., Yang Y.Y., Sardon H. *Langmuir*, **2017**, 33, 1959–1968.

CHAPTER 4. NON-ISOCYANATE POLYURETHANE NANOPARTICLES OBTAINED BY SURFACTANT-ASSISTED INTERFACIAL POLYMERIZATION

4.1. Introduction

In the previous chapter, the “acetone process” has been established to be effectively translated to the synthesis of waterborne NIPU-based stable dispersions. Use of bis-N-8-C, that is, a *N*-substituted bis-cyclic carbonate acting as an “internal emulsifier” has proven crucial for this purpose. Though versatile, this method relies on a multi-step procedure involving 1) the pre-synthesis of the polymer in bulk at high temperature for rather long reaction time and 2) subsequent dispersion in water. Moreover, the stability of the dispersion is affected by various parameters, such as the amount of internal surfactant, the degree of neutralization or the initial solid content. Consequently, the achievement of particles of well-defined morphology, size and distribution remains challenging. The control of latter physicochemical parameters is yet crucial as far as specific applications are concerned, for instance, in the biomedical field for the manufacture of drug delivery nanocarriers.[148]

Alternative techniques/processes have been implemented to access well-defined PU nanoparticles, including mini-emulsion or interfacial polymerization.[70–73] Typically, direct mini-emulsion consists in the preparation of thermodynamically stable monomer droplets (50-500 nm) *via* highly energetic shearing of a system containing water as the continuous phase, hydrophobic monomers, surfactant and a hydrophobic agent aimed at preventing coalescence of the droplets dispersed in water. In a second step, temperature is applied to the system to start the

polymerization. Polymerization of stable monomeric droplets leads to polymer particles of well-defined particle size and morphologies. One challenge of this strategy, however, when designing PU nanoparticles, is to keep the reagents hydrophobic enough to avoid their migration to the aqueous phase.

Previous works by Landfester *et al.* have demonstrated the potential of mini-emulsion polymerization as a specific process in preparing well-defined PU nanoparticles.[71,149] More recently, Cramail *et al*. have reported the synthesis of waterborne NIPUs-based latexes through mini-emulsion process, with up to 30 wt. % solid content.[75] In both cases, however, side reactions have been observed. The large amount of water surrounding the monomers droplets can indeed cause the formation of ureas *via* reaction of water with isocyanate groups. This side reaction changes the initial stoichiometry between isocyanate and hydroxyl groups, limiting the conversion and consequently, molecular weights as well. When applied to NIPU synthesis, hydrolysis of cyclic carbonates also occurs in mini-emulsion process, which leads to lower molecular weights in comparison to NIPU obtained in bulk polymerization.

Interfacial polymerization represents an alternative process for the preparation of step-growth polymers. This peculiar process has been industrially applied for the first time in the 1930s, namely, for the preparation of polyamides (Nylon®) from diacids and diamines. In its general sense, interfacial polymerization can be performed *via* either radical, or ionic or condensation polymerization mechanism occurring at the interface between two immiscible liquid phases. In the specific context of step-growth polymerization, each co-monomer of antagonist functionality is located in one of the two immiscible phases and diffuses at the interface, where repeated elementary reaction takes place; therefore this *de facto* guarantees perfect stoichiometry and achievement of high yields and molecular weights.[150–152]

The field has been reviewed by Landfester *et al.* who have emphasized that interfacial polymerization holds great promise and should expand in the near future.[150] Overall, it shows several advantages over mini-emulsion polymerization,

including very high reaction rates, mild conditions, and production of polymers of high molecular weight (**Figure 44**).[149,153,154]

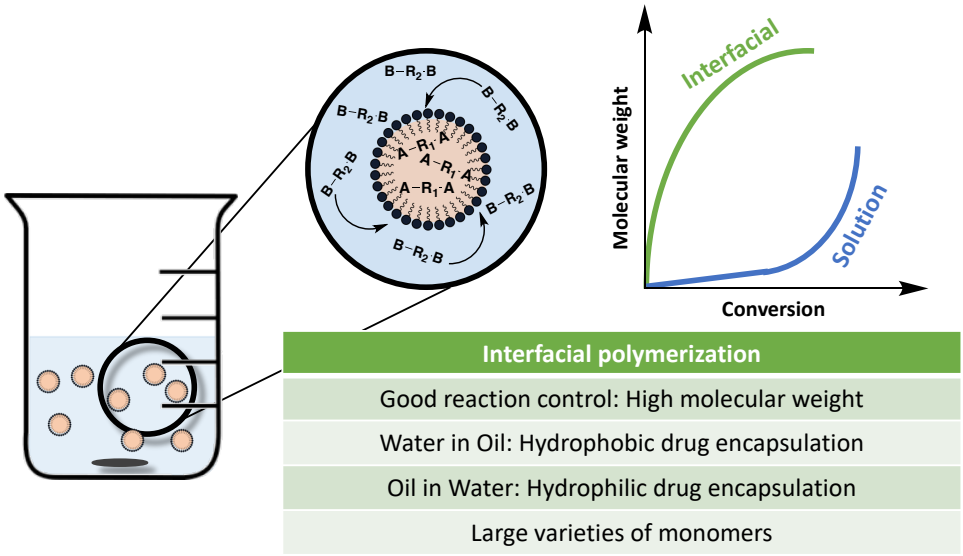

Figure 44. Main features of interfacial polymerization.

Moreover, the interface between hydrophilic and hydrophobic phases can be used to protect sensitive monomers, for instance isocyanates that are susceptible to hydrolysis.

Interfacial polymerization involves a pre-reaction mixture using high shear forces (*i.e.* sonication, microfluidic, etc.) and is composed of an organic phase containing a hydrophobic monomer, and the aqueous phase containing a surfactant. This leads to the formation of an oil-in-water (o/w) emulsion. Water-in-oil (w/o) emulsion can also be achieved by pre-mixing a hydrophilic monomer/surfactant aqueous solution with an organic continuous phase. Then, a second monomer-containing solution (either aqueous or organic depending on the type of emulsion) is added to the pre-emulsion mixture. As mentioned, polymerization occurs at the interface by diffusion of the monomers at the oil-water interface, when two droplets come in contact with each other (**Figure 45**).[150,151]

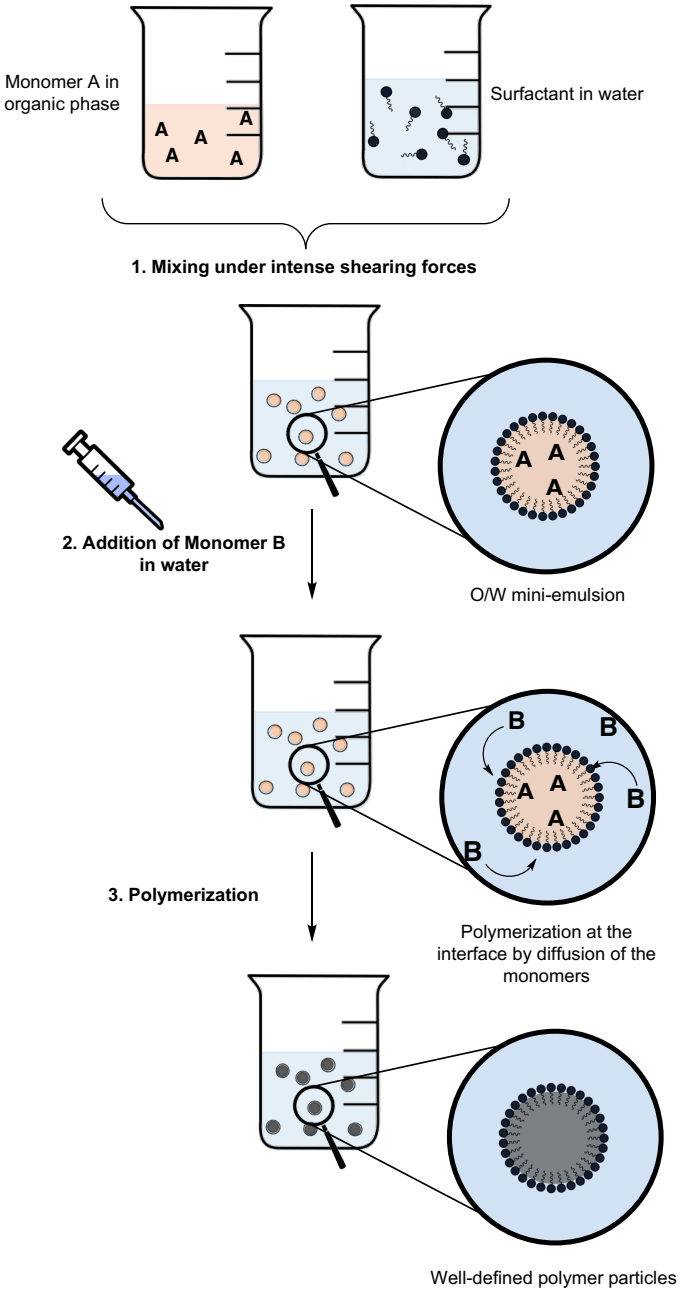

Figure 45. Principle of polymerization *via* interfacial polymerization.

Our motivation in this context was to resort to this interfacial process for the synthesis of waterborne NIPUs (WNIPUs). To the best of our knowledge, this has not been reported before. In order to avoid any side reactions and use of poorly reactive 5-membered cyclic carbonates, we turned in this chapter to activated dicarbonates and diamines of linear structure. Linear dicarbonates have indeed been reported to undergo polycondensation with diamines, resulting in the formation of PUs. In 1967, Morgan *et al.* reported for the first time the preparation of NIPU by the polycondensation of alkylene bis-chloroformates with diamines in chloroform at 60 °C in the presence of TEA (**Scheme 20**).[155] Under these conditions, high conversion and high molecular weight polymers were obtained within 10-30 min.

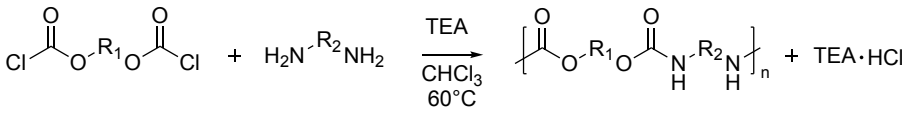

Scheme 20. Synthesis of NIPUs by the polycondensation of alkylene bis-chloroformates with diamines.

In 2013, Sardon *et al*. have reported the synthesis of PEG-based NIPUs in water, using polycondensation of a highly reactive linear pentafluorophenyl dicarbonate with *Jeffamine*.[46] A key feature for the success of this process lies in the high reactivity of the peculiar carbonate employed, which favors fast urethane formation rather than its decomposition in water.

In this chapter, we describe the one-pot synthesis of NIPUs based on surfactant-assisted interfacial polymerization (SAIP). For that purpose, we specifically designed three different linear activated dicarbonates containing pentafluorophenol, nitrophenol and phenol as leaving groups. Their reactivity towards bis-amino-(polyethylene glycol) (PEG-diamine) was compared to evaluate the influence of the leaving group on the reaction kinetics. Different conditions, *i.e.* o/w and w/o, were explored and a comprehensive computational study was performed to rationalize the effect of the solvation conditions on the reactivity of the

activated bicarbonates, and the role of water in lowering the activation energies of these reactions. Optimization of the reaction conditions, through variation of both the type and the concentration of the surfactant allowed us to achieve carious isocyanate-free PU nanoparticles. Finally, a straightforward method for incorporating carboxylic acid functionalities into these soft NIPU nanoparticles was developed, as a means to further encapsulate cargos *via* ionic interactions.

4.2. Results and discussion

4.2.1. Comparative study of the reactivity of different acyclic activated dicarbonates reactivity towards PEG diamine

As highlighted in **Chapter 1**, activated acyclic carbonates are suitable candidates for the preparation of NIPUs, especially for syntheses in waterborne conditions. They remain stable for up to 24 h in aqueous media and exhibits a high reactivity towards primary amines.[46] Thus, these monomers are able to form high molecular weight NIPUs in the presence of water, without limited – if any – side reactions.

In order to evaluate the most suitable activated dicarbonate for interfacial polymerization, aminolysis of PEG diamine was carried out at room temperature, using three different acyclic dicarbonate precursors, including 1,6-bis[(perfluorophenoxy)carbonyloxy] hexane (pentafluorophenolate) (monomer A), 1,6-bis[(4-nitrophenoxy)carbonyloxy] hexane (nitrophenolate) (monomer B), and 1,6-bis(phenoxycarbonyloxy) hexane (phenolate) (monomer C), (**Scheme S1** to **Scheme S3, Figure S41** to **Figure S43** and **Figure S47** to **Figure S49** in the appendix section), (**Figure 46.a & b**).

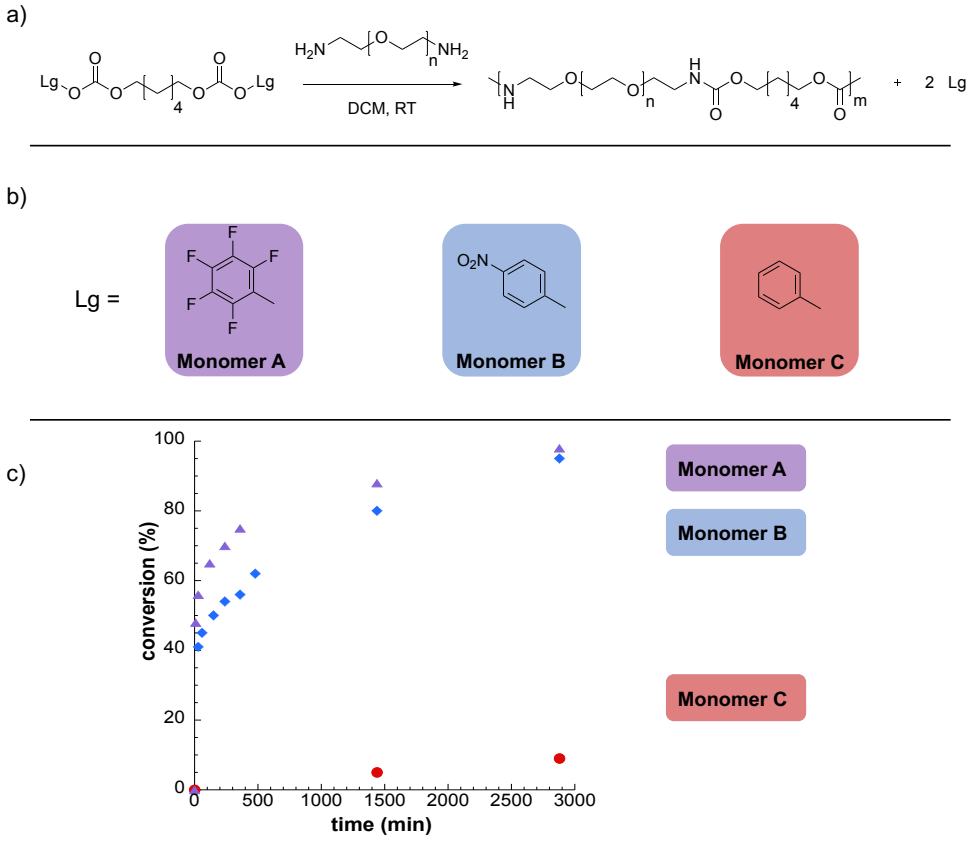

Figure 46. a) Condensation reaction between acyclic activated dicarbonates and PEG-diamine; b) leaving groups investigated for the synthesis of urethanes from activated dicarbonates; c) kinetics plot from the reaction between acyclic activated dicarbonates and PEG-diamine calculated as calculated by FTIR.

Reaction kinetics involving dicarbonates with PEG diamine in a 1:1 molar ratio in dichloromethane (DCM; 0.1 M) at 25 °C were monitored by FTIR (**Figure S50** to **Figure S52** in the appendix section). Conversion was determined using a similar method as detailed in **Chapter 2**, *i.e.* by following the decrease of the relative area integration value of the carbonate carbonyl characteristic band at 1760 cm^{-1}. Urethane formation was confirmed both through disappearance of the carbonate carbonyl characteristic band at 1760 cm^{-1} and the appearance of the

urethane stretching band (amide I) at 1720 cm^{-1}. Plotting the evolution of monomer conversion *vs.* time showed that dicarbonates featuring the pentafluorophenolate leaving group were more reactive than the other acyclic activated dicarbonates (**Figure 46.c**). This result is linked to the leaving group character during urethanization: the weaker the phenoxide conjugate base of the phenol is, the better the leaving group is and the faster is the reaction. This is confirmed by the pKa values of the respective phenols and phenoxide conjugate bases used in our study: the pKa value of ($PhOH/PHO^-$) is 9.95, while the pKa values of (NO_2PhOH/NO_2PhO^-) and (F_5PhOH/F_5PhO^-) are 7.15 and 5.5, respectively. Since pentafluorophenol is more acidic than the other leaving groups, its conjugated base will be weaker, hence pentafluorophenolate is the best leaving group in this series.

We next investigated the reactivity of monomer A in a heterogeneous process (**Figure 47**). Interfacial conditions were implemented by dissolving monomer A in DCM and PEG diamine in water. Water to DCM ratios were varied and conversion was monitored by FTIR (see **Figure S53** as example). Two observations could be made. Firstly, the reaction rate increased in all cases upon using interfacial conditions, a result in agreement with literature. Secondly, full and faster conversion could be reached upon using a water to DCM ratio of 80:20.

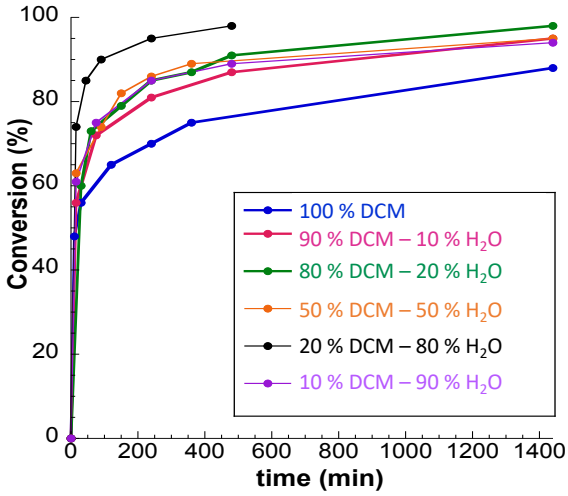

Figure 47. Kinetics plots from the condensation reaction between monomer A and PEG diamine using different DCM to H_2O ratios.

Two possible explanations could be put forward regarding the observation of higher reaction rate: a) the monomers are located in the organic phase and the local reagents concentration is higher and b) the possible coordination of water – acting as catalyst – with the carbonyl oxygen and the amine proton in the active transition state. The same reaction was then carried out, but by reducing the amount of DCM. When we compared the polymerization kinetics of 20 % DCM (0.4 mL) / 80 % H2O (1.6 mL) and the one with only DCM (0.4 mL), although there was a substantial increase on the reaction rate when performing the reaction at higher monomer concentration in solution, still the interfacial one was slightly faster (**Figure 48**).

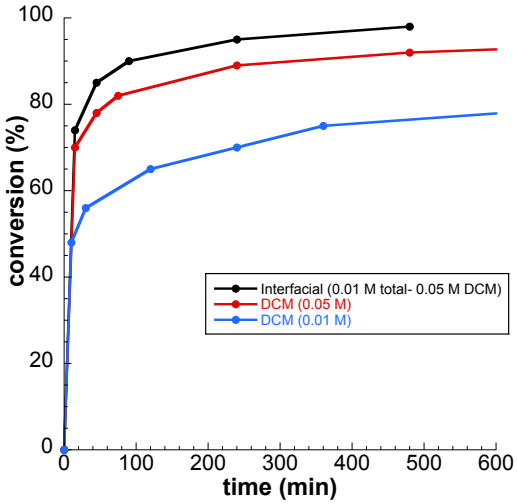

Figure 48. Kinetics plot from the interfacial polymerization of monomer A with PEG diamine at room temperature showing the effect of the concentration and the solvation condition (100 % DCM or deionized water/DCM mixture) on the conversion.

Therefore, a comprehensive computational study with GAMESS-US[156] using the dispersion-corrected[157] B3LYP[158–161] DFT method was conducted to provide insights into the experimentally observed reactivities during PU formation. Reaction profiles in four different types of solvation conditions were computed in order to explore how these reactions proceed under interfacial conditions. Thus, reaction mechanisms in implicit CH_2Cl_2 and implicit water using continuum dielectrics derived from the IEF-CPCM[162,163] method were explored as well as mechanisms involving the use of explicit water molecules bound to the carbonyl oxygen and the amine proton. The latter conditions are an attempt to account for the fact that water molecules can form hydrogen-bonds with the reactants at the interface of CH_2Cl_2 solvent molecules. Polymerizations were modeled from reactions involving methyl phenylcarbonate, methyl (4-nitrophenyl) carbonate, and methyl (perfluorophenyl) carbonate with methylamine, simple computational models of the carbonates and amine used in the experimental study.

Although different studies have suggested that an amphoteric tetrahedral intermediate or a six centered ring intermediate, considering a second amine molecule as proton shuttling, could be formed during the formation of urethanes from carbonates, a simple computational model is proposed in order to compare the reactivity of different carbonates (**Scheme 21**).[41,42] The first step involves formation of a reactant complex in which the amine is loosely bound to the carbonyl group. The zwitterionic INT1 is then formed by nucleophilic attack of the amino nitrogen on the carbonyl carbon in TS1. The next step of the reaction involves the transfer of the amine proton to the phenol oxygen concomitant with cleavage of the bond between the phenolic oxygen and the carbonyl carbon in TS2 which leads to formation of the product complex and finally to products.

Zabalov *et al*. have proposed the use of an additional molecule of amine in the transition state to facilitate proton transfer for condensation reactions involving cyclic carbonates and amines.[42] We believe that under the interfacial conditions used in the current study, where water serves as a medium, proton transfer by water molecules is more likely than the amine reactant/catalyst.[164] Thus, proton transfer was modeled by the use of two water molecules hydrogen-bonded to the carbonyl oxygen lone pairs of the carbonates and two water molecules hydrogen-bonded to the amine. These explicit water molecules facilitate proton transfer during nucleophilic attack in TS1 or product formation in TS2.

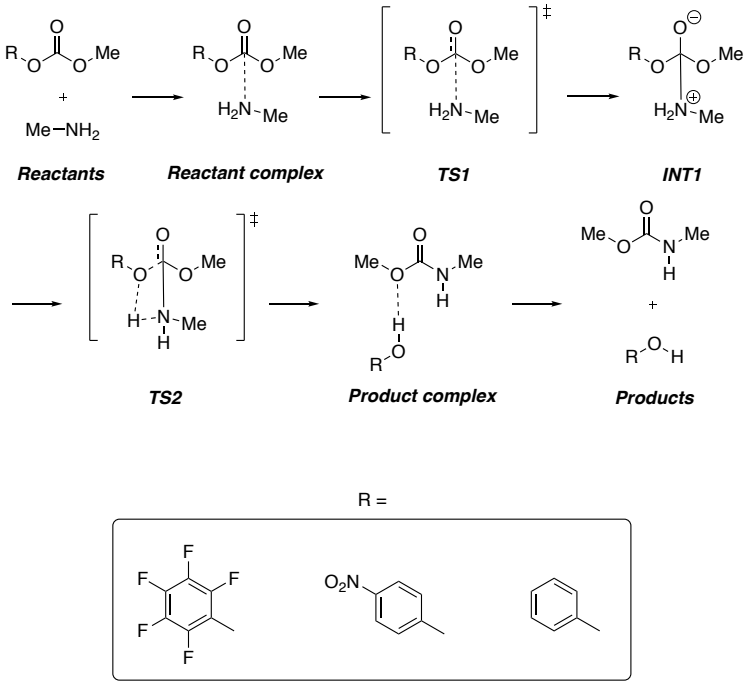

Scheme 21. Mechanisms for carbamate formation by reactions of various methyl (aryl) carbonates with methylamine. Water molecules have been omitted for clarity for mechanisms involving explicit water molecules participating as catalysts.

Free energies of activation for these rate-determining steps are shown in **Table 7**. These results show that alcohol loss is typically rate-determining in reactions involving phenyl carbonate. In addition, for reactions involving the activated carbonates, initial nucleophilic attack is only rate-determining when explicit water molecules are included, although perfluorophenoxide and para-nitrophenoxide are good leaving groups. Moreover, these results show that free energies of activation for rate-determining steps decrease in the order $H_5C_6O^-$ > $NO_2H_4C_6O^-$ > $F_5C_6O^-$ in all solvents.

Complexation of water molecules to carbonate and amine reactants lowers free energies of activation by 7-13 kcal/mol in comparison to reactions performed in implicit, purely organic or purely aqueous solvents. The effect is more dramatic in reactions involving phenyl carbonate for which free energies of activation are reduced by 12−13 kcal/mol by inclusion of explicit molecules of water. Free energies of activation are lowered to a smaller degree for reactions involving the 4-nitrophenylcarbonate and the perfluorophenyl carbonate when water molecules are explicitly included in the calculation.

Notably, the type of implicit solvent has only a small effect when explicit water molecules are included as catalysts in these reactions. Thus, free energies of activation only differ by at most 1 kcal/mol in implicit water or in implicit CH_2Cl_2 upon inclusion of explicit water molecules. In contrast, reactions performed in implicit CH_2Cl_2 alone possess free energies of activation that are 0.7 to 1.7 kcal/mol larger than reactions performed in implicit water without inclusion of explicit water molecules. Because of the small differences in the free energies of activation for reactions involving explicit water molecules, the calculations are inconclusive on whether reactions occur in a purely aqueous phase, or with water molecules on the interface between the two phases catalyzing reactions occurring in the organic phase. But they are consistent with experimental observations of a sharp increase in the reactivity when performing the reaction under interfacial conditions.

Overall, these calculations strongly suggest that no matter in which phase reactions occur, water molecules are always involved in the polymerization enhancing the polymerization rate. Moreover, it confirms that pentafluorophenol is the best leaving group in the reaction conditions used in this study, agreeing with the observations made experimentally.

Table 7. Free energies of activation (in kcal/mol), for the rate-determining step in reactions of methylamine with various types of methyl (aryl) carbonates in a variety of solvation conditions. Note: the identity of the rate-determining transition state is shown in parentheses.

Solvent	$-OC_6H_5$	$-OC_6H_4NO_2$	$-OC_6F_5$
CH_2Cl_2 (implicit)	22.6 (TS2)	16.1 (TS2)	13.6 (TS2)
H_2O (implicit)	21.9 (TS2)	14.9 (TS2)	12.5 (TS2)
H_2O (implicit/explicit)	10.0 (TS2)	8.6 (TS2)	5.6 (TS2)
CH_2Cl_2 (implicit)/H_2O (explicit)	10.2 (TS2)	9.6 (TS1)	5.0 (TS1)

In summary, the higher reactivity of the linear activated dicarbonate bearing pentafluorophenol as leaving groups was first demonstrated, in comparison with the other acyclic activated dicarbonates having nitrophenol and phenol. Clearly, polymerization performed fast under interfacial condition, with an optimal water to DCM ratio of 80:20. Moreover, computational studies are congruent with experimental findings. Nonetheless, a question has been raised: is it possible to obtain stable dispersions of NIPUs nanoparticles by interfacial polymerization?

4.2.2. Synthesis of non-isocyanate polyurethanes (NIPUs) soft nanoparticles by interfacial polymerization

After we have established that acyclic activated dicarbonates are excellent candidates for NIPU *via* interfacial polymerization, we next decided to examine the potential of monomer A for preparing NIPU-based soft nanoparticles under interfacial conditions, using the optimal water to DCM ratio elucidated earlier (**Figure 49.a**). Polymerizations were performed at room temperature using water and DCM in a volumetric ratio of 80:20, where monomer A was dissolved in DCM while PEG diamine was dissolved in aqueous media at 0.1 M. After dissolving both monomers in a pair of immiscible liquids. After they were mixed, a white solid

formed immediately. The pH was kept constant at 9 all along the polymerization thanks to the presence of TEA.

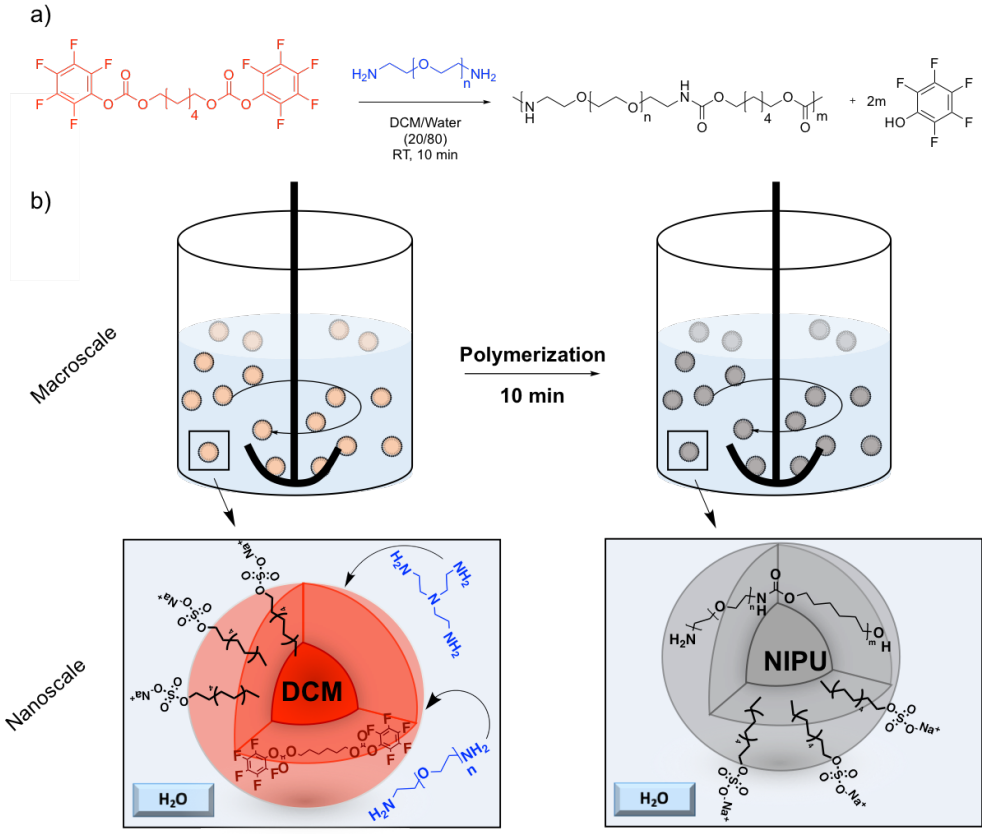

Figure 49. a) Interfacial polymerization of isocyanate free polyurethane using monomer A and PEG diamine. b) Schematic representation of surfactant-assisted interfacial polymerization of isocyanate free polyurethane soft nanoparticles.

Monitoring the reaction by ^{1}H NMR (**Figure 50**) showed that the polymerization was completed within 10 min, as evidenced by the disappearance of characteristic signals at 4.45 ppm (C*H*$_2$–OCO) of the methylene protons adjacent to the carbonate functionality, and the appearance of new signal of the methylene protons attached to the urethane groups at 4.2 ppm (C*H*$_2$–OCONH). Moreover, new

signals due to the methylene protons linked to the urethane moieties appeared at 3.36 ppm (C*H*$_2$–NHCOO).

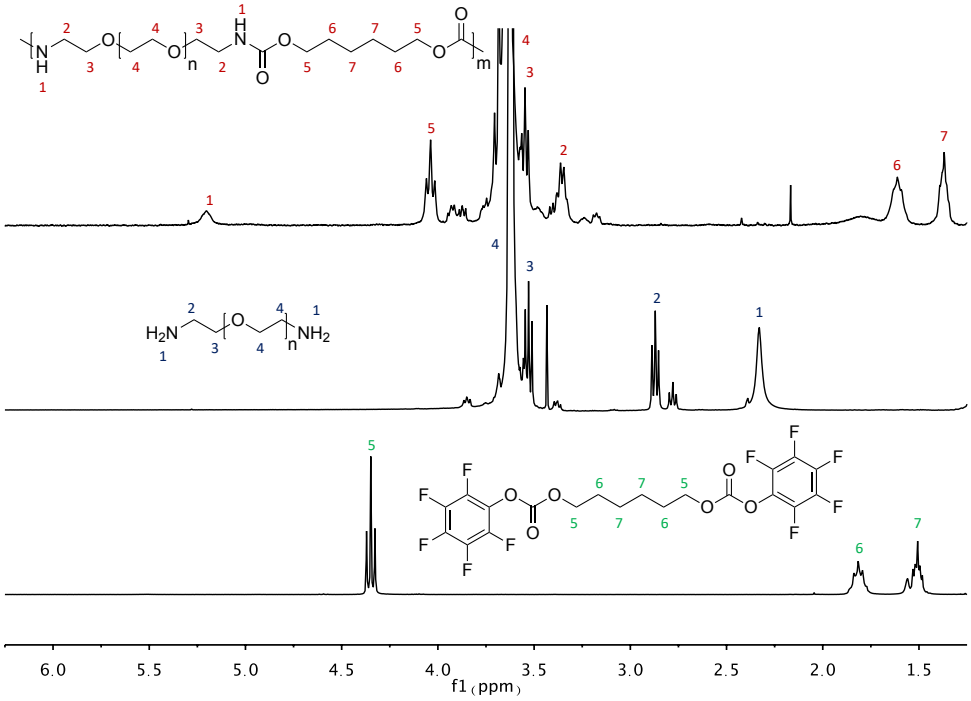

Figure 50. ^{1}H NMR (300 MHz, $CDCl_3$) of monomer A (bottom), PEG diamine (middle) and NIPU (top) synthesized from them by interfacial polymerization.

PU formation was further confirmed by FTIR analysis, showing a complete disappearance of the carbonate (C=O) stretching vibration at 1760 cm^{-1}. Two new bands appeared at 1720 cm^{-1} (C=O amide I) and at 1550 cm^{-1} (NH amide II), confirming successful urethane formation (**Figure 51**).

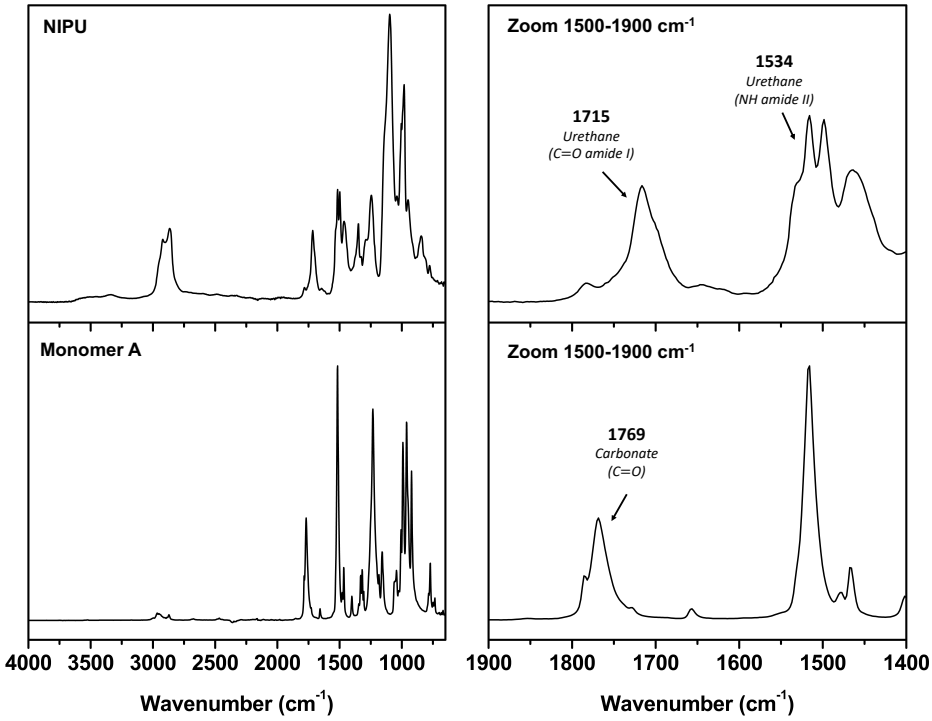

Figure 51. FTIR spectra of monomer A and the NIPU obtained by interfacial polymerization.

Finally, SEC analysis showed that high molecular weight PUs were obtained from this activated carbonate route (M_n = 27,700 Da; $Đ$ = 1.63), without any side reaction (**Figure 52**).

However, during the polymerization process, a tendency for polymer particles in suspension to settle down in water led to the formation of two distinct phases, as highlighted in **Figure 53.a**.

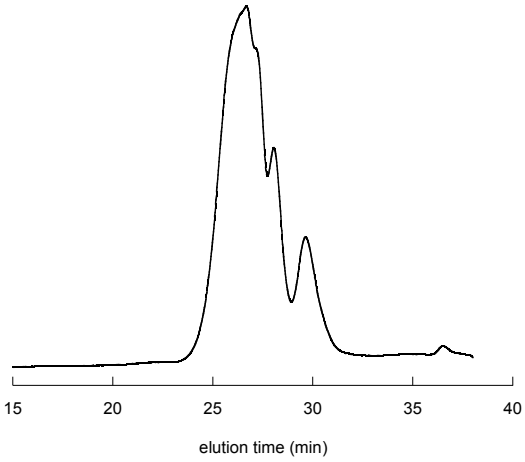

Figure 52. SEC trace of the polymerization of monomer A and PEG-diamine in 80/20 wt. % of deionized water/DCM mixture using *no surfactant* at room temperature for 10 min.

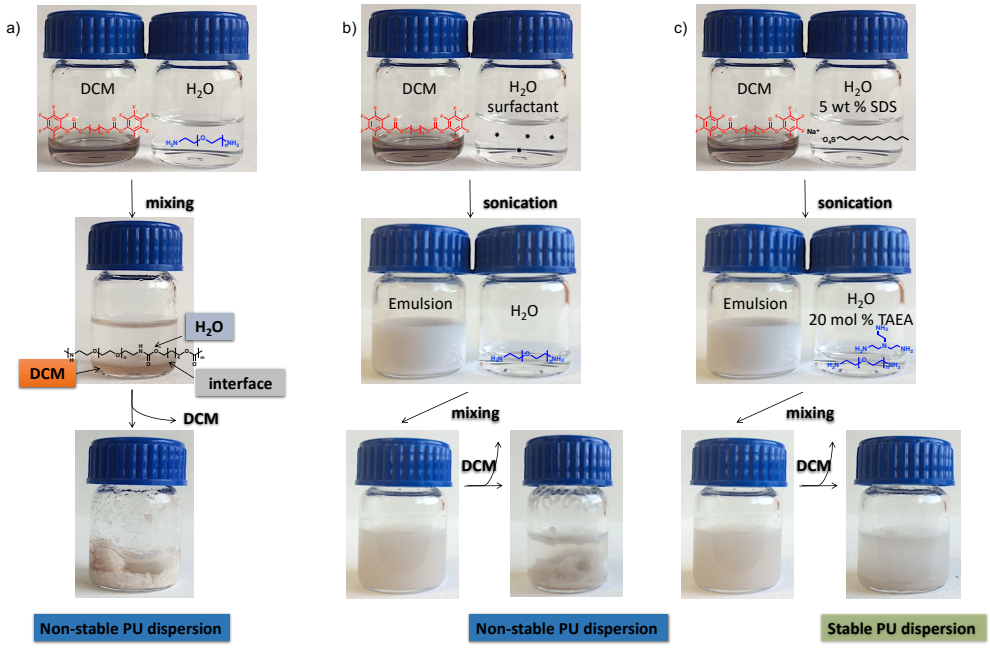

Figure 53. Pictures of interfacial polymerization of monomer A and PEG diamine using: a) no surfactant; b) anionic, cationic or non-ionic surfactants; c) the optimal condition of 5 wt. % of SDS as anionic surfactant and 20 mol. % of TAEA as crosslinker.

Use of an emulsifier was expected to improve the stability of the dispersed polymer prepared *via* interfacial polymerization in the water phase.[150] Critical features include the influence of the surfactant concentration (1.25, 2.5 and 5.0 wt. %), the nature of the surfactant (anionic, cationic and non-ionic) and the dispersion stability (**Table 8**). Thus, sodium dodecyl sulfate (SDS), dodecyltrimethylammonium bromide (DTAB) and pluronic F-68 were investigated as surfactants for the preparation of PUs by interfacial polymerization (**Figure 49.b**).

In an initial study, 5 wt. % of each of the three different surfactants were used in the interfacial polymerization reactions at room temperature with Monomer A and PEG diamine. An optimal value of 5 wt. % of SDS (**sample 4, Table 8**) was found, particles of around 170 nm being obtained under such conditions. Conversely, the non-ionic pluronic F-68 surfactant (**sample 7, Table 8**) provided a monodisperse suspension, where the resulting particle size was approximately 17 times the particle size of sample 4. High molecular weight NIPUs were obtained by this process. The use of the cationic DTAB surfactant (**sample 8, Table 8**), resulted in the precipitation of the reaction mixture. From this evaluation, SDS proved to be the best-suited surfactant for this interfacial polymerization.

The SDS concentration was then varied to achieve an optimal dispersion stability, which included samples 1 (no surfactant), 2 (1.25 wt. % SDS), 3 (2.5 wt. % SDS) and 4 (5 wt. % SDS) (**Table 8**). Although no significant difference in the final molecular weight was noted, stability of the final nanoparticles differed drastically from one experiment to another, the more stable and lower particle size distributions being achieved using 2.5 and 5 wt. % of SDS. It should be mentioned that this amount of surfactant is slightly higher than in the case of similar system obtained by mini-emulsion polymerization. This fact could be explained due to the DCM used in the interfacial reactions, which requires higher content in surfactant to stabilize the droplet.

Careful removal of DCM under vacuum was supposed to yield nanoparticles in aqueous solution. Yet, polymer particles tended to coalesce in water, as the particle size increased (**Figure 53.b**). To counter the softness of the particles

resulting in this phenomenon, we resorted to a trifunctional amine co-monomer, namely, tris(2-aminoethyl)amine (TAEA) as a crosslinking agent as a means to achieve a stable suspension after evaporating the organic solvent. Two different polymers were thus synthesized, using 10 and 20 mol. % of TAEA relative to the mole of acyclic activated dicarbonate (**samples 5** and **6, Table 8**). Comparing samples 4, 5 and 6, all the systems contain similar particle size and the particle size distribution before removing DCM. Once DCM was evaporated, however, changes were observed in the particle size and particle size distribution depending on the cross-linking concentration. Thus, by comparing of samples 5 and 6, one can note that varying the crosslinking density led to different particle size after removing DCM and thus, demonstrated that a minimum amount of cross-linker is required to form stable suspension (**Figure 53.c**).

TEM images of sample 6 are presented in **Figure 54**. As observed after careful removal of DCM and pentafluorophenol by dialysis, evaluated by ^{19}F NMR (**Figure S44** in the appendix section), we could confirm that the particles are in the nanometer scale. According to the results, we were able to form relatively stable suspensions even after removing the organic solvent by synthesizing harder particles using a suitable amount of a triamine cross-linking agent.

With this approach, we demonstrated that stable NIPUs dispersions with M_n = 27 kDa and nanoparticles sizes in the range of 200-300 nm could be obtained by interfacial polymerization, using 5 wt. % of emulsifier in combination with 20 mol. % of a trifunctional amine. Next, we investigated the preparation of waterborne NIPU soft nanoparticles functionalized with pendant carboxylic acid groups for potential drug delivery application.

Table 8. Molecular features of NIPUs synthesized in 80/20 volume % of deionized water/DCM mixture at room temperature for 10 min.

Entry	surfactant	surfactant concn (wt. %)[a]	TAEA (mol. %)	$D_{pwater/dcm}$ (nm)[b]	PDI[b]	D_{pwater} (nm)[c]	M_n (g/mol)[d]	*Đ*
1	no surfactant			-[e]	-[e]	-[e]	27700	1.63
2	SDS	1.25		300	0.47	2427	26600	1.26
3	SDS	2.5		274	0.28	3222	26700	1.22
4	SDS	5		162	0.17	1910	23300	1.55
5	SDS	5	10	146	0.15	1174	-[f]	-[f]
6	SDS	5	20	148	0.13	298	-[f]	-[f]
7	pluronic	5		2698	0.63	3127	29200	1.21
9	DTAB	5		-[g]	-[g]	-[g]	-[g]	-[g]

[a]Based on monomers (g) [b]Particle sizes and particle size distributions were calculated using dynamic light scattering (DLS) in water/DCM mixture. [c]Particle sizes and particle size distributions were calculated using DLS after DCM removal. [d]M_n values were calculated by SEC in DMF. [e]Phase separation was observed in that case (non-stable suspension). [f]M_n values were unobtainable due to cross-linking. [g]Precipitation occurred due to the complex formation between the bromide counter ion and pentafluorophenolate.

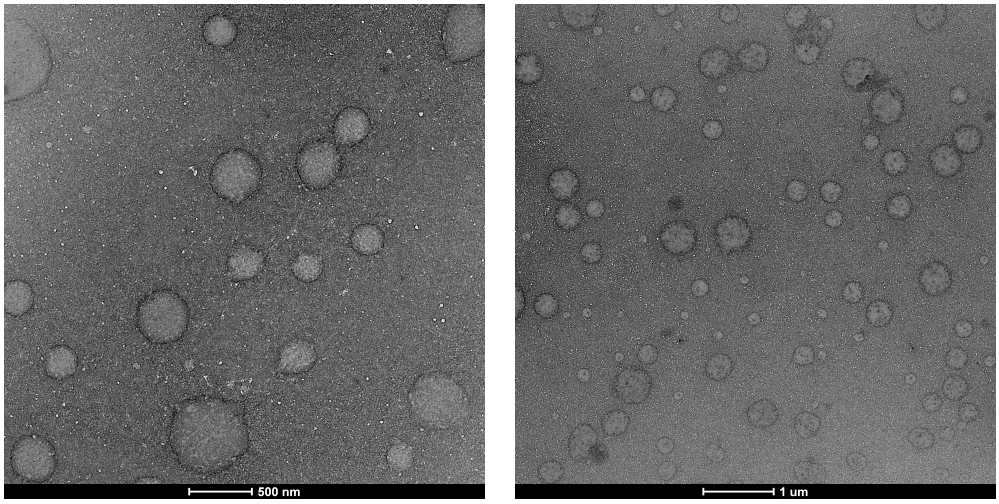

Figure 54. TEM images of sample 6 after dialysis.

4.2.3. Functionalization of NIPU soft nanoparticles

NIPU nanoparticles containing molecular recognition groups that specifically interact with the cargo are expected to enhance the drug loading capacity.[165,166] A number of anticancer drugs contain amine groups in their molecular structures, including doxorubicin (DOX). Acid-containing groups polymers are prone to sequester such amine-containing drugs.[166] We thus explored a simple way to incorporate functionality into the soft nanoparticles by designing an acid-containing dicarbonate co-monomer.[80,167,168]

After preparing the monomer bearing the protected acid functionality,[169] 2 equiv. of a monomer derived from 2,2-bis(methylol)propionic acid bearing pendant *tert*-butyl groups (MTC-tBAC) were reacted with 1 equiv. of ethylenediamine, the diol being activated with bis(pentafluorophenyl) carbonate (**Figure 55** and **Figure S45**).

Corresponding NIPUs were obtained in a two-step approach, involving 1) the formation of the NIPU by surfactant-assisted interfacial polymerization and 2) the conversion of the *t*-butyl ester moiety into carboxylic acid groups (**Figure 56**). After dissolving both monomers in a pair of immiscible liquids, activated carbonate was reacted with PEG diamines and 20 mol. % of trifunctional amine TAEA.

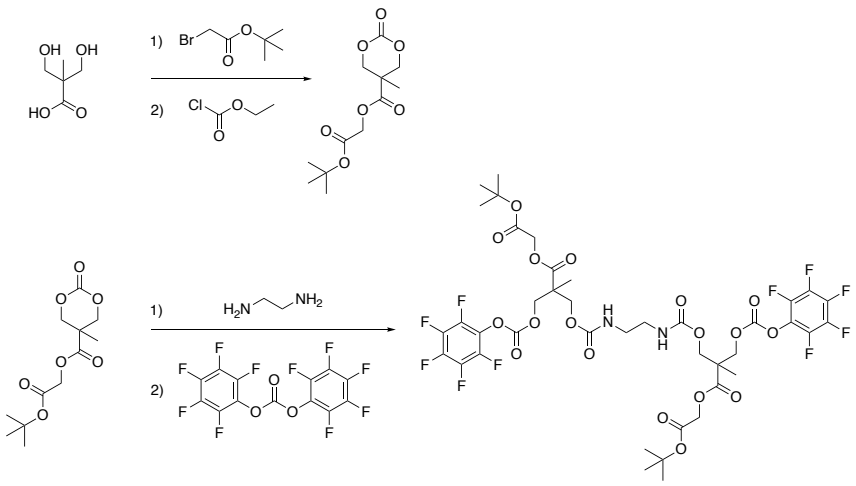

Figure 55. Method for the synthesis of bis-pentafluorophenyl carbonate monomer containing protected carboxylic acid group (monomer D).

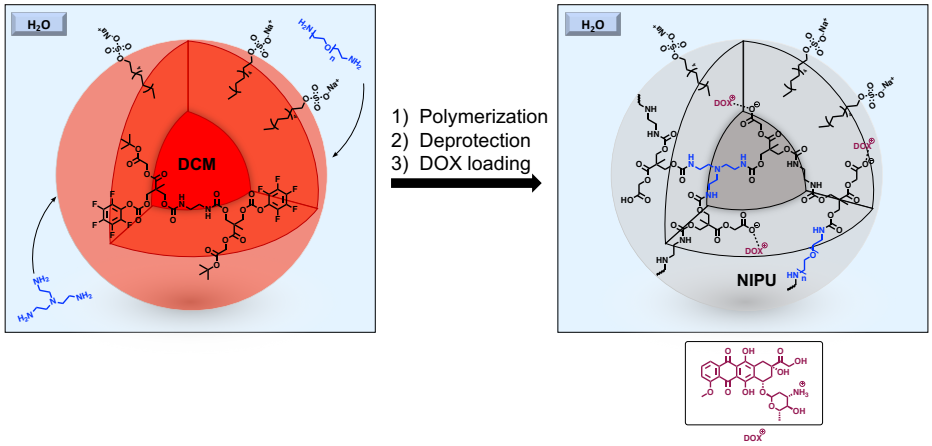

Figure 56. Schematic representation of functionalized NIPU containing -COOH groups that specifically interact with the cargo -NH_2 of doxorubicin.

The reaction was characterized by ^{1}H NMR (**Figure 57**). In all cases, > 98 % conversion by FTIR was observed within 60 min, demonstrating high monomer reactivity. In the last step, the *tert*-butyl ester groups were selectively converted to

carboxylic acid groups by mixing the resulting PU soft nanoparticles with DCM:trifluoroacetic acid (1:1 vol/vol) to achieve NIPU-COOH. Evidence of the successful deprotection of carboxylic acid was shown by ^{1}H NMR analyses, which revealed the disappearance of the residual *tert*-butoxy methyl proton resonance at 1.48 ppm without affecting the polyurethane backbone chemical shifts (**Figure S46**).

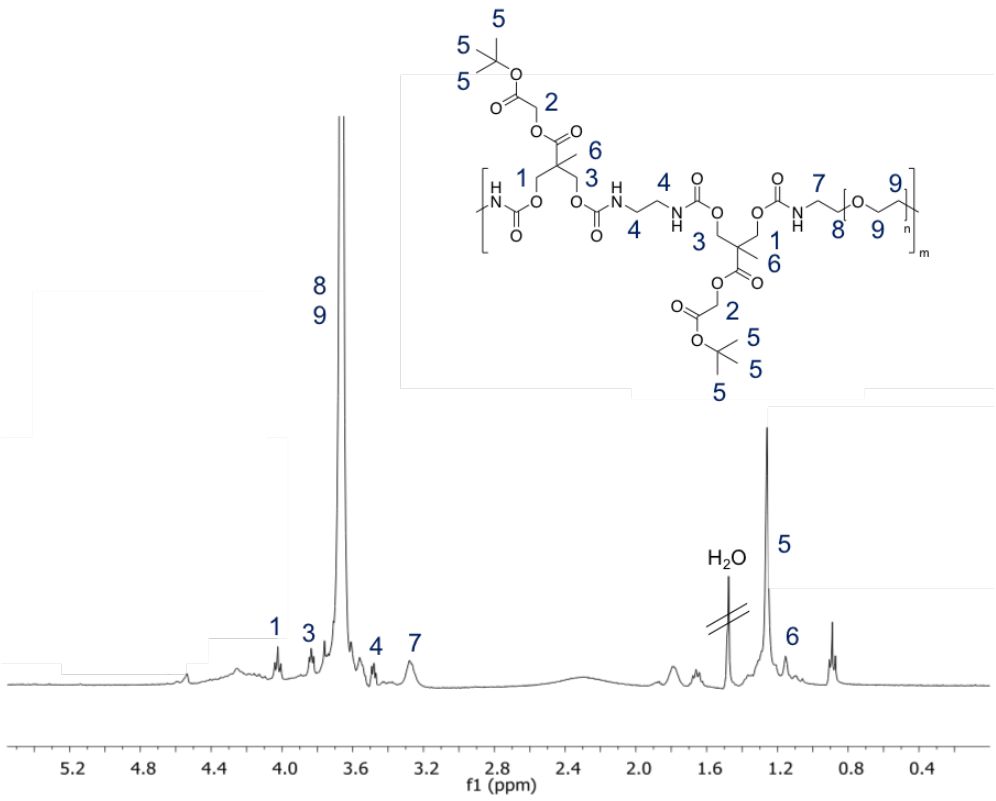

Figure 57. ^{1}H NMR (300 MHz, $CDCl_3$) of the polymer obtained from the interfacial polymerization of monomer D with PEG-diamine (80/20 wt. % deionized water/DCM mixture) before deprotection.

Doxorubicin (DOX) is considered as an amphiphilic anticancer drug. Loading of DOX into the soft NIPU nanoparticles was carried out by first neutralizing a fixed amount of DOX·HCl with 3-molar equivalent of triethylamine. Subsequently, the DOX solution was added dropwise to the NIPU soft nanoparticles-containing

aqueous solution under stirring. The mixture was added dropwise into 10 mL of deionized water while being sonicated and the resultant suspension was equilibrated at 25° C for 24 h. After 48 h of dialysis, the DOX-loaded nanoparticles were isolated by freeze-drying. To determine the DOX-loading level, a known amount of soft nanoparticles was suspended in 10 mL of DMF and vortexed vigorously. NIPU carriers were able to load up to 10.6 mg of DOX per 100 mg of polymer. In addition, after DOX loading the particle size was below 200 nm (D_p = 195 nm) with narrow particle size distribution (PDI = 0.1), ideal for drug delivery applications.

Compared with previous isocyanate-based PUs containing molecular recognition groups,[170,171] these NIPUs have two main advantages: 1) the PU soft nanoparticles can be directly prepared in aqueous media and 2) the toxic isocyanate is replaced by much more benign acyclic activated carbonates. This is the first example where well-defined isocyanate free polyurethane soft nanoparticles have been prepared by ultrafast surfactant assisted interfacial polymerization. In addition, we showed that functionality can be easily incorporated without affecting the polymerization.

4.3. Conclusion

This chapter describes a new method for the preparation of well-defined non-isocyanate polyurethane soft nanoparticles through the use of activated linear dicarbonates and polyamines, following a surfactant-assisted interfacial polymerization process. Pentafluorophenyl activated carbonates (monomer A) and heterogeneous polymerization conditions, typically 80 % H_2O / 20 % DCM, were found best suited to achieve stable NIPU particles. DFT calculations indicated that the nature of the leaving group, as well as solvation conditions, greatly affect the polymerization rate. In addition, the complexation of explicit water molecules to

carbonate and amine reactants lowers free energies of activation by 7-13 kcal/mol enhancing the overall kinetics. Moreover, a minimum of 5 wt. % of external surfactant was required, in combination with a trifunctional amine, to avoid NIPU particle aggregation. Using this method, NIPU nanoparticles with sizes in the range of 200−300 nm could be achieved. Finally, carboxylic acid-functionalized NIPU nanoparticles were prepared and were found to show excellent ability for loading a chemotherapeutic drug, namely, doxorubicin through ionic interactions. In view of the increasing demand for biocompatible nanocarriers, it is believed that this new waterborne synthetic method to functionalized NIPU soft nanoparticles holds great promise for the preparation of drug delivery nanocarriers.

4.4. Experimental part

Instrumentation

Nuclear Magnetic Resonance (NMR). ^{1}H and ^{13}C spectra were recorded with Bruker Avance DPX 300 or Bruker Avance 400 spectrometers. The NMR chemical shifts were reported as δ in parts per million (ppm) relative to the traces of non-deuterated solvent (*e.g.* δ = 2.50 ppm for DMSO-d_6 or δ = 7.26 for $CDCl_3$). Data were reported as: chemical shift, multiplicity (s = singlet, d = doublet, t = triplet, m = multiplet, br = broad) and integration.

Size Exclusion Chromatography (SEC). SEC was performed using a set of PSS GRAM columns with pore sizes of 10 µm (guard column) and 30 and 1000 Å calibrated with narrow polystyrene standards from Polymer Laboratories, using both refractometric and UV detectors (Varian). DMF was used as eluent (0.8 mL.min^{-1}) and toluene as a flow marker (300 µL toluene/100 mL DMF) at 50 °C, in the presence of LiBr (2.17 g.L^{-1}).

Fourier Transform Infrared Spectroscopy. FT-IR spectra were obtained by FT-IR spectrophotometer (Nicolet 6700 FT-IR, Thermo Scientific Inc., USA) using attenuated total reflectance (ATR) technique (Golden Gate, spectra Tech). Spectra

were recorded between 4000-525 cm^{-1} with a spectrum resolution of 4 cm^{-1}. All spectra were averaged over 10 scans.

Dynamic Light Scattering. The particle size (Dp) and particle size distribution (PDI) of the PHU dispersions were measured by Dynamic Light Scattering (DLS) using a Zetasizer-Nano S from Malvern operating with a 4 mW He–Ne laser (633 nm wavelength) and a fixed detector angle of 173 (non-invasive backscattering geometry NIBSTM) and with the cell holder maintained at constant temperature by means of a Peltier element. The samples were diluted with deionized water before the measurements to avoid multiple light scattering. The final value was an average of three measurements.

Transmission Electron Microscopy (TEM). TEM was performed using a Philips Tecnai 20 microscope working at accelerating voltage of 200 kV. Diluted samples of the emulsions (0.005-0.01 wt. %) were prepared.

Materials

1,6-Hexanediol (99 %), 1,8-bis(dimethylamino)naphthalene (Proton-Sponge®) (99 %), sodium methoxide (95 %), triethylamine (≥ 99 %), tris(2-aminoethyl)amine (96 %), ethylene diamine (≥ 99 %), sodium dodecyl sulfate (98,5 %), Pluronic-F68 (M_n = 8,400 Da), dodecyltrimethylammonium bromide (≥ 98 %), DCM (≥ 99.9 %), 4-nitrophenyl chloroformate (96 %), 1,1'-carbonyldiimidazole (≥ 97 %), phenyl chloroformate (97 %), ethyl chloroformate (97 %), doxorubicin hydrochloride, 2,2-bis(methylol) propionic acid (98 %), *tert*-butyl bromoacetate (98 %), trifluoroacetic acid (99 %), dimethyl acetamide (≥ 99 %), dimethyl sulfoxide (≥ 99.5 %) and THF (≥ 99.8 %) were purchased from Sigma Aldrich. DMF (GPC grade) and diethyl ether (99 %) were purchased from Fisher. Hexane (reagent grade) was purchased from Scharlab. Polyoxyethylene (bis)amine (M_w = 1,000 Da and M_w = 3,600 Da) were purchased from Alfa Aesar. (bis)-Pentafluorophenyl carbonate (PFC) (97 %) was purchased from Manchester Organics. Deuterated solvents such as $CDCl_3$, DMSO-d_6 were purchased from Euro-top. All materials were used without further purification.

Computational Methodology. All calculations were performed with GAMESS-US using the dispersion-corrected B3LY density functional theory (DFT) method. Geometry optimizations were performed with the 6-311+G(2d,p) basis set. All geometry optimizations were followed by single point energy calculations with the aug-cc-pVTZ basis set. Reported energies are free energies in kcal/mol. Only vibrational free energy corrections to the electronic energy at 298 K were used in accordance with recommendations for molecules optimized in implicit solvent. Reaction conditions were represented with a continuum dielectric derived from the IEF-CPCM method.[172]

Synthesis of $C_6F_5O–COO–(CH_2)_6–OCO–OC_6F_5$ (Monomer A). Monomer A was prepared according to literature.[46] PFC (2.2 equiv., 1.8 g, 4.4 mmol) and Proton-Sponge® (0.25 equiv., 0.11 g, 0.50 mmol) were dissolved in THF (8.0 mL) and stirred for 30 min. 1,6-Hexanediol (1.0 equiv., 0.24 g, 2.0 mmol) dissolved in 2.0 mL of THF was added dropwise to the reaction mixture and allowed to react at room temperature until completion (4 h). The reaction mixture was evaporated to dryness and cold dichloromethane was added to the residue, in which much of the pentafluorophenol byproduct was precipitated and recovered (0.65 g, 68 % recovery, with analytical purity higher than 95 %). The product-containing filtrate was rinsed with saturated aqueous $NaHCO_3$ and water, dried over $MgSO_4$, and concentrated. The crude product was recrystallized from hexane to afford monomer A as a white crystalline powder (0.77 g, 73 % yield). The structure was confirmed by ^1H, ^{13}C, and ^{19}F NMR spectroscopy. ^1H NMR ($CDCl_3$, 400 MHz, δ) 4.28 (t, $OCOOCH_2$, 4H), 1.75 (t, $OCOOCH_2CH_2$, 4H), 1.44 (t, CH_2, 4H); ^{13}C NMR ($CDCl_3$, 400 MHz, δ) 151.0 (OCOO), 142.0, 140.0, 139.0, 136.0 (CAr), 70.0 (s, $COOCH_2$), 28.0 ($COOCH_2CH_2$), 25.0 (CH_2); ^{19}F NMR ($CDCl_3$, 400 MHz): −154 (d, Ar-F, 4F), −158 (t, Ar-F, 4F), −162 (q, Ar-F, 2F).

Synthesis of $C_6H_4NO_2O–COO–(CH_2)_6–OCO–OC_6H_4NO_2$ (Monomer B). 4-Nitrophenyl chloroformate (2.2 equiv., 0.58 g, 2.9 mmol) and triethylamine (TEA, 0.29 g, 2.9 mmol, 2.2 equiv.) were dissolved in THF (8.0 mL), stirred for 30 minutes, and cooled down to 0 °C. 1,6-Hexanediol (0.24 g, 2.0 mmol, 1.0 equiv.) dissolved in 2.0 mL of THF was added dropwise to the reaction mixture. The mixture was stirred at room temperature for 4 h and filtered to remove triethylamine hydrochloride salt. The filtrate was concentrated and recrystallized from hexanes to afford monomer B as a yellow crystalline powder (0.53 g, 76 % yield). The structure was confirmed by ^{1}H NMR ($CDCl_3$, 400 MHz, δ) 8.40-7.20 (d, C_{Ar}, 4H), 4.35 (t, OCOOCH_2, 4H), 1.82 (t, OCOOCH$_2$CH_2, 4H), 1.52 (t, CH_2, 4H).

Synthesis of $C_6H_5O–COO–(CH_2)_6–OCO–OC_6H_5$ (Monomer C). Phenyl chloroformate (2.2 equiv., 0.45 g, 2.9 mmol) and TEA (0.29 g, 2.9 mmol, 2.2 equiv.) were dissolved in THF (8.0 mL) and stirred for 30 min. 1,6-hexanediol (0.24 g, 2.0 mmol, 1.0 equiv.) dissolved in 2.0 mL of THF was added dropwise to the reaction mixture and the mixture was stirred at room temperature 4 h. The reaction mixture was filtered to remove triethylamine hydrochloride salt. The product-containing filtrate was concentrated and the crude product was recrystallized from hexanes to afford monomer C as a white crystalline powder (0.38 g, 68 % yield). The structure was confirmed by ^{1}H NMR ($CDCl_3$, 400 MHz, δ) 7.50-7.10 (m, C_{Ar}, 5H), 4.30 (t, OCOOCH_2, 4H), 1.80 (t, OCOOCH$_2$CH_2, 4H), 1.50 (t, CH_2, 4H).

Synthesis of bis-pentafluorophenyl carbonate monomer containing protected carboxylic acid (Monomer D). The cyclic monomer containing protected acid was prepared in 3 steps according to literature.[169] Briefly, in the first step 2,2-bis(hydroxymethyl) propionic acid (DMPA) was modified with *tert*-butyl bromoacetate (TBBA) to form the protected acid TBMPA in the presence of NaOH. In a typical modification procedure, DMPA (10 g, 74.6 mmol, 1 equiv.) and NaOH (2.98 g, 74.6 mmol, 1 equiv.) were placed in DMSO (50 mL) at 80 °C and stirred for 24 h prior to the drop-wise addition of a solution of *tert*-butyl bromoacetate (14.25 g,

73.1 mmol, 0.98 equiv.) dissolved in DMSO (10 mL). The reaction was stirred at 80 °C for about 8 h, at which time the reaction was diluted 10-fold with water and the product was extracted with diethyl ether. The product solution containing TBMPA was rinsed with saturated $NaHCO_3$, dried over $MgSO_4$, and concentrated. Yellow liquid was obtained (17 g, 69 % yield). The ^1H NMR spectrum of TBMPA was consistent with published data. In the second step, the synthesized diol, TBMPA, was reacted with ethyl chloroformate (ECF) in the presence of TEA to form the 6-membered cyclic carbonate, MTC-TB. In a typical modification procedure, TBMPA (4 g, 17.1 mmol, 1 equiv.) was dissolved in dry THF (40 mL) and the resulting solution was cooled in an ice bath to 0° C prior to the addition of ECF (4.43 g, 37.6 mmol, 2.2 equiv.). Subsequently, TEA (3.79 g, 37.6 mmol, 2.2 equiv.) was dissolved in dry THF (20 mL) and added drop-wise to the reaction mixture, which was maintained under N_2. Upon completion (about 8 h), the reaction was concentrated and recrystallized in diethyl ether to give cyclic carbonate monomer trimethylenecarbonate-5-methyl-5-carboxy-*tert*-butylacetate (MTC-tBAc) (2.2 g, yield 50 %). The ^1H NMR spectrum of MTC-tBAc was consistent with published data. In the third step, the cyclic monomer MTC-tBAc was ring opened with ethylene diamine and functionalized with the bis-pentafluorophenyl carbonate in the presence of proton sponge to form the activated carbonate Monomer D. In a typical modification procedure, MTC-tBAc (1 g, 0.0036 mmol, 1 equiv.) was dissolved in dry THF (4 mL). The resulting solution was cooled in an ice bath prior to the drop-wise addition of ethylene diamine (0.108 g, 0.0018 mmol, 0.5 equiv.). Upon completion (about 1 h), bis-pentafluorophenyl carbonate (1.1 g, 0.0022 mmol, 1.2 equiv.) and proton sponge (0.12 g, 0.00055 mmol, 0.25 equiv.) were dissolved in dry THF (4 mL), and the resulting solution was added drop-wise to the reaction mixture. The reaction was carried out at 20 °C under nitrogen. Upon completion (about 12 h), the reaction mixture was concentrated and dissolved in DCM, upon which much of the pentafluorophenol by-product precipitated and was recovered. The solution containing the product monomer D was then rinsed with saturated aqueous $NaHCO_3$ followed by water, dried over $MgSO_4$, and concentrated. The

crude product monomer D was recrystallized in hexane to afford a viscous liquid (1.2 g, 73 % yield). ^{1}H NMR spectrum of monomer D clearly shows that the methylene groups linked to the pentafluorophenyl carbonate are shifted to 4.5 ppm. Moreover, the *t*-butyl group is not affected by the pentafluorophenyl carbonate modification. ^{1}H NMR ($CDCl_3$, 400 MHz, δ) 4.65-4.55 (m, $OCOOCH_2$, 4H), 4.40-4.20 (m, $OCOOCH_2$, 4H), 3.28 (m, $OCONHCH_2$, 4H), 1.48 (s, CH_3, 18H), 1.40 (s, CH_3, 6H).

General procedure for the comparative study of acyclic activated dicarbonates reactivity toward PEG diamine. In a typical procedure, carbonate (1 equiv., 82.5 umol) was added into a vial and dissolved in DCM (0.01 M). Separately, PEG diamine (1 equiv., 82.5 µmol) and TEA (2.1 equiv., 175 µmol) was dissolved in DCM (0.01 M) and added dropwise into the carbonate solution. The reaction was then stirred for 48 h at room temperature. Aliquots were taken at specific intervals of time and dried under reduce pressure prior to FTIR analysis.

General procedure for the comparative study of different DCM/H_2O ratio in the interfacial polymerization. In a typical procedure, Monomer A (1 equiv., 165 µmol) was dissolved in DCM. Separetely, PEG diamine (1 equiv., 165 µmol) and TEA (2.1 equiv., 350 µmol) was dissolved in deionized water and added dropwise into the carbonate solution. The reaction was then stirred for 24 h at room temperature. Aliquots were taken at specific intervals of time and dried under reduce pressure prior to FTIR analysis.

Synthesis of isocyanate free linear polyurethanes using the surfactant assisted interfacial polymerization. In a typical procedure, Monomer A (1 equiv., 82.5 µmol) was dissolved in 0.25 mL of DCM. Separately, PEG diamine (M_w = 1,000 Da) (1 equiv., 82.5 µmol) was dissolved in 0.25 mL of deionized water, TEA (2.1 equiv., 175 µmol) and surfactant were dissolved in 0.75 mL of deionized

water. Monomer A solution and surfactant solution were mixed together to form a pre-reaction mixture. The pre-reaction mixture was then sonicated for 10 sec followed by the “one shot” insertion of the polyoxyethylene (bis)amine solution. The reaction mixture was further stirred at room temperature for 10 min prior to DLS, ^{1}H NMR and FTIR analysis

Synthesis of isocyanate free polyurethane soft nanoparticles bearing functionalities using the surfactant assisted interfacial polymerization. Monomer D (0.1g, 0.09 mmol, 1 equiv.) was dissolved in 3 mL of DCM to form an organic phase. Sodium dodecyl sulfate (SDS) (0.02 g) was dissolved in distilled water (15 mL) to form an aqueous phase. Both phases were mixed vigorously using a sonicator cup to form a stable emulsion. Subsequently, PEG diamine (M_w = 3600 Da, 0.32 g, 0.09 mmol, 0.8 equiv.) and TAEA (0.005 g, 0.034 mmol, 0.2 equiv.) were dissolved in distilled water (8 mL) and the resulting solution was added dropwise at 10 mL/h to the emulsion. The polymerization was carried out at room temperature for 1 h. The reaction was followed by ^{1}H NMR. The characteristic signal of the activated carbonate end units at 4.45 ppm disappeared completely and a new signal attributed to the methylene group linked to the O-CO-NH appeared at 4.2 ppm. The average particle size for this system was 245 nm having a polydispersity of 0.145. In the third step, the *t*-butyl ester groups were selectively converted to carboxylic acid groups by mixing the resulting polyurethane solution with trifluoroacetic acid (TFA) (1:1 vol/vol). The modification was confirmed by ^{1}H NMR following the dissipation of *tert*-butyl group ^{1}H NMR signal.

DOX loading. DOX encapsulation was done through equilibrium adsorption method. DOX·HCl (5 mg) was neutralized with 3 mole excess of triethylamine and dissolved in 1.5 mL of *N*,*N*-dimethylacetamide (DMAc). The DOX solution was mixed with NIPU soft nanoparticles solution made from Monomer D (10 mg in 0.5 mL DMAc) by vortexing, and the mixture was added dropwise into 10 mL of deionized (DI) water while being sonicated. After this, the mixture was dialyzed

against 1 L of DI water using a 1000 Da molecular weight cut-off membrane for 48 h and lyophilized. Each experiment was performed in triplicate. To determine the DOX loading level, a known amount of lyophilized DOX-polymer was dissolved in 1 mL of dimethyl sulfoxide (DMSO) and the absorbance of the solution was measured using the UV-vis spectrometer at 480 nm. The DOX loading level was determined using well-established protocol.[173]

Chapter 5

Conclusions and Outlooks

CHAPTER 5. CONCLUSIONS AND OUTLOOKS

As discussed in this thesis, there is an urgent need to develop alternatives to the conventional synthetic method to PUs, which relies on the reaction of polyols with toxic polyisocyanates, due to major environmental concerns. In this context, synthesis of non-isocyanate polyurethanes (NIPUs) is a fast-developing field that holds great promise for specific applications. Nevertheless, many challenges still remain in view of their production to be competitive with the current process. The literature survey indicates that the method involving the step-growth polyaddition of 5-membered cyclic carbonates with diamines likely represents the most promising route for a large-scale production of NIPUs. However, this system is limited by the low reactivity of the cyclic carbonates, which requires harsh polymerization conditions, such as high temperatures, bulk conditions, long reaction times and the use catalysts, to push the reaction to completion and obtain high molecular weight polymers. These conditions imply the formation of side reactions, like the transamidations inter- or intra-molecular, leading to urea.

A rational study about the influence of organocatalysts, not only in the polymerization kinetics, but also on the structure and properties of the resulting NIPUs, has been carried out in **Chapter 2**. A complete study of the effect of different organocatalysts on the step-growth polyaddition of diglycerol dicarbonate with *Jeffamine* ED-2003 in bulk at 120 °C was successfully carried out. Our investigations concluded that the reaction was dramatically influenced by the type of catalyst, being the strong bases, such as P_4 or TBD, the most efficient catalysts. Unexpectedly, we found that the as-formed urethane moieties were transformed into urea. We took advantage of this reaction, to develop a synthetic route to access a range of poly(hydroxyurea-urethane) (PHUU) with controlled urethane-to-urea ratio in a one-pot process. Interestingly, it was found that increasing the urea ratio led to PHUUs with improved physical properties and phase separated

morphologies. These results can be of great interest considering not only the industrial importance of poly(urea-urethanes) but also the restrictions on the use of isocyanates.

Another important challenge for the preparation of non-isocyanate polyurethanes derived from 5-membered cyclic carbonates is the preparation of NIPU latexes. For that purpose, in **Chapter 3**, we adapted for the first time the most popular strategy to obtain aqueous polyurethane dispersions, the so-called acetone process, to access water-dispersible non-isocyanate polyurethane (WNIPU). To do so, we took advantage of 8-membered *N*-substituted cyclic carbonate (bis-N-8-C); which upon ring-opening with amines produces tertiary amines which act as internal surfactants, allowing the subsequent stabilization of NIPU particles in water. We were able to prepare stable poly(hydroxyurethanes) dispersions with average particle size around 200 nm using a minimum of 30 mol. % of bis-N-8-C.

Unfortunately, the mechanical properties of the films derived from these latexes were insufficient, as a result of the low T_g given by PDMS. One method to increase the mechanical properties of polymers is through the synthesis of crosslinked materials. In this sense we took advantage of the ionic interactions given by the tertiary amines, to prepare supramolecular networks. Using citric acid, a trifunctional acid, dynamic non-covalent structures were formed *via* the formation of ionic bonds between carboxylate and ammonium moieties. Hence, the physical properties of the films obtained from the optimal dispersion could be tuned. As a result of the subsequent formation of the dynamic ionic interactions, the films obtained showed improved mechanical properties and great healing abilities. Overall, this facile and versatile strategy based on water-dispersible non-isocyanate polyurethanes shows the potential to be used to design novel materials, such as for coating or adhesive applications.

In spite of the successful preparation of water NIPU dispersions using the acetone process, using this process it is difficult to obtain well-control over the particle morphology, size and distribution. While this fact is not critical for large scale applications such as in paints or coatings, it is highly relevant in applications related with nanomedicine where control over the particle size is crucial. Therefore, in **Chapter 4**, we have developed an innovative approach based on the surfactant-assisted interfacial polymerization of linear activated dicarbonates and diamines. This process enabled us to obtain crosslinked soft nanoparticles in the range of 200-300 nm with narrow polydispersities. The versatility of this process permitted to incorporate into the NIPU nanoparticles, functional groups such as carboxylic acids. These carboxylic groups allowed us to encapsulate the chemotherapeutic drug Doxorubicin (DOX). The obtained NIPU carriers were able to load up to 10.6 mg of DOX per 100 mg of polymer. In addition, after DOX loading, the particle size was below 200 nm (Dp = 195 nm) with narrow particle size distribution (PDI = 0.1), ideal for drug delivery applications. Compared with previous isocyanate-based PUs containing molecular recognition groups, these NIPUs have two main advantages: (1) the PU soft nanoparticles can be directly prepared in aqueous media, and (2) the toxic isocyanate is replaced by much more benign acyclic activated carbonates.

Based on the new synthetic methods presented in this thesis, several research areas are still underway and others could be developed. First, it could be interesting to combine the mechanically improved poly(hydroxyurea-urethane)s (PHUU)s synthesis using organocatalysis with the acetone process to prepare NIPU coatings with better mechanical properties. Interestingly, we could also take advantage of the onium ions coming from bis-N-8-C during the acetone process, to incorporate different functionalities into the NIPU nanoparticles. For example, addition of a sulfonic/carboxylic acid comprising of an allyl group could open the door to the preparation of UV curable NIPU films which could find application in 3D printing. The development of more efficient catalytic centers, such as dual catalysts, by combining for example, Lewis bases and Lewis acids to form Lewis pairs (*e.g.*

TBD/trimethylsilyl triflate) could benefit the polymerization kinetic of 5-membered cyclic carbonates with diamines. As another research area, the interfacial polymerization process could be optimized by changing the nature of the leaving group in the linear activated dicarbonates to better fulfill the requirements of the biomedical field. Finally, others amino group-containing molecules could be incorporating into the NIPU nanoparticles, such as the dye Rhodamine B, for biotechnology applications such as fluorescence microscopy.

Overall, this PhD thesis demonstrates the great potential and broaden the scope of organocatalyzed polymerization reactions combined with waterborne processes in addition to utilizing isocyanate-free chemistry, to prepare new functional polyurethanes for a wide range of applications.

Chapter 6

References and Lists

CHAPTER 6. REFERENCES AND LISTS

6.1. References

1 PlasticsEurope, *Plastics – the Facts 2017*, 2017.
2 O. Bayer, *Angew. Chem.*, 1947, **59**, 257–272.
3 E. Delebecq, J.-P. Pascault, B. Boutevin and F. Ganachaud, *Chem. Rev.*, 2013, **113**, 80–118.
4 H.-W. Engels, H.-G. Pirkl, R. Albers, R. W. Albach, J. Krause, A. Hoffmann, H. Casselmann and J. Dormish, *Angew. Chem. Int. Ed.*, 2013, **52**, 9422–9441.
5 C. Hepburn, *Polyurethane Elastomers*, Springer Science & Business Media, 2012.
6 D. C. Allport, D. S. Gilbert and S. M. Outterside, *MDI and TDI: Safety, Health and the Environment: A Source Book and Practical Guide*, John Wiley & Sons, 2003.
7 S. Diamond, The Bhopal Disaster: How It Happened, *N. Y. Times*, 1985.
8 W. Biddle, Nerve Gases and Pesticides: Links Are Close, *N. Y. Times*, 1984.
9 R. Devendra, N. R. Edmonds and T. Söhnel, *J. Mol. Catal. Chem.*, 2013, **366**, 126–139.
10 W. J. Blank, Z. A. He and E. T. Hessell, *Prog. Org. Coat.*, 1999, **35**, 19–29.
11 O. Kreye, H. Mutlu and M. A. R. Meier, *Green Chem.*, 2013, **15**, 1431–1455.
12 A. Nachtergael, O. Coulembier, P. Dubois, M. Helvenstein, P. Duez, B. Blankert and L. Mespouille, *Biomacromolecules*, 2015, **16**, 507–514.
13 H. Sardon, L. Irusta and M. J. Fernández-Berridi, *Prog. Org. Coat.*, 2009, **66**, 291–295.
14 Y. Salánki, Y. D'eri, A. Platokhin and K. Sh-Rózsa, *Neurosci. Behav. Physiol.*, 2000, **30**, 63–73.
15 G. Schwach, J. Coudane, R. Engel and M. Vert, *J. Polym. Sci. Part Polym. Chem.*, 1997, **35**, 3431–3440.
16 J. Yang, S. Zhang, X. Liu and A. Cao, *Polym. Degrad. Stab.*, 2003, **81**, 1–7.
17 L. Mølhave, B. Bach and O. F. Pedersen, *Environ. Int.*, 1986, **12**, 167–175.
18 W. N. Ottou, H. Sardon, D. Mecerreyes, J. Vignolle and D. Taton, *Prog. Polym. Sci.*, 2016, **56**, 64–115.
19 H. Sardon, A. Pascual, D. Mecerreyes, D. Taton, H. Cramail and J. L. Hedrick, *Macromolecules*, 2015, **48**, 3153–3165.
20 R. H. Lambeth and T. J. Henderson, *Polymer*, 2013, **54**, 5568–5573.
21 B. Ochiai, H. Kojima and T. Endo, *J. Polym. Sci. Part Polym. Chem.*, 2014, **52**, 1113–1118.
22 H. Matsukizono and T. Endo, *RSC Adv.*, 2015, **5**, 71360–71369.
23 H. Tomita, F. Sanda and T. Endo, *J. Polym. Sci. Part Polym. Chem.*, 2001, **39**, 851–859.

24 B. Ochiai, M. Matsuki, T. Miyagawa, D. Nagai and T. Endo, *Tetrahedron*, 2005, **61**, 1835–1838.
25 B. Ochiai, Y. Satoh and T. Endo, *Green Chem.*, 2005, **7**, 765–767.
26 O. Lamarzelle, P.-L. Durand, A.-L. Wirotius, G. Chollet, E. Grau and H. Cramail, *Polym. Chem.*, 2016, **7**, 1439–1451.
27 H. Tomita, F. Sanda and T. Endo, *J. Polym. Sci. Part Polym. Chem.*, 2001, **39**, 860–867.
28 L. Maisonneuve, A. S. More, S. Foltran, C. Alfos, F. Robert, Y. Landais, T. Tassaing, E. Grau and H. Cramail, *RSC Adv.*, 2014, **4**, 25795–25803.
29 H. Tomita, F. Sanda and T. Endo, *J. Polym. Sci. Part Polym. Chem.*, 2001, **39**, 162–168.
30 H. Tomita, F. Sanda and T. Endo, *J. Polym. Sci. Part Polym. Chem.*, 2001, **39**, 4091–4100.
31 A. Yuen, A. Bossion, E. Gómez-Bengoa, F. Ruipérez, M. Isik, J. L. Hedrick, D. Mecerreyes, Y. Y. Yang and H. Sardon, *Polym. Chem.*, 2016, **7**, 2105–2111.
32 M. S. Kathalewar, P. B. Joshi, A. S. Sabnis and V. C. Malshe, *RSC Adv.*, 2013, **3**, 4110–4129.
33 S. J. Groszos, E. K. Drechsel, Method of preparing a polyurethane, United States, US2802022A, 1957.
34 L. Maisonneuve, O. Lamarzelle, E. Rix, E. Grau and H. Cramail, *Chem. Rev.*, 2015, **115**, 12407–12439.
35 V. Besse, F. Camara, F. Méchin, E. Fleury, S. Caillol, J.-P. Pascault and B. Boutevin, *Eur. Polym. J.*, 2015, **71**, 1–11.
36 E. K. Leitsch, G. Beniah, K. Liu, T. Lan, W. H. Heath, K. A. Scheidt and J. M. Torkelson, *ACS Macro Lett.*, 2016, **5**, 424–429.
37 G. Beniah, X. Chen, B. E. Uno, K. Liu, E. K. Leitsch, J. Jeon, W. H. Heath, K. A. Scheidt and J. M. Torkelson, *Macromolecules*, 2017, **50**, 3193–3203.
38 C. Hahn, H. Keul and M. Möller, *Polym. Int.*, 2012, **61**, 1048–1060.
39 H. Matsukizono and T. Endo, *Macromol. Chem. Phys.*, 2017, **218**, 1700043.
40 H. Tomita, F. Sanda and T. Endo, *J. Polym. Sci. Part Polym. Chem.*, 2001, **39**, 3678–3685.
41 R. M. Garipov, V. A. Sysoev, V. V. Mikheev, A. I. Zagidullin, R. Y. Deberdeev, V. I. Irzhak and A. A. Berlin, *Dokl. Phys. Chem.*, 2003, **393**, 289–292.
42 M. V. Zabalov, R. P. Tiger and A. A. Berlin, *Russ. Chem. Bull.*, 2012, **61**, 518–527.
43 M. K. Kiesewetter, E. J. Shin, J. L. Hedrick and R. M. Waymouth, *Macromolecules*, 2010, **43**, 2093–2107.
44 C. D. Diakoumakos and D. L. Kotzev, *Macromol. Symp.*, 2004, **216**, 37–46.
45 M. Kathalewar, A. Sabnis and D. D'Mello, *Eur. Polym. J.*, 2014, **57**, 99–108.
46 H. Sardon, A. C. Engler, J. M. W. Chan, D. J. Coady, J. M. O'Brien, D. Mecerreyes, Y. Y. Yang and J. L. Hedrick, *Green Chem.*, 2013, **15**, 1121–1126.
47 M. Blain, L. Jean-Gérard, R. Auvergne, D. Benazet, S. Caillol and B. Andrioletti, *Green Chem.*, 2014, **16**, 4286–4291.

48 Q. Chen, K. Gao, C. Peng, H. Xie, Z. K. Zhao and M. Bao, *Green Chem.*, 2015, **17**, 4546–4551.
49 A. Cornille, S. Dworakowska, D. Bogdal, B. Boutevin and S. Caillol, *Eur. Polym. J.*, 2015, **66**, 129–138.
50 M. Unverferth, O. Kreye, A. Prohammer and M. A. R. Meier, *Macromol. Rapid Commun.*, 2013, **34**, 1569–1574.
51 M. Firdaus and M. A. R. Meier, *Green Chem.*, 2013, **15**, 370–380.
52 C. Duval, N. Kébir, A. Charvet, A. Martin and F. Burel, *J. Polym. Sci. Part Polym. Chem.*, 2015, **53**, 1351–1359.
53 A. Martin, L. Lecamp, H. Labib, F. Aloui, N. Kébir and F. Burel, *Eur. Polym. J.*, 2016, **84**, 828–836.
54 M. Blain, H. Yau, L. Jean-Gérard, R. Auvergne, D. Benazet, P. R. Schreiner, S. Caillol and B. Andrioletti, *ChemSusChem*, 2016, **9**, 2269–2272.
55 A. Cornille, C. Guillet, S. Benyahya, C. Negrell, B. Boutevin and S. Caillol, *Eur. Polym. J.*, 2016, **84**, 873–888.
56 A. Cornille, R. Auvergne, O. Figovsky, B. Boutevin and S. Caillol, *Eur. Polym. J.*, 2017, **87**, 535–552.
57 P. R. Schreiner, *Chem. Soc. Rev.*, 2003, **32**, 289–296.
58 N. E. Kamber, W. Jeong, R. M. Waymouth, R. C. Pratt, B. G. G. Lohmeijer and J. L. Hedrick, *Chem. Rev.*, 2007, **107**, 5813–5840.
59 J. Alsarraf, Y. A. Ammar, F. Robert, E. Cloutet, H. Cramail and Y. Landais, *Macromolecules*, 2012, **45**, 2249–2256.
60 D. Dieterich, *Prog. Org. Coat.*, 1981, **9**, 281–340.
61 A. K. Nanda and D. A. Wicks, *Polymer*, 2006, **47**, 1805–1811.
62 Y. Wei, Y. Luo, B. Li and B. Li, *Colloid Polym. Sci.*, 2005, **283**, 1289–1297.
63 M. C. Delpech and F. M. B. Coutinho, *Polym. Test.*, 2000, **19**, 939–952.
64 H. Sardon, L. Irusta, M. J. Fernández-Berridi, J. Luna, M. Lansalot and E. Bourgeat-Lami, *J. Appl. Polym. Sci.*, 2011, **120**, 2054–2062.
65 H. Sardon, L. Irusta, M. J. Fernández-Berridi, M. Lansalot and E. Bourgeat-Lami, *Polymer*, 2010, **51**, 5051–5057.
66 B. K. Kim, *Colloid Polym. Sci.*, 1996, **274**, 599–611.
67 A. Barni and M. Levi, *J. Appl. Polym. Sci.*, **88**, 716–723.
68 S. Ma, H. Zhang, R. J. Sablong, C. E. Koning and R. A. T. M. van Benthem, *Macromol. Rapid Commun.*, 2018, **39**, 1800004.
69 S. Ma, E. P. A. van Heeswijk, B. A. J. Noordover, R. J. Sablong, R. A. T. M. van Benthem and C. E. Koning, *ChemSusChem*, 2018, **11**, 149–158.
70 G. Morral-Ruíz, C. Solans, M. L. García and M. J. García-Celma, *Langmuir*, 2012, **28**, 6256–6264.
71 F. Tiarks, K. Landfester and M. Antonietti, *J. Polym. Sci. Part Polym. Chem.*, 2001, **39**, 2520–2524.
72 B. G. Zanetti-Ramos, E. Lemos-Senna, V. Soldi, R. Borsali, E. Cloutet and H. Cramail, *Polymer*, 2006, **47**, 8080–8087.
73 H. J. MSc and R. B. Schmid, *J. Microencapsul.*, 2007, **24**, 731–742.
74 G. G. Odian, in *Principles of Polymerization*, Wiley-Blackwell, 2004, pp. 350–371.

75 E. Rix, E. Grau, G. Chollet and H. Cramail, *Eur. Polym. J.*, 2016, **84**, 863–872.
76 J. Guan, Y. Song, Y. Lin, X. Yin, M. Zuo, Y. Zhao, X. Tao and Q. Zheng, *Ind. Eng. Chem. Res.*, 2011, **50**, 6517–6527.
77 O. Lamarzelle, P.-L. Durand, A.-L. Wirotius, G. Chollet, E. Grau and H. Cramail, *Polym. Chem.*, 2016, **7**, 1439–1451.
78 D. J. Fortman, J. P. Brutman, C. J. Cramer, M. A. Hillmyer and W. R. Dichtel, *J. Am. Chem. Soc.*, 2015, **137**, 14019–14022.
79 L. Maisonneuve, A. S. More, S. Foltran, C. Alfos, F. Robert, Y. Landais, T. Tassaing, E. Grau and H. Cramail, *RSC Adv.*, 2014, **4**, 25795–25803.
80 D. P. Sanders, K. Fukushima, D. J. Coady, A. Nelson, M. Fujiwara, M. Yasumoto and J. L. Hedrick, *J. Am. Chem. Soc.*, 2010, **132**, 14724–14726.
81 T. F. Al-Azemi and K. S. Bisht, *Polymer*, 2002, **43**, 2161–2167.
82 G. Rokicki, T. Kowalczyk and M. Glinski, *Polym. J.*, 2000, **32**, 381–390.
83 Y. Du, F. Cai, D.-L. Kong and L.-N. He, *Green Chem.*, 2005, **7**, 518–523.
84 S. Klaus, M. W. Lehenmeier, C. E. Anderson and B. Rieger, *Coord. Chem. Rev.*, 2011, **255**, 1460–1479.
85 A. Decortes, A. M. Castilla and A. W. Kleij, *Angew. Chem. Int. Ed Engl.*, 2010, **49**, 9822–9837.
86 M. Alvaro, C. Baleizao, D. Das, E. Carbonell and H. García, *J. Catal.*, 2004, **228**, 254–258.
87 H. Kawanami, A. Sasaki, K. Matsui and Y. Ikushima, *Chem. Commun.*, 2003, 896–897.
88 B. Chatelet, L. Joucla, J.-P. Dutasta, A. Martinez, K. C. Szeto and V. Dufaud, *J. Am. Chem. Soc.*, 2013, **135**, 5348–5351.
89 G. Fiorani, W. Guo and A. W. Kleij, *Green Chem.*, 2015, **17**, 1375–1389.
90 M. Alves, B. Grignard, R. Mereau, C. Jerome, T. Tassaing and C. Detrembleur, *Catal. Sci. Technol.*, 2017, **7**, 2651–2684.
91 S. Gennen, B. Grignard, T. Tassaing, C. Jérôme and C. Detrembleur, *Angew. Chem. Int. Ed.*, 2017, **56**, 10394–10398.
92 G. Jakab, C. Tancon, Z. Zhang, K. M. Lippert and P. R. Schreiner, *Org. Lett.*, 2012, **14**, 1724–1727.
93 J. H. Clements, *Ind. Eng. Chem. Res.*, 2003, **42**, 663–674.
94 Q.-W. Lu, T. R. Hoye and C. W. Macosko, *J. Polym. Sci. Part Polym. Chem.*, 2002, **40**, 2310–2328.
95 P. N. Lan, S. Corneillie, E. Schacht, M. Davies and A. Shard, *Biomaterials*, 1996, **17**, 2273–2280.
96 A. P. Dove, *Chem. Commun.*, 2008, 6446–6470.
97 R. C. Pratt, B. G. G. Lohmeijer, D. A. Long, R. M. Waymouth and J. L. Hedrick, *J. Am. Chem. Soc.*, 2006, **128**, 4556–4557.
98 A. P. Dove, R. C. Pratt, B. G. G. Lohmeijer, R. M. Waymouth and J. L. Hedrick, *J. Am. Chem. Soc.*, 2005, **127**, 13798–13799.
99 X. Zhang, G. O. Jones, J. L. Hedrick and R. M. Waymouth, *Nat. Chem.*, 2016, **8**, 1047–1053.
100 Y. S. Yang and L. J. Lee, *J. Appl. Polym. Sci.*, 1988, **36**, 1325–1342.

101 J. Mattia and P. Painter, *Macromolecules*, 2007, **40**, 1546–1554.
102 J. L. J. van Velthoven, L. Gootjes, D. S. van Es, B. A. J. Noordover and J. Meuldijk, *Eur. Polym. J.*, 2015, **70**, 125–135.
103 M. Tryznowski, A. Świderska, Z. Żołek-Tryznowska, T. Gołofit and P. G. Parzuchowski, *Polymer*, 2015, **80**, 228–236.
104 L. H. Chan-Chan, G. González-García, R. F. Vargas-Coronado, J. M. Cervantes-Uc, F. Hernández-Sánchez, A. Marcos-Fernandez and J. V. Cauich-Rodríguez, *Eur. Polym. J.*, 2017, **92**, 27–39.
105 X. Chen, L. Li, K. Jin and J. M. Torkelson, *Polym. Chem.,* 2017, **8**, 6349–6355.
106 S.-H. Pyo and R. Hatti-Kaul, *Adv. Synth. Catal.*, 2016, **358**, 834–839.
107 D. J. Fortman, J. P. Brutman, M. A. Hillmyer and W. R. Dichtel, *J. Appl. Polym. Sci.*, 2017, **134**, 44984.
108 E. Yamazaki, H. Hanahata, J. Hiwatari and Y. Kitahama, *Polym. J.*, 1997, **29**, 811–817.
109 Michael Szycher, *Szycher's Handbook of Polyurethanes, First Edition*, CRC Press, 1999.
110 M. M. Coleman, D. J. Skrovanek, J. Hu and P. C. Painter, *Macromolecules*, 1988, **21**, 59–65.
111 S. Li, J. Zhao, Z. Zhang, J. Zhang and W. Yang, *RSC Adv.*, 2014, **5**, 6843–6852.
112 D. Tang, D.-J. Mulder, B. A. J. Noordover and C. E. Koning, *Macromol. Rapid Commun.*, 2011, **32**, 1379–1385.
113 S. Ma, C. Liu, R. J. Sablong, B. A. J. Noordover, E. J. M. Hensen, R. A. T. M. van Benthem and C. E. Koning, *ACS Catal.*, 2016, **6**, 6883–6891.
114 M. Tryznowski, A. Świderska, Z. Żołek-Tryznowska, T. Gołofit and P. G. Parzuchowski, *Data Brief*, 2016, **6**, 77–82.
115 H. Blattmann, M. Fleischer, M. Bähr and R. Mülhaupt, *Macromol. Rapid Commun.*, 2014, **35**, 1238–1254.
116 V. Besse, F. Camara, C. Voirin, R. Auvergne, S. Caillol and B. Boutevin, *Polym. Chem.*, 2013, **4**, 4545–4561.
117 G. Rokicki, P. G. Parzuchowski and M. Mazurek, *Polym. Adv. Technol.*, 2015, **26**, 707–761.
118 A. Cornille, G. Michaud, F. Simon, S. Fouquay, R. Auvergne, B. Boutevin and S. Caillol, *Eur. Polym. J.*, 2016, **84**, 404–420.
119 G. Beniah, W. H. Heath, J. Jeon and J. M. Torkelson, *J. Appl. Polym. Sci.*, 2017, **134**, 44942.
120 S. Gennen, B. Grignard, J.-M. Thomassin, B. Gilbert, B. Vertruyen, C. Jerome and C. Detrembleur, *Eur. Polym. J.*, 2016, **84**, 849–862.
121 A. Cornille, M. Blain, R. Auvergne, B. Andrioletti, B. Boutevin and S. Caillol, *Polym. Chem.*, 2017, **8**, 592-604.
122 M. Barrère and K. Landfester, *Macromolecules*, 2003, **36**, 5119–5125.
123 D. K. Chattopadhyay and K. V. S. N. Raju, *Prog. Polym. Sci.*, 2007, **32**, 352–418.
124 W. J. Blank and V. J. Tramontano, *Prog. Org. Coat.*, 1996, **27**, 1–15.

125 L. Brunsveld, B. J. B. Folmer, E. W. Meijer and R. P. Sijbesma, *Chem. Rev.*, 2001, **101**, 4071–4098.
126 L. Yang, X. Tan, Z. Wang and X. Zhang, *Chem. Rev.*, 2015, **115**, 7196–7239.
127 Y. Yang and M. W. Urban, *Adv. Mater. Interfaces*, 2015, **5**, 1800384.
128 A. Campanella, D. Döhler and W. H. Binder, *Macromol. Rapid Commun.*, 2018, **39**, 1700739.
129 M. A. Aboudzadeh, M. E. Muñoz, A. Santamaría, M. J. Fernández-Berridi, L. Irusta and D. Mecerreyes, *Macromolecules*, 2012, **45**, 7599–7606.
130 A. Aboudzadeh, M. Fernandez, M. E. Muñoz, A. Santamaría and D. Mecerreyes, *Macromol. Rapid Commun.*, 2014, **35**, 460–465.
131 D. Wang, H. Zhang, B. Cheng, Z. Qian, W. Liu, N. Zhao and J. Xu, *J. Polym. Sci. Part Polym. Chem.*, 2016, **54**, 1357–1366.
132 K. S. Partridge, D. K. Smith, G. M. Dykes and P. T. McGrail, *Chem. Commun.*, 2001, **0**, 319–320.
133 A. Noro, K. Ishihara and Y. Matsushita, *Macromolecules*, 2011, **44**, 6241–6244.
134 L. Zhang, L. R. Kucera, S. Ummadisetty, J. R. Nykaza, Y. A. Elabd, R. F. Storey, K. A. Cavicchi and R. A. Weiss, *Macromolecules*, 2014, **47**, 4387–4396.
135 D. Wang, J. Guo, H. Zhang, B. Cheng, H. Shen, N. Zhao and J. Xu, *J. Mater. Chem. A*, 2015, **3**, 12864–12872.
136 Y. Miwa, J. Kurachi, Y. Kohbara and S. Kutsumizu, *Commun. Chem.*, 2018, **1**, 5.
137 M. Comí, M. Fernández, A. Santamaría, G. Lligadas, J. C. Ronda, M. Galià and V. Cádiz, *Macromol. Chem. Phys.*, 2017, **218**, 1700379.
138 M. Comí, G. Lligadas, J. C. Ronda, M. Galià and V. Cádiz, *Eur. Polym. J.*, 2017, **91**, 408–419.
139 H. Daemi, M. Barikani and H. Sardon, *Carbohydr. Polym.*, 2017, **157**, 1949–1954.
140 C. Duval, N. Kébir, R. Jauseau and F. Burel, *J. Polym. Sci. Part Polym. Chem.*, 2016, **54**, 758–764.
141 L. K. Saw, B. W. Brooks, K. J. Carpenter and D. V. Keight, *J. Colloid Interface Sci.*, 2003, **257**, 163–172.
142 M. A. Aboudzadeh, M. E. Muñoz, A. Santamaría, R. Marcilla and D. Mecerreyes, *Macromol. Rapid Commun.*, 2012, **33**, 314–318.
143 K. E. Feldman, M. J. Kade, E. W. Meijer, C. J. Hawker and E. J. Kramer, *Macromolecules*, 2009, **42**, 9072–9081.
144 J. D. Ferry and J. D. Ferry, *Viscoelastic Properties of Polymers*, John Wiley & Sons, 1980.
145 S. B. Ross-Murphy, *Polym. Gels Netw.*, 1994, **2**, 229–237.
146 G. M. Kavanagh and S. B. Ross-Murphy, *Prog. Polym. Sci.*, 1998, **23**, 533–562.
147 A. Bossion, R. H. Aguirresarobe, L. Irusta, D. Taton, H. Cramail, E. Grau, D. Mecerreyes, C. Su, G. Liu, A. J. Müller and H. Sardon, *Macromolecules*, 2018, **51**, 5556-5566.

148 A. Z. Wilczewska, K. Niemirowicz, K. H. Markiewicz and H. Car, *Pharmacol. Rep.*, 2012, **64**, 1020–1037.
149 D. Crespy and K. Landfester, *Beilstein J. Org. Chem.*, 2010, **6**, 1132–1148.
150 K. Piradashvili, E. M. Alexandrino, F. R. Wurm and K. Landfester, *Chem. Rev.*, 2016, **116**, 2141–2169.
151 Y. Song, J.-B. Fan and S. Wang, *Mater. Chem. Front.*, 2017, **1**, 1028–1040.
152 C. N. R. Rao and K. P. Kalyanikutty, *Acc. Chem. Res.*, 2008, **41**, 489–499.
153 D. Crespy, M. Stark, C. Hoffmann-Richter, U. Ziener and K. Landfester, *Macromolecules*, 2007, **40**, 3122–3135.
154 J. M. Asua, *Prog. Polym. Sci.*, 2002, **27**, 1283–1346.
155 S. L. Kwolek and P. W. Morgan, *J. Polym. Sci. A*, 1964, **2**, 2693–2703.
156 M. W. Schmidt, K. K. Baldridge, J. A. Boatz, S. T. Elbert, M. S. Gordon, J. H. Jensen, S. Koseki, N. Matsunaga, K. A. Nguyen, S. Su, T. L. Windus, M. Dupuis and J. A. Montgomery, *J. Comput. Chem.*, 1993, **14**, 1347–1363.
157 S. Grimme, J. Antony, S. Ehrlich and H. Krieg, *J. Chem. Phys.*, 2010, **132**, 154104.
158 A. D. Becke, *J. Chem. Phys.*, 1993, **98**, 5648–5652.
159 C. Lee, W. Yang and R. G. Parr, *Phys. Rev. B*, 1988, **37**, 785–789.
160 S. H. Vosko, L. Wilk and M. Nusair, *Can. J. Phys.*, 1980, **58**, 1200–1211.
161 P. J. Stephens, F. J. Devlin, C. F. Chabalowski and M. J. Frisch, *J. Phys. Chem.*, 1994, **98**, 11623–11627.
162 V. Barone and M. Cossi, *J. Phys. Chem. A*, 1998, **102**, 1995–2001.
163 M. Cossi, N. Rega, G. Scalmani and V. Barone, *J. Comput. Chem.*, 2003, **24**, 669–681.
164 G. O. Jones, J. M. García, H. W. Horn and J. L. Hedrick, *Org. Lett.*, 2014, **16**, 5502–5505.
165 C. Yang, J. P. K. Tan, W. Cheng, A. B. E. Attia, C. T. Y. Ting, A. Nelson, J. L. Hedrick and Y.-Y. Yang, *Nano Today*, 2010, **5**, 515–523.
166 C. Yang, A. B. Ebrahim Attia, J. P. K. Tan, X. Ke, S. Gao, J. L. Hedrick and Y.-Y. Yang, *Biomaterials*, 2012, **33**, 2971–2979.
167 S. García-Gallego, A. M. Nyström and M. Malkoch, *Prog. Polym. Sci.*, 2015, **48**, 85–110.
168 S. Tempelaar, L. Mespouille, O. Coulembier, P. Dubois and A. P. Dove, *Chem. Soc. Rev.*, 2013, **42**, 1312–1336.
169 C. Bartolini, L. Mespouille, I. Verbruggen, R. Willem and P. Dubois, *Soft Matter*, 2011, **7**, 9628–9637.
170 A. Wang, H. Gao, Y. Sun, Y. Sun, Y.-W. Yang, G. Wu, Y. Wang, Y. Fan and J. Ma, *Int. J. Pharm.*, 2013, **441**, 30–39.
171 H. Li, Y. Cui, J. Sui, S. Bian, Y. Sun, J. Liang, Y. Fan and X. Zhang, *ACS Appl. Mater. Interfaces*, 2015, **7**, 15855–15865.
172 E. Cancès, B. Mennucci and J. Tomasi, *J. Chem. Phys.*, 1997, **107**, 3032–3041.
173 H. Sardon, J. P. K. Tan, J. M. W. Chan, D. Mantione, D. Mecerreyes, J. L. Hedrick and Y. Y. Yang, *Macromol. Rapid Commun.*, 2015, **36**, 1761–1767.

6.2. List of figures

6.3. List of schemes

6.4. List of tables

6.5. List of publications

- **Amaury Bossion**, Ion Olazabal, Robert H. Aguirresarobe, Sara Marina, Lourdes Irusta, Daniel Taton and Haritz Sardon. *Synthesis of self-healable waterborne isocyanate-free poly(hydroxyurethane)-based supramolecular networks by ionic interactions*. ACS Sustainable Chemistry and Engineering. In preparation, 2018

- **Amaury Bossion**, Katherine V Heifferon, Leire Meabe, Nicolas Zivic, Daniel Taton, James L. Hedrick, Timothy E. Long, Haritz Sardon. *Opportunities of organocatalysis in the synthesis of polymers via step-growth methods*. Progress in Polymer Science. Minor revision, 2018.

- **Amaury Bossion**, Katherine V Heifferon, Nicolas Zivic, Daniel Taton, Timothy E. Long, Haritz Sardon. *Organocatalyzed Step-Growth Polymerization*. Polymer Chemistry Series; The Royal Society of Chemistry, 2018.

- **Amaury Bossion**, Robert H. Aguirresarobe, Lourdes Irusta, Daniel Taton, Henri Cramail, Etienne Grau, David Mecerreyes, Cui Su, Guoming Liu, Alejandro J. Müller and Haritz Sardon. *Unexpected synthesis of segmented poly(hydroxyurea-urethane)s from dicyclic carbonates and diamines by organocatalysis*. Macromolecules, 2018, 51 (15), 5556–5566.

- Alexander Y. Yuen, **Amaury Bossion**, Antonio Veloso, David Mecerreyes, James L. Hedrick, Andrew P. Dove and Haritz Sardon. *Efficient polymerization and post-modification of N-substituted eight-membered cyclic carbonates containing allyl groups.* Polym. Chem., 2018, 9, 2458-2467.

- Alexander Y. Yuen, Elena Lopez-Martinez, Enrique Gomez-Bengoa, Aitziber L. Cortajarena, Robert H. Aguirresarobe, **Amaury Bossion**, David Mecerreyes, James L. Hedrick, Yi Yan Yang, and Haritz Sardon. *Preparation of Biodegradable Cationic Polycarbonates and Hydrogels Through the Direct Polymerization of Quaternized Cyclic Carbonates.* ACS Biomater. Sci. Eng., 2017, *3* (8), 1567–1575.

- **Amaury Bossion**, Gavin O. Jones, Daniel Taton, David Mecerreyes, James L. Hedrick, Zhan Yuin Ong, Yi Yan Yang, and Haritz Sardon. *Non-Isocyanate Polyurethane Soft Nanoparticles Obtained by Surfactant-Assisted Interfacial Polymerization.* Langmuir, 2017, 33, 1959−1968.

- Alexander Yuen, **Amaury Bossion**, Enrique Gómez-Bengoa, Fernando Ruipérez, Mehmet Isik, James L. Hedrick, David Mecerreyes, Yi Yan Yang and Haritz Sardon. *Room temperature synthesis of non-isocyanate polyurethanes (NIPUs) using highly reactive N-substituted 8-membered cyclic carbonates.* Polym. Chem., 2016, 7, 2105-2111

Appendix

APPENDIX CHAPTER 2

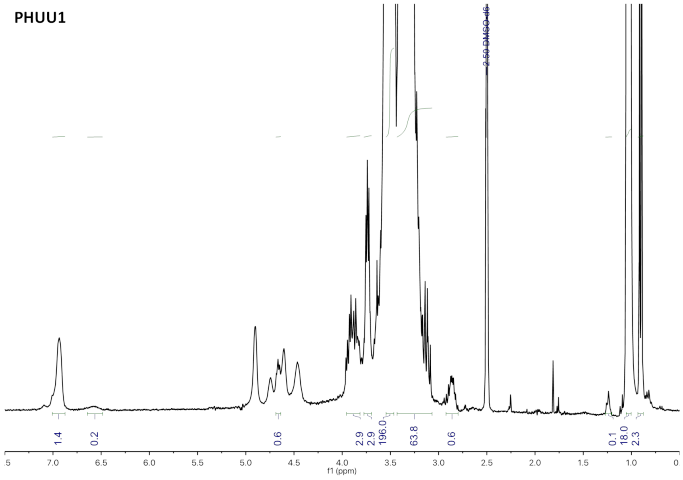

Figure S1. ^{1}H NMR of PHUU1 (300 MHz, DMSO-d_6) δ (ppm) = 6.93 (bs, 1.4H, N*H*(CO)O), 6,58 (bs, 0.2H, N*H*(CO)O), 4.90 (bs, O*H*), 4.74 (bs, O*H*), 4.67 (m, 0.6H, *CH*O(CO)N), 3.96-3.82 (m, 2.9H, CH_2OCH_2), 3.74 (m, 2.9H, C*H*OH), 3.64-2.80 (m, 260H, CH_2O and CH_2NH), 1.24 (s, 0.1H, CH_3), 1.03 (m, 18H, CH_3), 0.91-0.89 (m, 2.3H, CH_3). The ratio urethane/urea calculated from the ^{1}H NMR is 100/0.

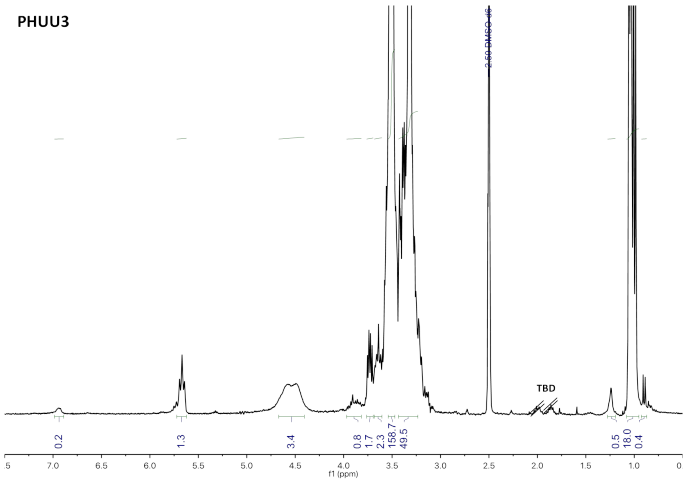

Figure S2. ^{1}H NMR of PHUU3 (300 MHz, DMSO-d_6) δ (ppm) = 6.94 (bs, 0.2H, N*H*(CO)O), 5.67 (m, 1.5H, N*H*(CO)N*H*), 4.57-4.48 (bs, O*H* and *CH*O(CO)N), 3.96-3.83 (m, 0.8H, CH_2OCH_2), 3.74 (m, 1.7H, C*H*OH), 3.64-3.20 (m, 210H, CH_2O and CH_2NH), 1.24 (s, 0.5H, CH_3), 1.03 (m, 18H, CH_3), 0.91-0.89 (m, 0.4H, CH_3). The ratio urethane/urea calculated from the ^{1}H NMR is 23/77.

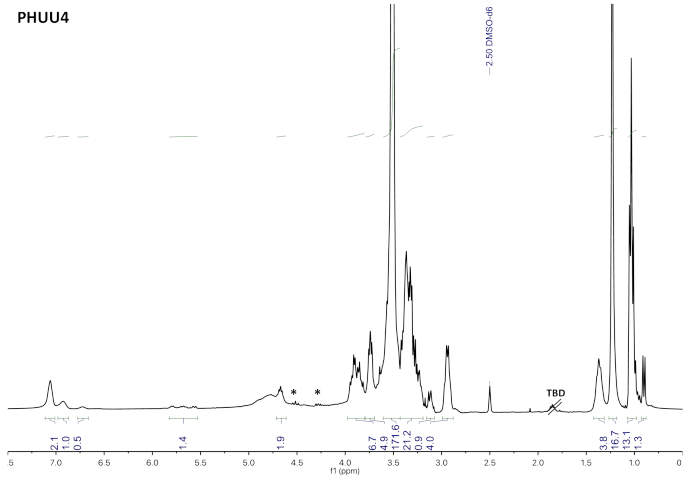

Figure S3. ^{1}H NMR of PHUU4 (300 MHz, DMSO-d_6) δ (ppm) = 7.06 (bs, 2.1H, N*H*(CO)O), 6.92 (bs, 1.0H, N*H*(CO)O), 6,72 (bs, 0.5H, N*H*(CO)O), 5.80-5.65 (m, 1.4H, N*H*(CO)N*H*), 4.90 (s, O*H*), 4.80 (s, O*H*), 4.67 (m, 1.9H, *CH*O(CO)N), 3.95-3.82 (m, 6.7H, CH_2OCH_2), 3.74 (m, 4.9H, C*H*OH), 3.51-3.11 (m, 194H, CH_2O), 2.94 (q, 4H, CH_2NH), 1.37 (m, 3.8H, CH_2), 1.23 (s, 16.7H, CH_2), 1.03 (m, 13.1H, CH_3), 0.91-0.89 (m, 1.3H, CH_3). Residual monomer has been labeled with *.

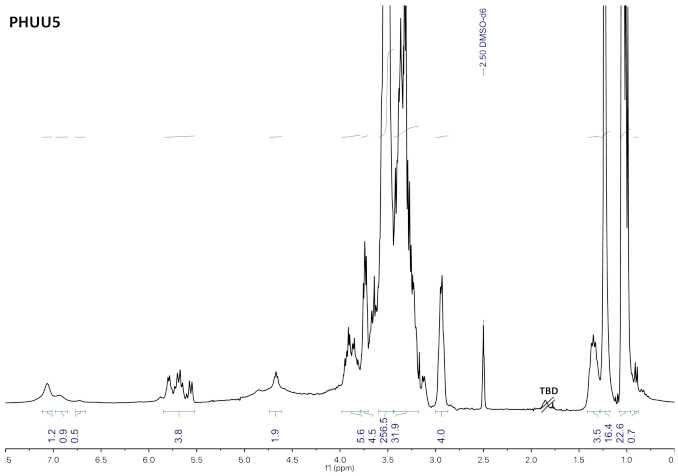

Figure S4. ^{1}H NMR of PHUU5 (300 MHz, DMSO-d_6) δ (ppm) = 7.06 (bs, 1.2H, N*H*(CO)O), 6.92 (bs, 0.9H, N*H*(CO)O), 6,72 (bs, 0.5H, N*H*(CO)O), 5.80-5.65 (m, 3.8H, N*H*(CO)N*H*), 4.90 (s, O*H*), 4.80 (s, O*H*), 4.67 (m, 1.9H, *CH*O(CO)N), 3.95-3.82 (m, 5.6H, CH_2OCH_2), 3.74 (m, 4.5H, C*H*OH), 3.51-3.11 (m, 288H, CH_2O), 2.94 (q, 4H, CH_2NH), 1.37 (m, 3.5H, CH_2), 1.23 (s, 16.4H, CH_2), 1.03 (m, 22.6H, CH_3), 0.91-0.89 (m, 0.7H, CH_3). The ratio urethane/urea calculated from the ^{1}H NMR is 58/42**.**

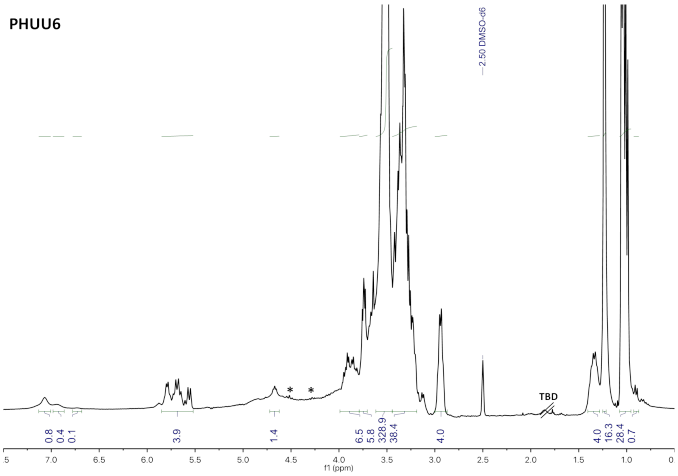

Figure S5. ^{1}H NMR of PHUU6 (300 MHz, DMSO-d_6) δ (ppm) = 7.07 (bs, 0.8H, N*H*(CO)O), 6.93 (bs, 0.4H, N*H*(CO)O), 6,72 (bs, 0.1H, N*H*(CO)O), 5.80-5.65 (m, 3.9H, N*H*(CO)N*H*), 4.90 (s, O*H*), 4.80 (s, O*H*), 4.67 (m, 1.4H,*CH*O(CO)N), 3.95-3.82 (m, 6.5H, CH_2OCH_2), 3.74 (m, 5.8H, C*H*OH), 3.51-3.11 (m, 367H, CH_2O), 2.94 (q, 4H, CH_2NH), 1.37 (m, 4H, CH_2), 1.23 (s, 16.3H, CH_2), 1.03 (m, 28.4H, CH_3), 0.91-0.89 (m, 0.7H, CH_3). Residual monomer has been labeled with *. The ratio urethane/urea calculated from the ^{1}H NMR is 40/60.

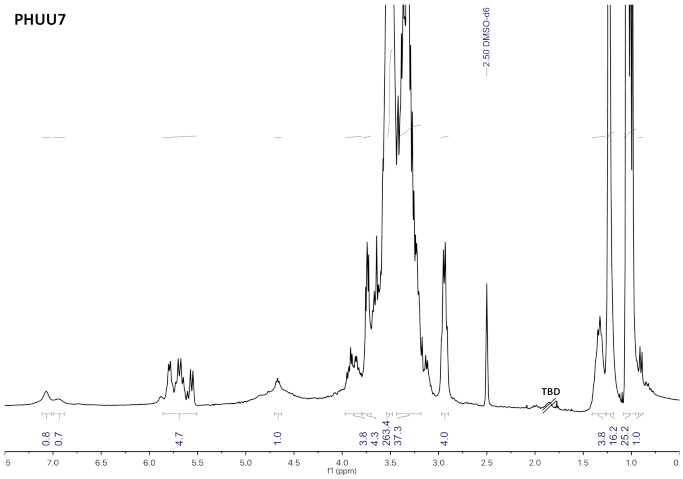

Figure S6. ^{1}H NMR of PHUU7 (300 MHz, DMSO-d_6) δ (ppm) = 7.06 (bs, 0.8H, N*H*(CO)O), 6.95 (bs, 0.7H, N*H*(CO)O), 5.80-5.65 (m, 4.7H, N*H*(CO)N*H*), 4.90 (s, O*H*), 4.80 (s, O*H*), 4.67 (m, 1H, *CH*O(CO)N), 3.95-3.82 (m, 3.8H, CH_2OCH_2), 3.74 (m, 4.3H, C*H*OH), 3.51-3.11 (m, 300H, CH_2O), 2.94 (q, 4H, CH_2NH), 1.37 (m, 3.8H, CH_2), 1.23 (s, 16.2H, CH_2), 1.03 (m, 25.2H, CH_3), 0.91-0.89 (m, 1H, CH_3). The ratio urethane/urea calculated from the ^{1}H NMR is 39/61.

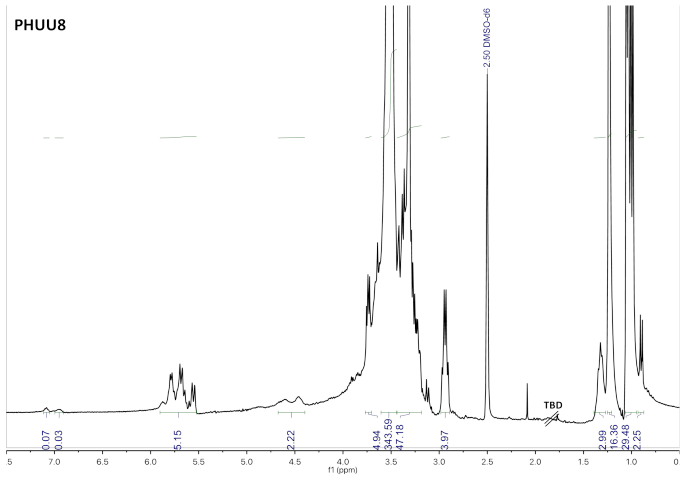

Figure S7. ^{1}H NMR of PHUU8 (300 MHz, DMSO-d_6) δ (ppm) = 7.06 (bs, 0.1H, N*H*(CO)O), 6.92 (bs, 0.03H, N*H*(CO)O), 5.80-5.65 (m, 5.2H, N*H*(CO)N*H*), 4.60 (m, 2.2H, *CH*O(CO)N), 3.74 (m, 4.9H, C*H*OH), 3.51-3.11 (m, 391H, CH_2O), 2.94 (q, 4H, CH_2NH), 1.37 (m, 3H, CH_2), 1.23 (s, 16.4H, CH_2), 1.03 (m, 29.5H, CH_3), 0.91-0.89 (m, 2.3H, CH_3). The ratio urethane/urea calculated from the ^{1}H NMR is 5/95.

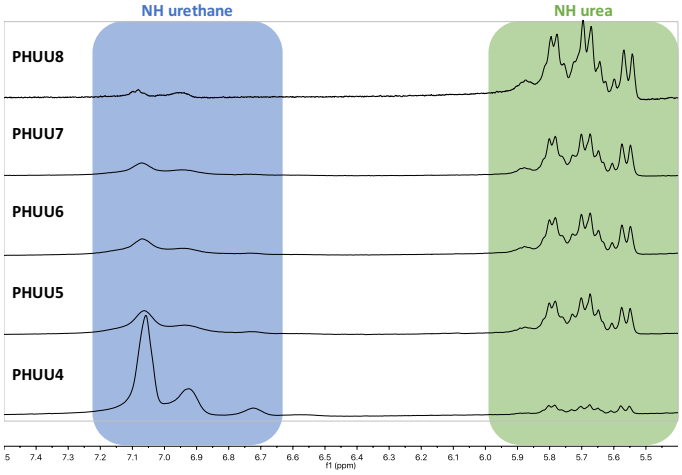

Figure S8. Evolution of the NH bands in the ^{1}H NMR from PHUU4 to PHUU8.

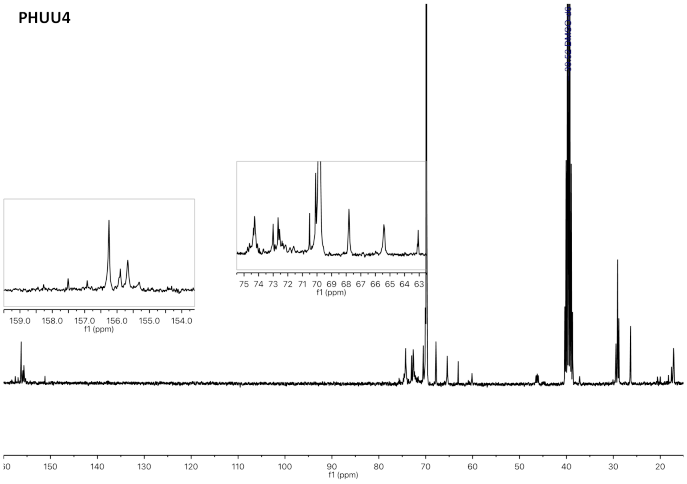

Figure S9. ^{13}C NMR of PHUU4 (75 MHz, DMSO-d_6) δ (ppm) = 158.3, 157.5, 156.9 (–NH–(C=O)–NH–), 156.3, 155.9, 155.7, 155.3 (–NH–(C=O)–O–), 75.8, 75.7, 75.5, 74.7-74.0 (m), 73.0-71.6 (m), 70.5, 70.1, 69.8, 67.8, 65.4, 63.1, 60.1 (CH_2O and CHO), 46.5, 46.4, 46.3, 46.2, 46.1, 46.0, 45.0, 44.8, 44.7, 44.6 (CH_2NH), 29.4, 29.1, 28.8, 26.3, 20.6, 19.9, 18.3, 17.6, 17.3, 17.2, 17.1 (CH_3).

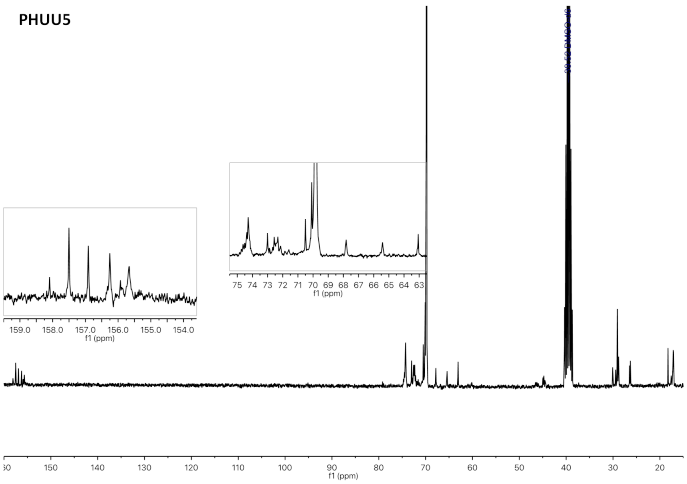

Figure S10. ^{13}C NMR of PHUU5 (75 MHz, DMSO-d_6) δ (ppm) = 158.1, 157.5, 156.9 (–NH–(C=O)–NH–), 156.3, 155.9, 155.7 (–NH–(C=O)–O–),74.7-74.0 (m), 73.0-71.6 (m), 70.5, 70.1, 67.8, 65.4, 63.1 (CH_2O and CHO), 46.5, 46.3, 46.2, 46.0, 44.9, 44.8, 44.7, 44.6, 44.5 (CH_2NH), 30.1, 29.4, 29.1, 28.9, 28.8, 26.5, 26.3, 18.3, 17.6, 17.2, 17.1 (CH_3).

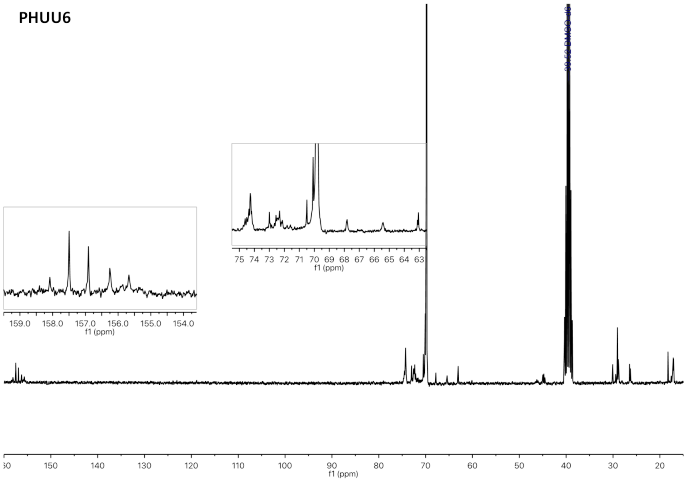

Figure S11. ^{13}C NMR of PHUU6 (75 MHz, DMSO-d_6) δ (ppm) = 158.1, 157.5, 156.9 (–NH–(C=O)–NH–), 156.3, 155.9, 155.7 (–NH–(C=O)–O–), 74.7-74.0 (m), 73.0-71.6 (m), 70.5, 70.1, 69.8, 67.8, 65.4, 63.1 (CH_2O and CHO), 46.5, 46.3, 46.2, 46.1, 46.0, 44.9, 44.8, 44.7, 44.6, 44.5 (CH_2NH), 30.1, 20.6, 19.9, 18.3, 17.6, 17.3, 17.2, 17.1 (CH_3).

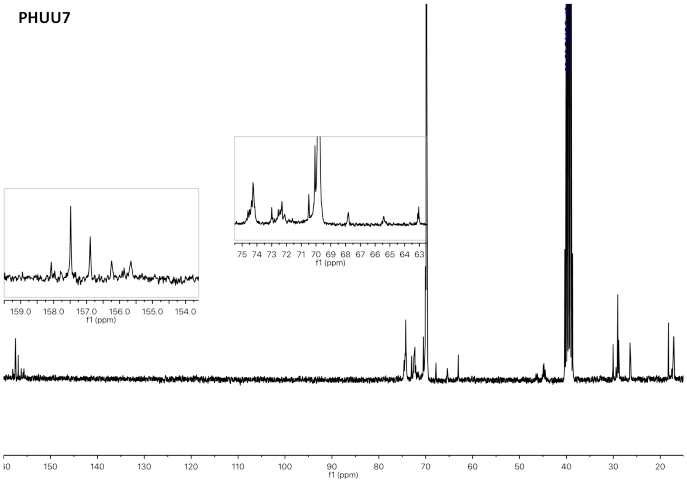

Figure S12. ^{13}C NMR of PHUU7 (75 MHz, DMSO-d_6) δ (ppm) = 158.1, 157.5, 156.9 (–NH–(C=O)–NH–), 156.3, 155.9, 155.7, 155.3 (–NH–(C=O)–O–), 74.7-74.0 (m), 73.0-71.6 (m), 70.5, 70.1, 69.8, 67.8, 65.4, 63.1 (CH_2O and CHO), 46.5, 46.2, 46.0, 44.9, 44.8, 44.7, 44.6, 44.5 (CH_2NH), 30.1, 29.4, 29.1, 29.0, 28.9, 28.8, 26.5, 26.3, 18.3, 17.6, 17.2, 17.1 (CH_3).

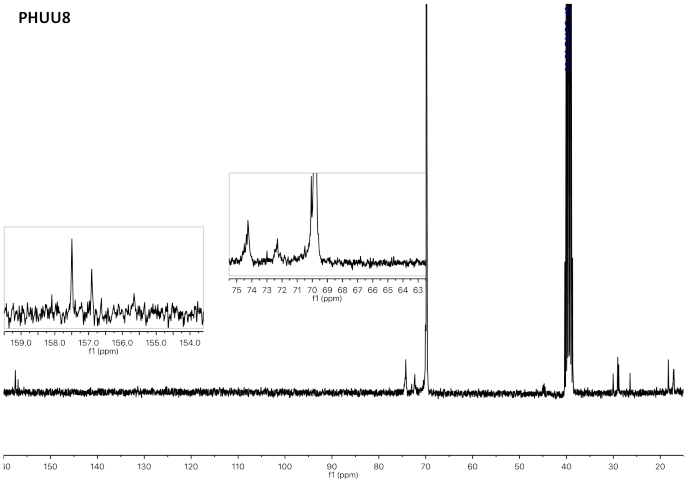

Figure S13. ^{13}C NMR of PHUU8 (75 MHz, DMSO-d_6) δ (ppm) = 158.1, 157.5, 156.9 (–NH–(C=O)–NH–), 155.7, 155.3 (–NH–(C=O)–O–), 74.6-74.0 (m), 73.0-72.1 (m), 70.5, 70.1, 69.8 (CH_2O and CHO), 44.9, 44.8, 44.7, 44.6, 44.5 (CH_2NH), 30.1, 29.1, 29.0, 28.9, 28.8, 26.4, 18.3, 17.3, 17.2, 17.1 (CH_3).

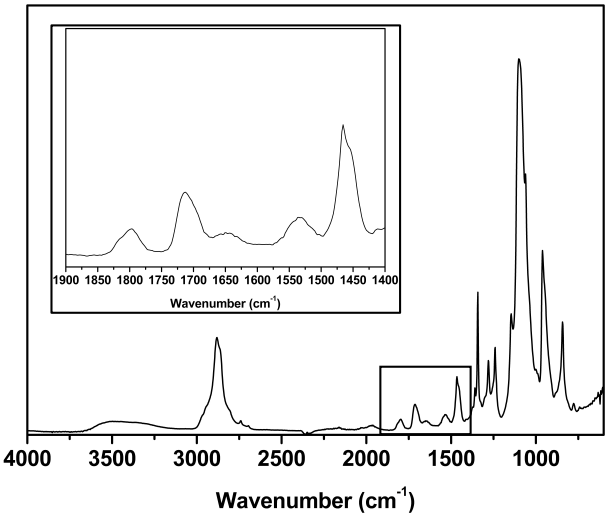

Figure S14. FTIR spectrum of PHUU1.

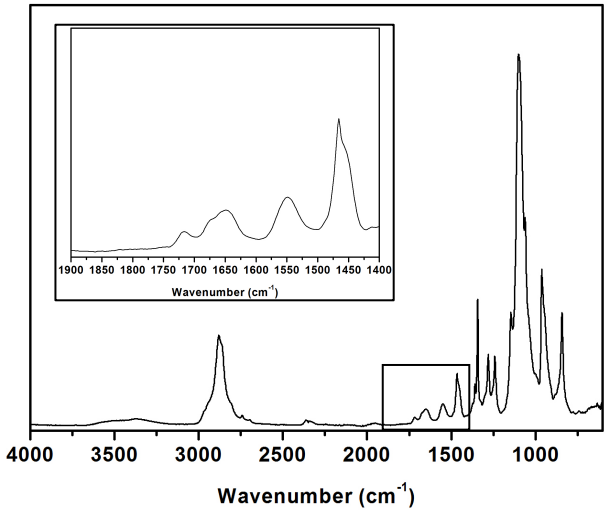

Figure S15. FTIR spectrum of PHUU3.

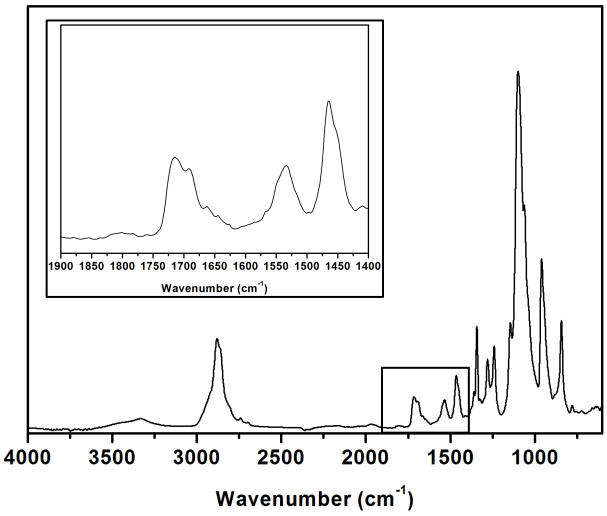

Figure S16. FTIR spectrum of PHUU4.

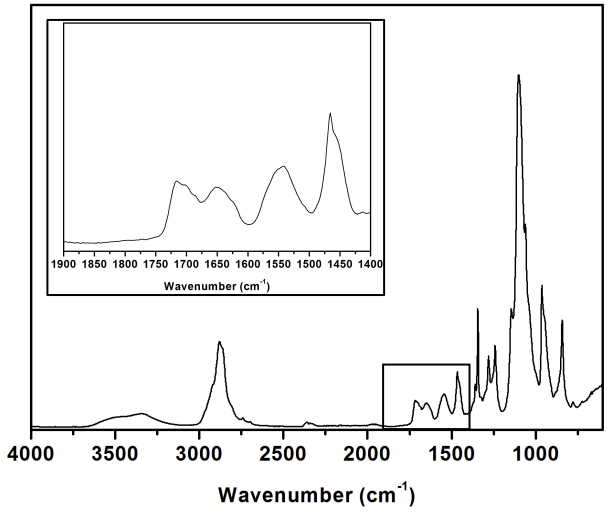

Figure S17. FTIR spectrum of PHUU5.

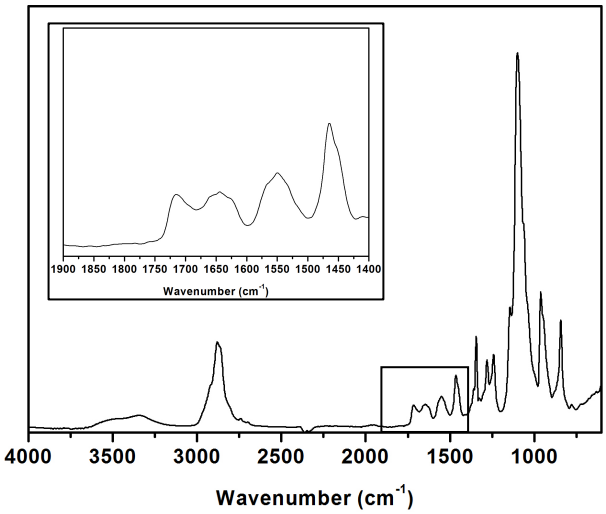

Figure S18. FTIR spectrum of PHUU6.

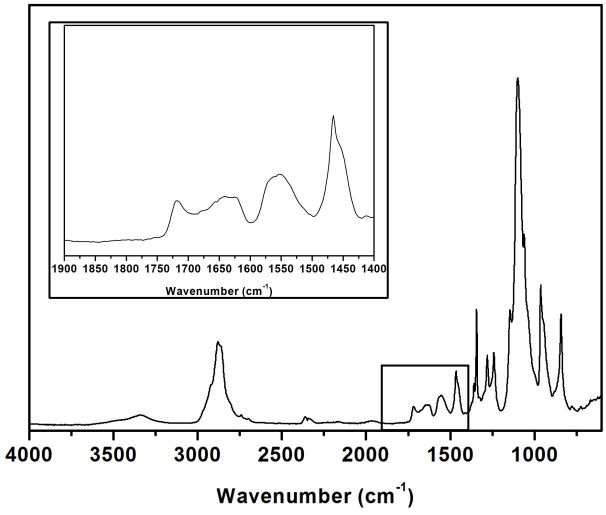

Figure S19. FTIR spectrum of PHUU7.

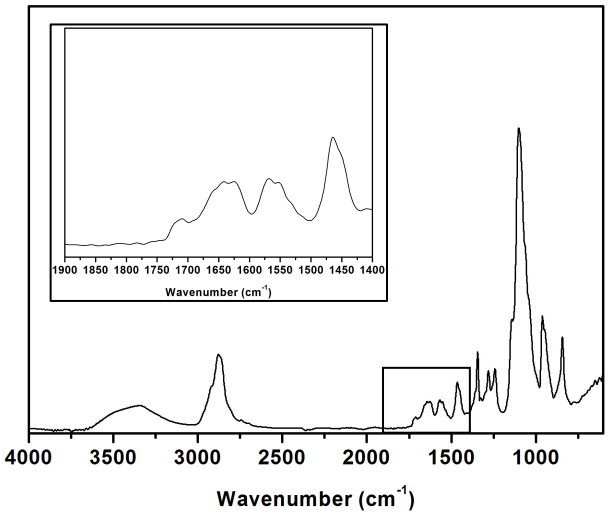

Figure S20. FTIR spectrum of PHUU8.

APPENDIX CHAPTER 3

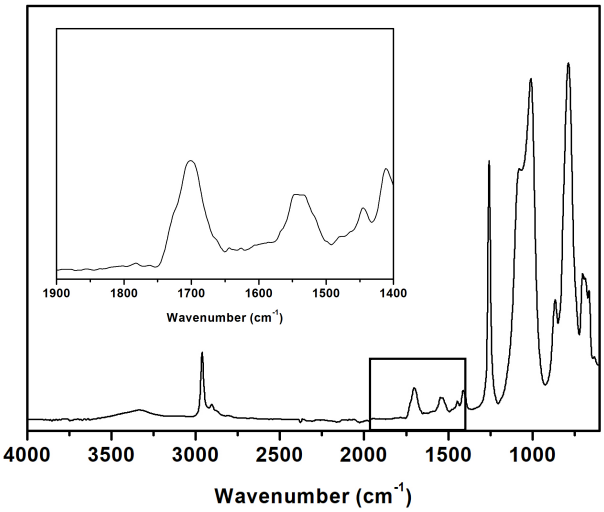

Figure S21. FTIR spectrum of WNIPU1.

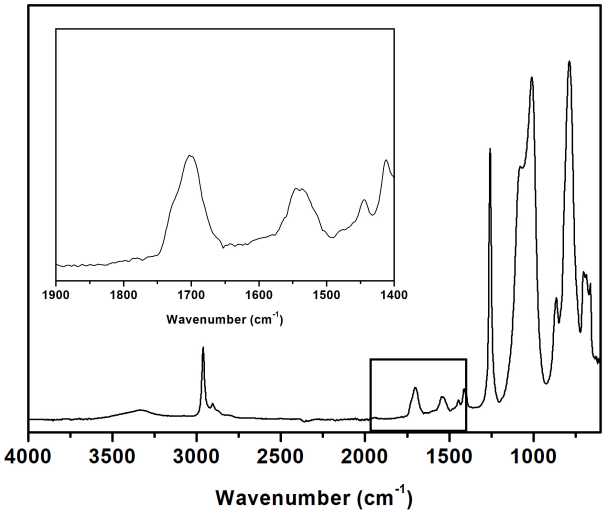

Figure S22. FTIR spectrum of WNIPU2.

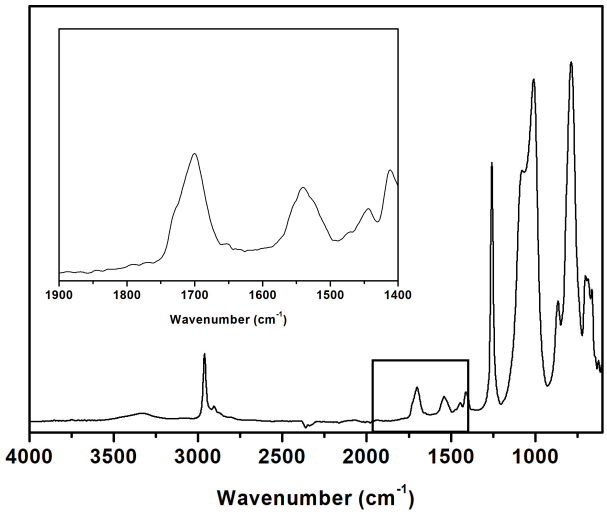

Figure S23. FTIR spectrum of WNIPU3.

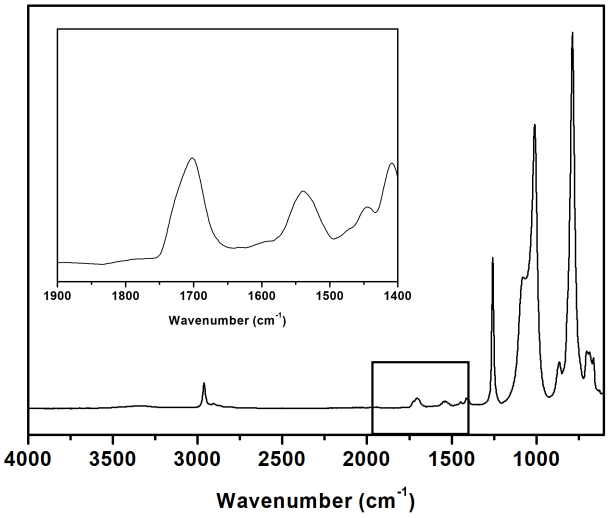

Figure S24. FTIR spectrum of WNIPU4.

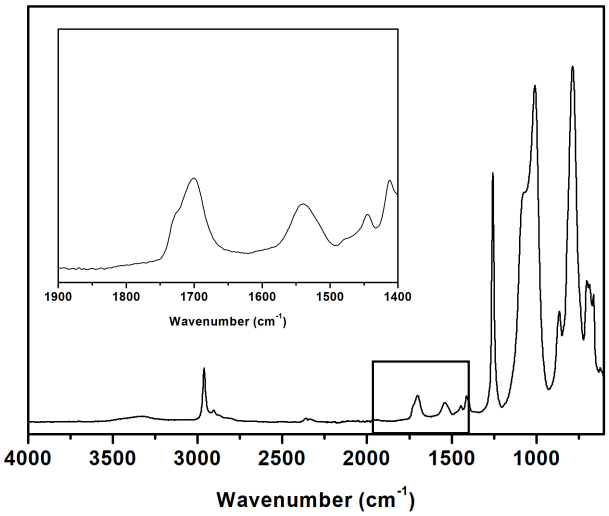

Figure S25. FTIR spectrum of WNIPU5.

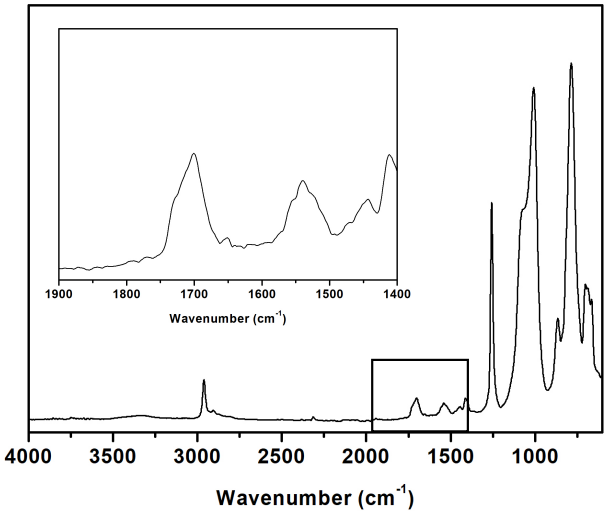

Figure S26. FTIR spectrum of WNIPU6.

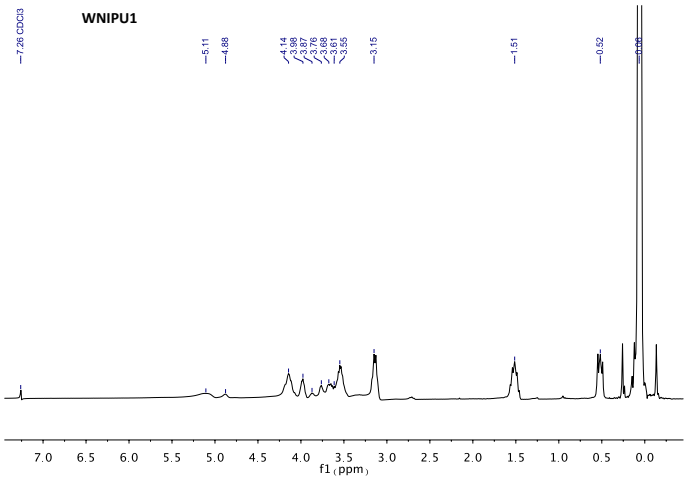

Figure S27. ^{1}H NMR of WNIPU1 (300 MHz, $CDCl_3$) δ (ppm) = 5.11 (bs, CHO*H*), 4.88 (bs, *CH*O(CO)N), 4.14 (m, *CH*$_2$O(CO)N), 3.98 (m, CHC*H*$_2$O), 3.87 (m, C*H*OH), 3.76 (m, CH$_2$CHC*H*$_2$O), 3.68-3.55 (m, C*H*$_2$OH), 3.15 (q, C*H*$_2$NH), 1.51 (quintuplet, SiCH$_2$C*H*$_2$CH$_2$NH), 0.52 (t, SiC*H*$_2$), 0.06 (s, SiC*H*$_3$).

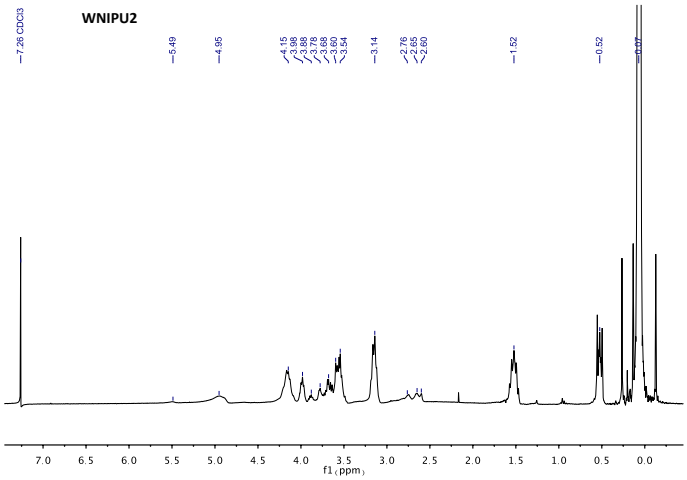

Figure S28. ^{1}H NMR of WNIPU2 (300 MHz, $CDCl_3$) δ (ppm) = 5.49 (s, CHO*H*), 4.95 (bs, *CH*O(CO)N), 4.15 (m, *CH*$_2$O(CO)N), 3.98 (m, CHC*H*$_2$O), 3.88 (m, C*H*OH), 3.78 (m, CH$_2$CHC*H*$_2$O), 3.68-3.54 (m, C*H*$_2$OH), 3.14 (q, C*H*$_2$NH), 2.76-2.60 (m, C*H*$_2$N), 1.52 (quintuplet, SiCH$_2$C*H*$_2$CH$_2$NH), 0.52 (t, SiC*H*$_2$), 0.07 (s, SiC*H*$_3$).

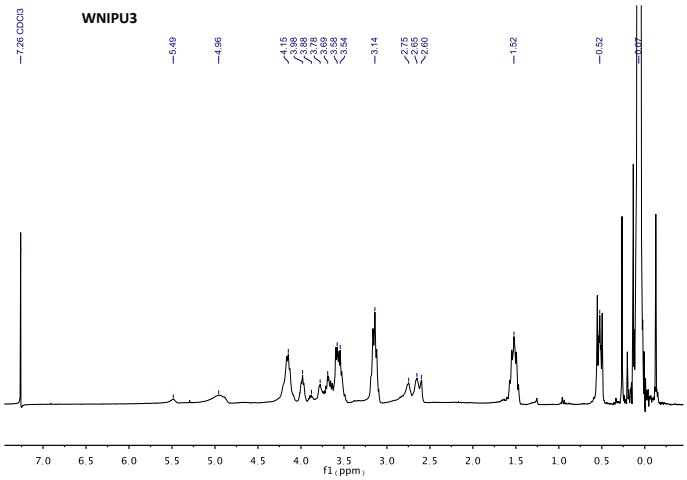

Figure S29. ^{1}H NMR of WNIPU3 (300 MHz, $CDCl_3$) δ (ppm) = 5.49 (s, CHO*H*), 4.96 (bs, *CH*O(CO)N), 4.15 (m, *CH*$_2$O(CO)N), 3.98 (m, CHC*H*$_2$O), 3.88 (m, C*H*OH), 3.78 (m, CH$_2$CHC*H*$_2$O), 3.69-3.54 (m, C*H*$_2$OH), 3.14 (q, C*H*$_2$NH), 2.75-2.60 (m, C*H*$_2$N), 1.52 (quintuplet, SiCH$_2$C*H*$_2$CH$_2$NH), 0.52 (t, SiC*H*$_2$), 0.07 (s, SiC*H*$_3$).

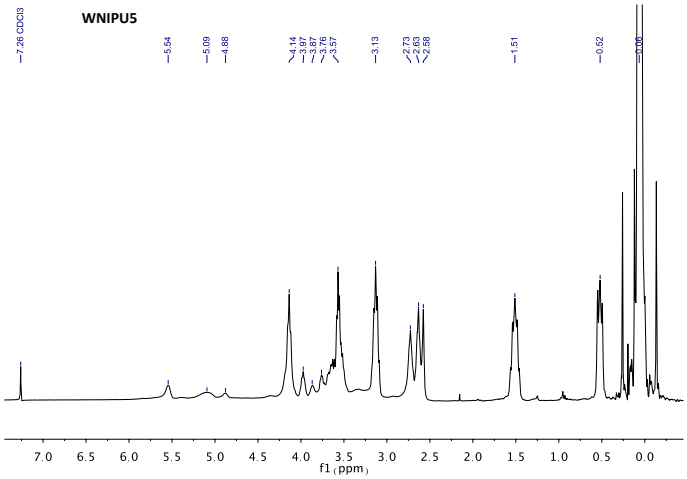

Figure S30. ^{1}H NMR of WNIPU5 (300 MHz, $CDCl_3$) δ (ppm) = 5.54 (s, CHO*H*), 5.09 (bs, CHO*H*), 4.88 (bs, *CH*O(CO)N), 4.14 (m, *CH*$_2$O(CO)N), 3.97 (m, CHC*H*$_2$O), 3.87 (m, C*H*OH), 3.76 (m, CH$_2$CHC*H*$_2$O), 3.68-3.55 (m, C*H*$_2$OH), 3.13 (q, C*H*$_2$NH), 2.73-2.58 (m, C*H*$_2$N), 1.51 (quintuplet, SiCH$_2$C*H*$_2$CH$_2$NH), 0.52 (t, SiC*H*$_2$), 0.06 (s, SiC*H*$_3$).

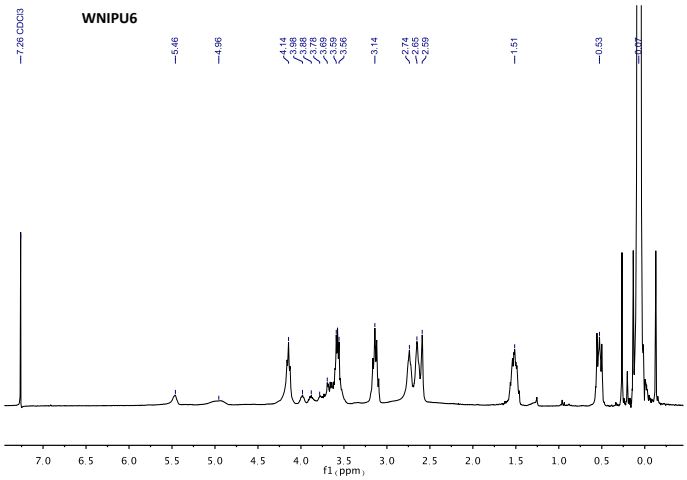

Figure S31. ^{1}H NMR of WNIPU6 (300 MHz, $CDCl_3$) δ (ppm) = 5.49 (s, CHO*H*), 4.96 (bs, *CH*O(CO)N), 4.14 (m, *CH*$_2$O(CO)N), 3.98 (m, CHC*H*$_2$O), 3.88 (m, C*H*OH), 3.78 (m, CH$_2$CHC*H*$_2$O), 3.69-3.56 (m, C*H*$_2$OH), 3.14 (q, C*H*$_2$NH), 2.74-2.59 (m, C*H*$_2$N), 1.51 (quintuplet, SiCH$_2$C*H*$_2$CH$_2$NH), 0.53 (t, SiC*H*$_2$), 0.07 (s, SiC*H*$_3$).

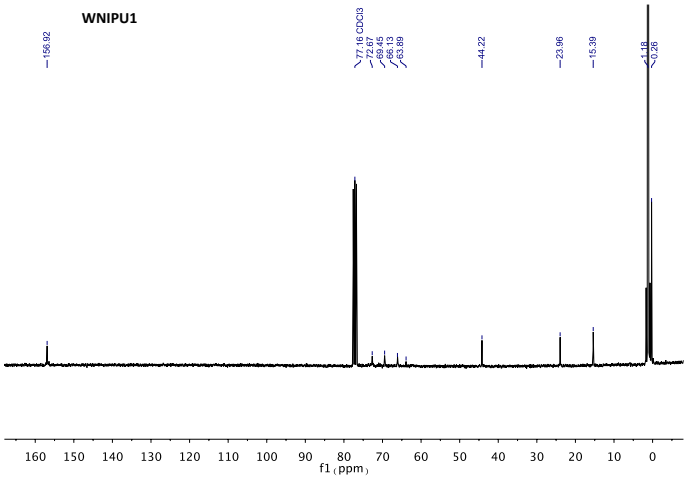

Figure S32. ^{13}C NMR of WNIPU1 (75 MHz, $CDCl_3$) δ (ppm) = 156.9 (–NH–(C=O)–O–), 72.7, 69.4, 66.1, 63.9 (CH_2O and CHO), 44.2 (CH_2NH), 23.9 (CH_2), 15.4 ($SiCH_2$), 1.2, 0.26 ($SiCH_3$).

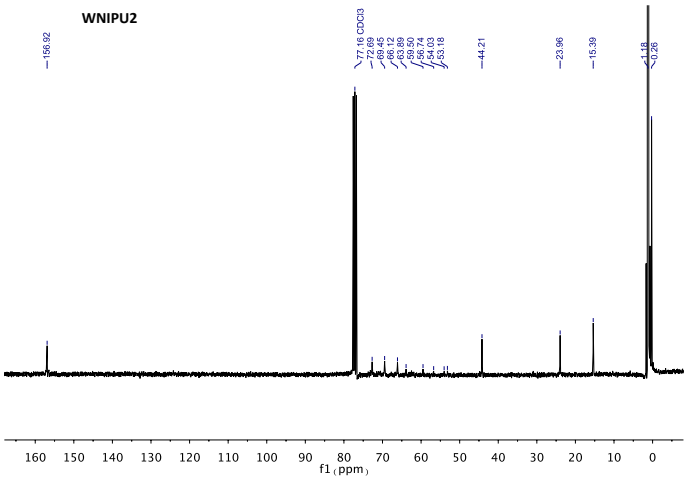

Figure S33. ^{13}C NMR of WNIPU2 (75 MHz, $CDCl_3$) δ (ppm) = 156.9 (–NH–(C=O)–O–), 72.7, 69.4, 66.1, 63.9, 59.5, 56.7, 54.0, 53.2 (CH_2O, CHO and CH_2N), 44.2 (CH_2NH), 23.9 (CH_2), 15.4 ($SiCH_2$), 1.2, 0.26 ($SiCH_3$).

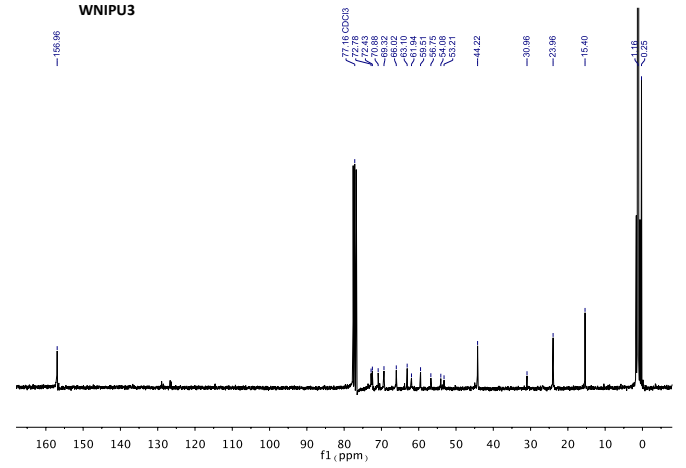

Figure S34. ^{13}C NMR of WNIPU3 (75 MHz, $CDCl_3$) δ (ppm) = 156.9 (–NH–(C=O)–O–), 72.8, 72.4, 70.1, 69.3, 66.0, 63.1, 61.9, 59.5, 56.7, 54.0, 53.2 (CH_2O, CHO and CH_2N), 44.2 (CH_2NH), 30.9, 23.9 (CH_2), 15.4 ($SiCH_2$), 1.2, 0.25 ($SiCH_3$).

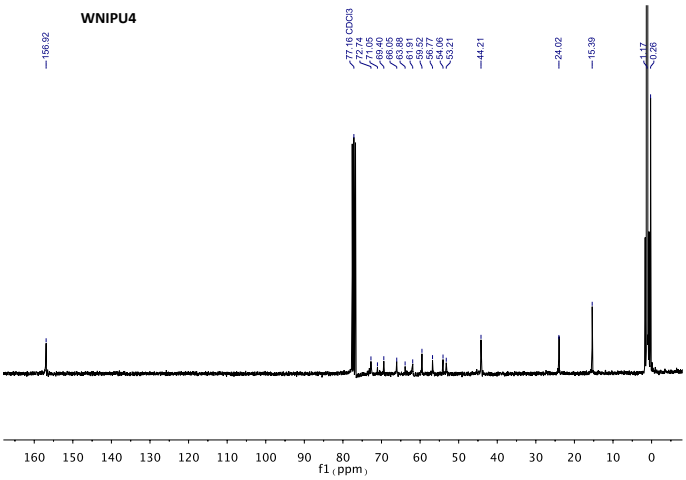

Figure S35. ^{13}C NMR of WNIPU4 (75 MHz, $CDCl_3$) δ (ppm) = 156.9 (–NH–(C=O)–O–), 72.7, 71.0, 69.4, 66.1, 63.9, 61.9, 59.5, 56.7, 54.0, 53.2 (CH_2O, CHO and CH_2N), 44.2 (CH_2NH), 24.0 (CH_2), 15.4 ($SiCH_2$), 1.2, 0.26 ($SiCH_3$).

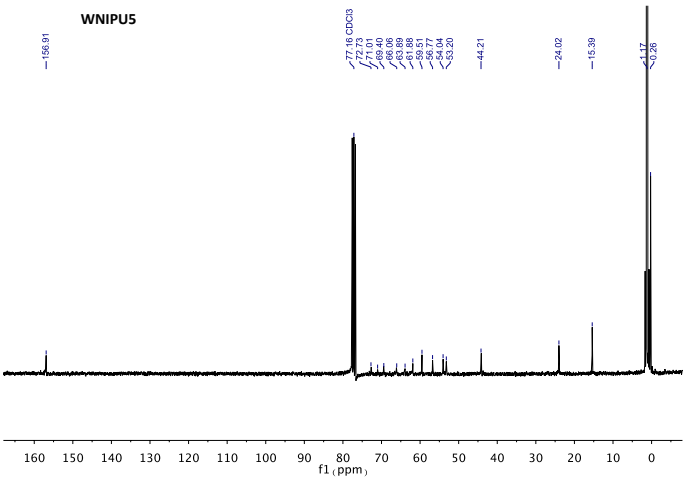

Figure S36. ^{13}C NMR of WNIPU5 (75 MHz, $CDCl_3$) δ (ppm) = 156.9 (–NH–(C=O)–O–), 72.7, 71.0, 69.4, 66.1, 63.9, 61.9, 59.5, 56.7, 54.0, 53.2 (CH_2O, CHO and CH_2N), 44.2 (CH_2NH), 24.0 (CH_2), 15.4 ($SiCH_2$), 1.2, 0.26 ($SiCH_3$).

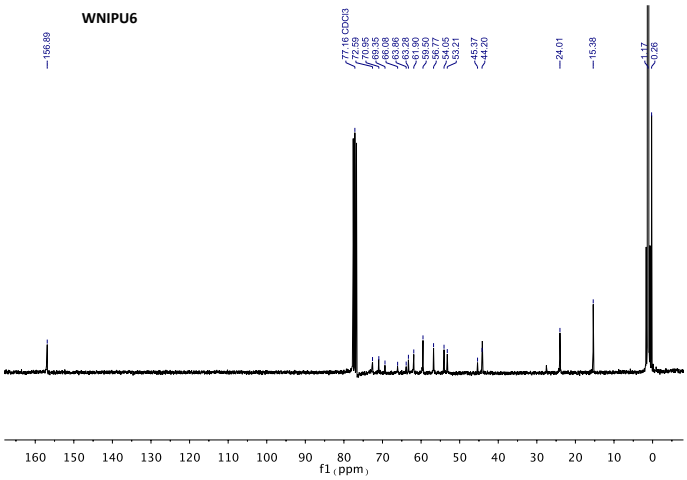

Figure S37. ^{13}C NMR of WNIPU6 (75 MHz, $CDCl_3$) δ (ppm) = 156.9 (–NH–(C=O)–O–), 72.6, 70.1, 69.3, 66.1, 63.3, 61.9, 59.5, 56.8, 54.0, 53.2 (CH_2O, CHO and CH_2N), 45.4, 44.2 (CH_2NH), 24.0 (CH_2), 15.4 ($SiCH_2$), 1.2, 0.26 ($SiCH_3$).

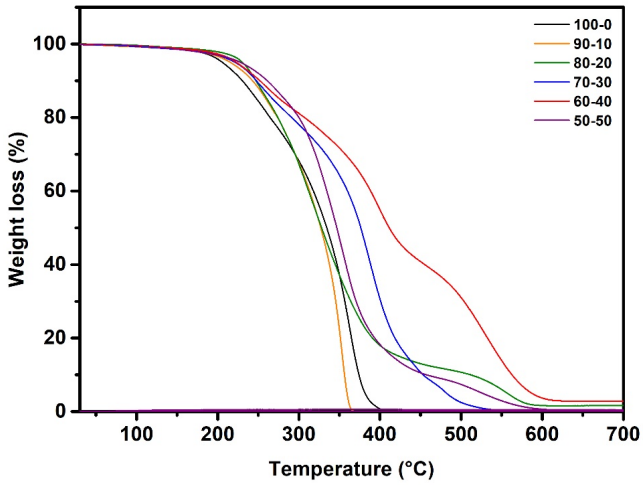

Figure S38. TGA thermograms of the synthesized poly(hydroxyurethanes).

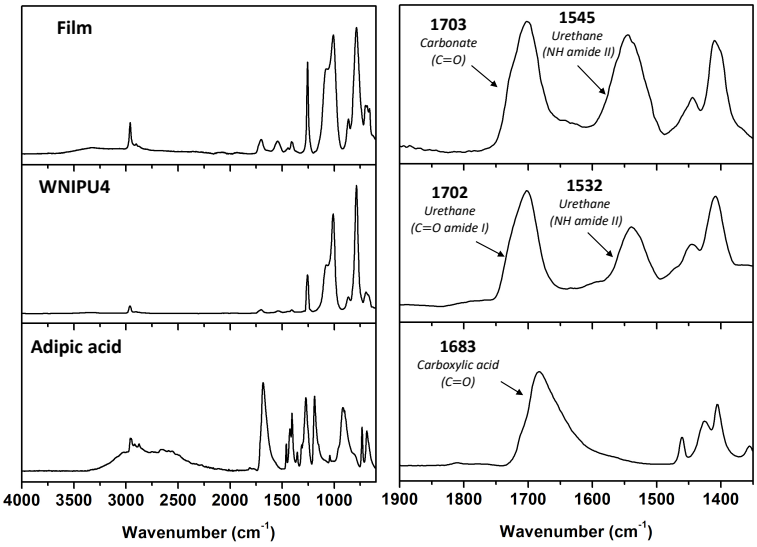

Figure S39. FTIR spectra of adipic acid, WNIPU4 and WNIPU4/adipic acid film.

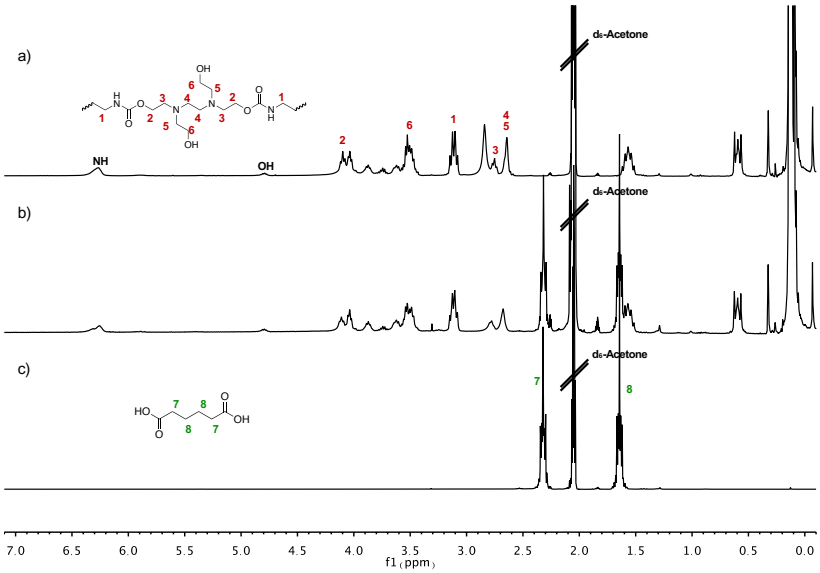

Figure S40. ^{1}H NMR (300 MHz, d_6-acetone) of a) WNIPU4, b) WNIPU4/adipic acid film and c) adipic acid showing no proton shift associated with the formation of ionic hydrogen bonds.

APPENDIX CHAPTER 4

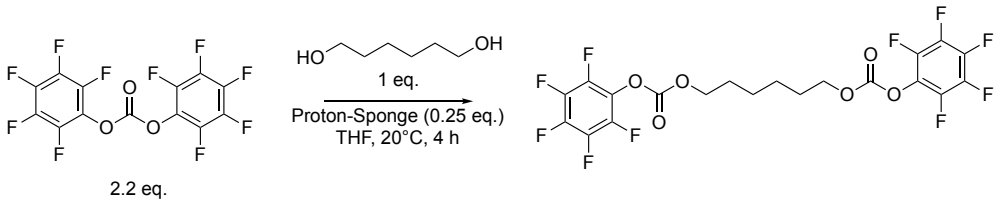

Scheme S1. Method for the synthesis of $C_6F_5O–COO–(CH_2)_6–OCO–OC_6F_5$ (Monomer A).

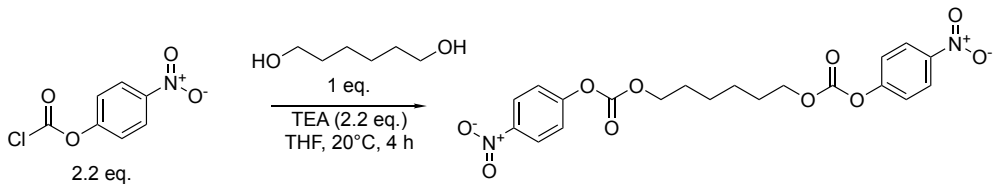

Scheme S2. Method for the synthesis of $C_6H_4NO_2O–COO–(CH_2)_6–OCO–OC_6H_4NO_2$ (Monomer B).

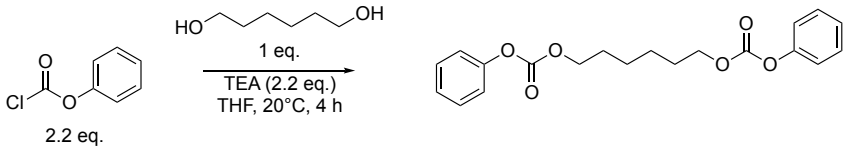

Scheme S3. Method for the synthesis of $C_6H_5O–COO–(CH_2)_6–OCO–OC_6H_5$ (Monomer C).

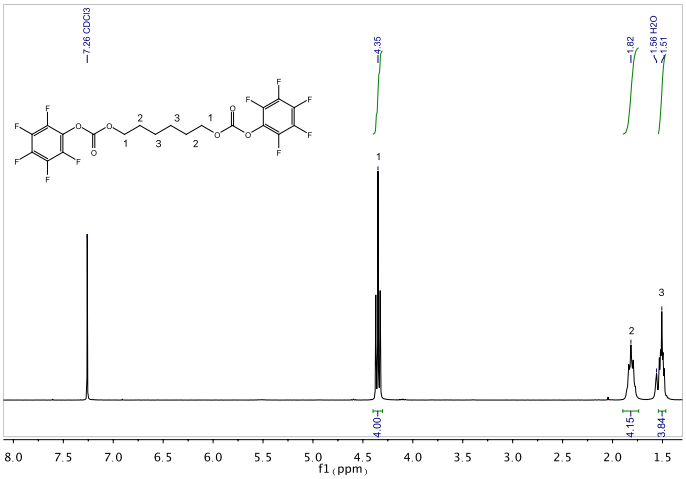

Figure S41. ^{1}H NMR (300 MHz, $CDCl_3$) of $C_6F_5O–COO–(CH_2)_6–OCO–OC_6F_5$ (Monomer A). (73% yield)

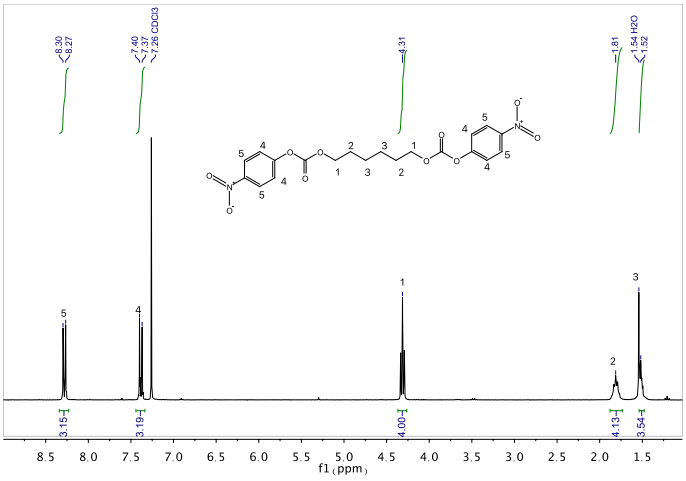

Figure S42. ^{1}H NMR (300 MHz, $CDCl_3$) of $C_6H_4NO_2O–COO–(CH_2)_6–OCO–OC_6H_4NO_2$ (Monomer B). (76% yield)

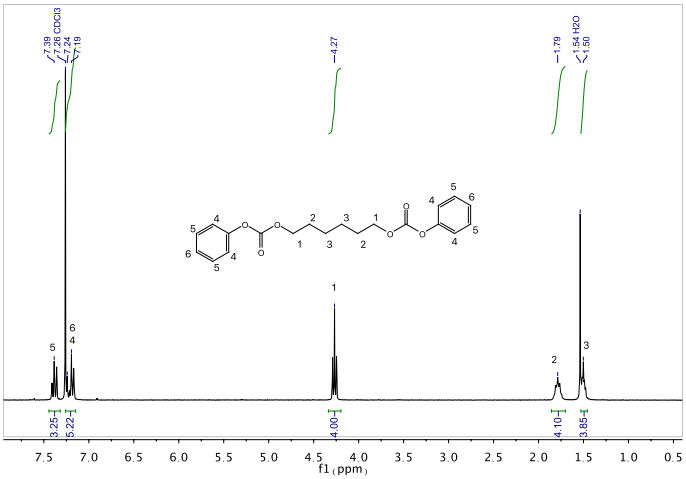

Figure S43. ^{1}H NMR (300 MHz, $CDCl_3$) of $C_6H_5O–COO–(CH_2)_6–OCO–OC_6H_5$ (Monomer C). (68% yield)

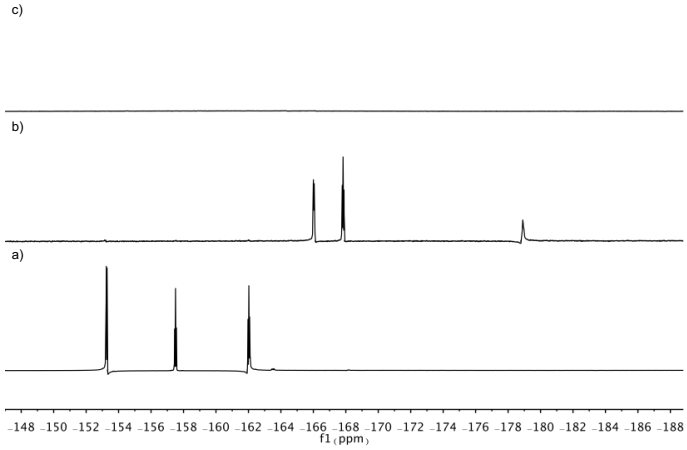

Figure S44. ^{19}F NMR (282 MHz, $CDCl_3$) of a) Monomer A, and the NIPU obtained by the interfacial polymerization (80/20 wt. % deionized water/DCM mixture) of Monomer A with PEG-diamine b) before dialysis and c) after dialysis.

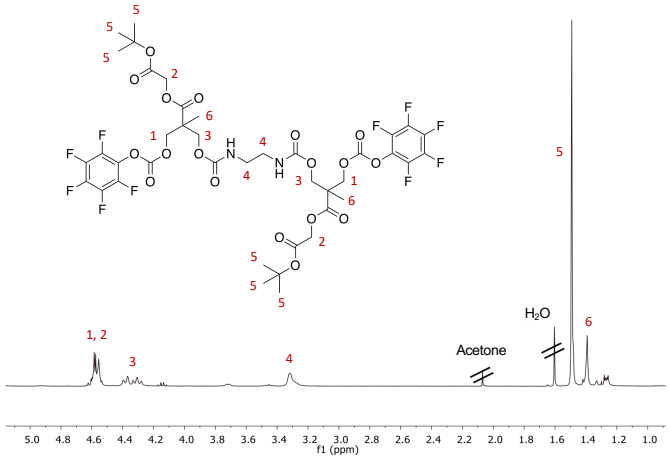

Figure S45. ^{1}H NMR (300 MHz, $CDCl_3$) of Monomer D. (73% yield)

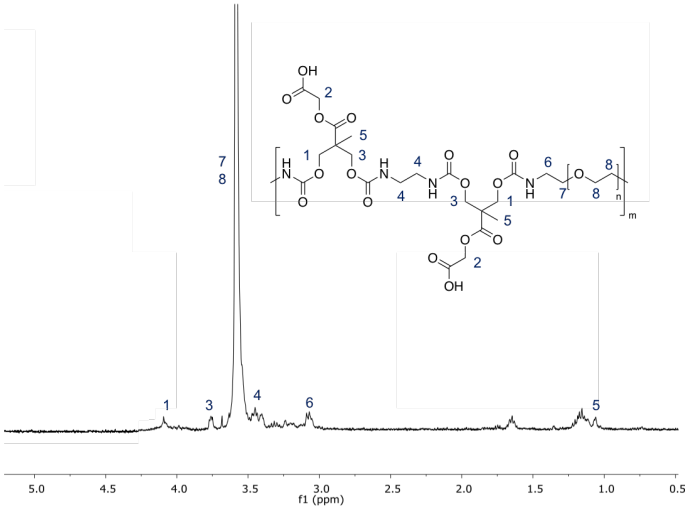

Figure S46. ^{1}H NMR (300 MHz, $CDCl_3$) of the polymer obtained from the interfacial polymerization of Monomer D with PEG-diamine (80/20 wt. % deionized water/DCM mixture) after deprotection.

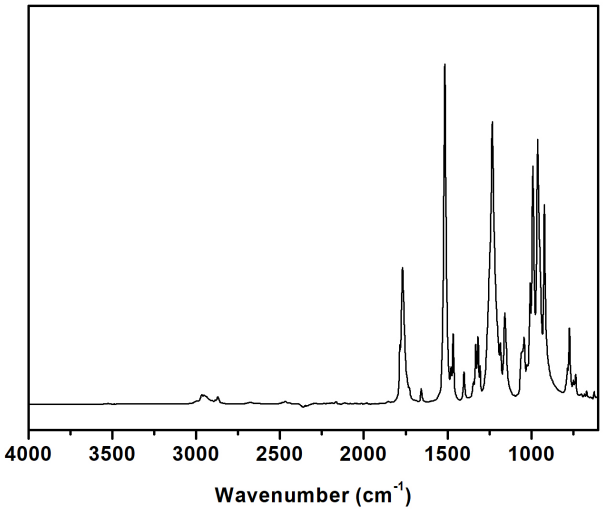

Figure S47. FTIR spectrum of $C_6F_5O–COO–(CH_2)_6–OCO–OC_6F_5$ (Monomer A).

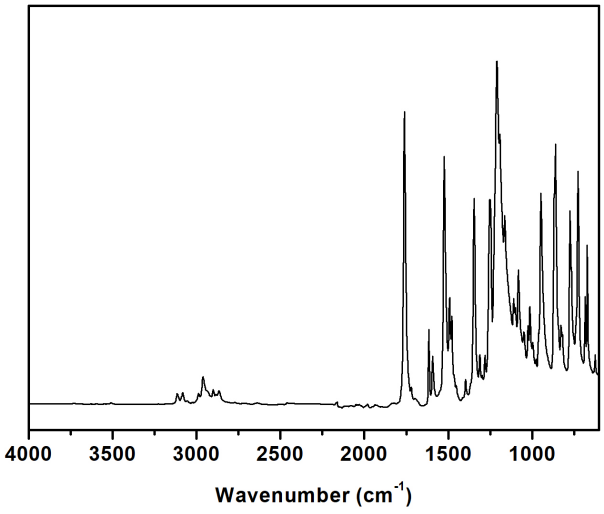

Figure S48. FTIR spectrum of $C_6H_4NO_2O–COO–(CH_2)_6–OCO–OC_6H_4NO_2$ (Monomer B).

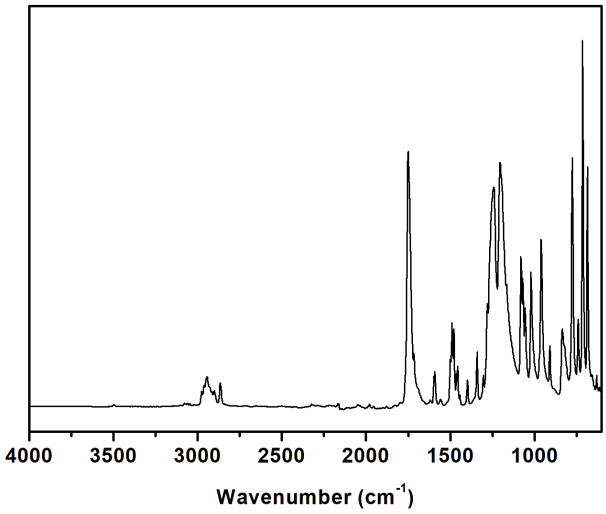

Figure S49. FTIR spectrum of $C_6H_5O–COO–(CH_2)_6–OCO–OC_6H_5$ (Monomer C).

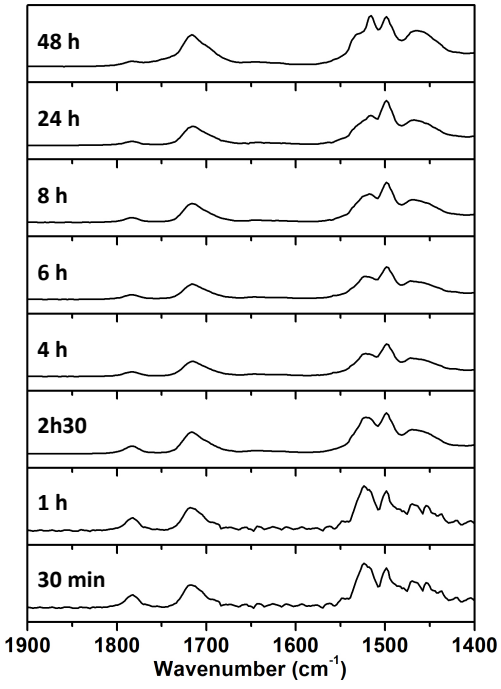

Figure S50. Scale expanded FTIR spectra at different reaction times of the polymerization between Monomer A and PEG diamine.

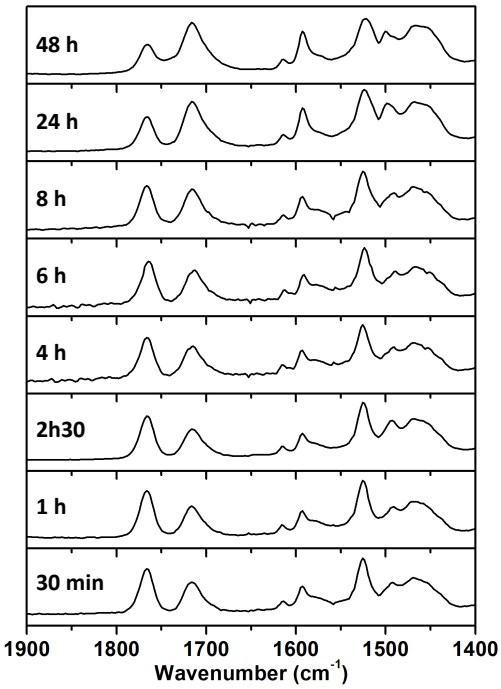

Figure S51. Scale expanded FTIR spectra at different reaction times of the polymerization between Monomer B and PEG diamine.

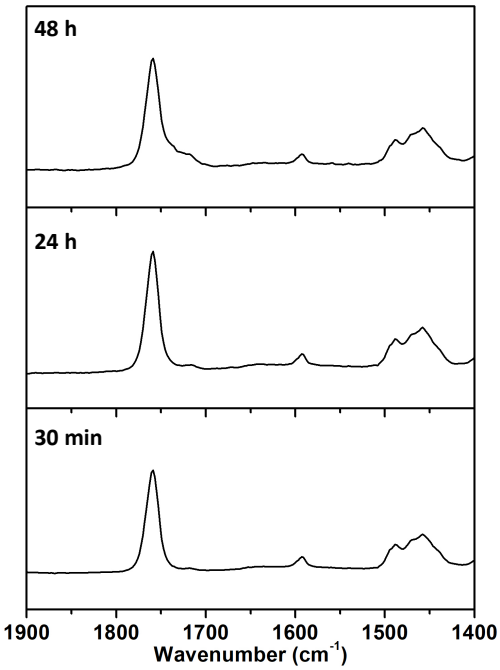

Figure S52. Scale expanded FTIR spectra at different reaction times of the polymerization between Monomer C and PEG diamine.

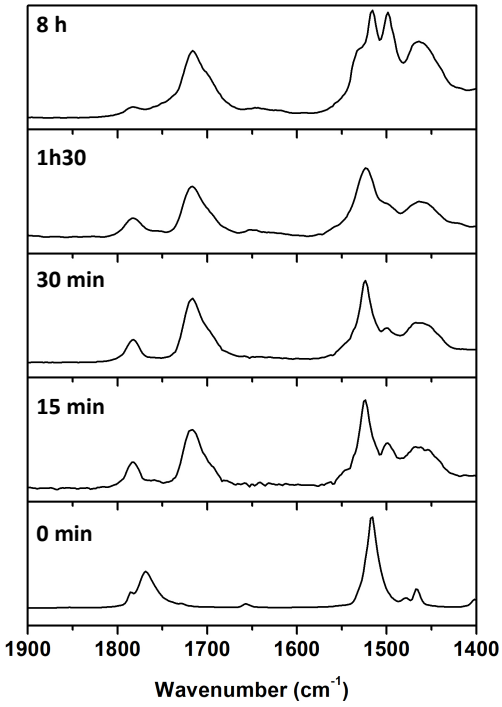

Figure S53. Scale expanded FTIR at different reaction times of the polymerization between Monomer A and PEG diamine in interfacial condition (80 % H_2O / 20 % DCM) as example.

Resumen

RESUMEN

Hoy en día, los polímeros están omnipresentes en nuestra sociedad, ya sea en los sectores de embalaje, construcción, automoción, electrónica, recreación o medicina. En 2016 la producción mundial de plásticos alcanzó los 335 millones de toneladas y en 2018 el crecimiento de la producción aumentó un 1,5 % principalmente debido a la creciente demanda de los países emergentes.

De entre todos los plásticos, los poliuretanos (PUs) representan la sexta clase de polímeros más utilizada en el mundo, con una producción mundial estimada de 18 millones de toneladas en 2016. La demanda de PU está aumentando en un promedio de 4,5 % por año. En Europa, esta demanda aumentó un 7,5 % en 2016. Estos polímeros tienen excelentes propiedades físicas y mecánicas, como su dureza, durabilidad, biocompatibilidad, elasticidad y resistencia a la abrasión. Los PUs se usan convencionalmente como espumas flexibles y rígidas para aislamiento, como materiales de sellado, para recubrimientos de alto rendimiento, como adhesivos o en el campo biomédico. Descubiertos por Otto Bayer en 1947, los PUs generalmente se sintetizan por la reacción entre un diol y un diisocianato en presencia de un catalizador metálico, proceso que actualmente se sigue empleando en la industria. Cabe también resaltar que los PUs a menudo se sintetizan en presencia de un disolvente orgánico para reducir la viscosidad global de la reacción y para obtener polímeros de alto peso molecular.

Sin embargo, su síntesis presenta importantes problemas ambientales y de salud. En primer lugar, se ha demostrado que los isocianatos y algunos reactivos que se utilizan en su síntesis, como el fosgeno, son muy tóxicos. Además, la presencia de compuestos orgánicos volátiles (VOC, de sus siglas en inglés) en la síntesis de PUs para aplicaciones de recubrimiento y pintura ha demostrado ser peligrosa para la salud humana con efectos a largo plazo o muy nocivos para el

medio ambiente. Finalmente, las trazas de metal residual del catalizador pueden permanecer en la matriz del polímero. Estas trazas no solo se han asociado con efectos adversos sobre las propiedades de los polímeros, sino que también restringen su uso como polímero de alto rendimiento en aplicaciones biomédicas o electrónicas. La nueva regulación promovida por la Unión Europea y la Agencia de Protección Ambiental de los Estados Unidos (EPA, de sus siglas en inglés) estipula la prohibición no solo del uso de sustancias que contengan más del 0,1% en peso de diisocianato libre, sino también de limitar la cantidad de VOC que se puede liberar a la atmósfera. Por estas razones, la búsqueda de nuevas rutas de síntesis de poliuretanos sin isocianatos (NIPUs, de sus siglas en inglés) en medios acuosos y en presencia de un catalizador orgánico, que permitan competir con los poliuretanos convencionales, es un verdadero desafío para la ciencia de los polímeros.

En este contexto, durante la última década, se ha producido un gran avance en esta área el cual ha llevado a una serie de procesos sin isocianato. Las cuatro vías más estudiadas para la producción de NIPUs son (1) la poliadición de carbonatos bis-cíclicos con diaminas, (2) la policondensación de dicarbonatos lineales con diaminas, (3) la policondensación de dicarbamatos lineales con dioles y (4) la polimerización con apertura de anillo de carbamatos cíclicos. Entre estos métodos, el más popular y prometedor, propuesto por primera vez en 1957, es la poliadición de carbonatos bis-cíclicos de 5 miembros con diaminas para conducir a la formación de poli(hidroxiuretanos) (PHUs). Sin embargo, este sistema está limitado por la baja reactividad de los carbonatos cíclicos, que a menudo requieren altas temperaturas, condiciones de polimerización en masa, largos tiempos de reacción y el uso de catalizadores para obtener polímeros de alto peso molecular. Además, estas condiciones a menudo implican la formación de reacciones secundarias, tales como transamidaciones inter o intramoleculares, que conducen a la urea. Todas estas limitaciones representan un verdadero obstáculo para el desarrollo industrial de PHUs sin isocianatos a partir de carbonatos cíclicos de 5

miembros. A pesar del gran número de estudios relacionados con el uso de catalizadores en la polimerización por etapas, entre carbonatos cíclicos y aminas, el número de investigaciones acerca del efecto de estos (organo)catalizadores sobre las propiedades finales de los resultantes PHUs son escasos.

Por lo tanto, parte de este manuscrito está dedicado al estudio de la influencia de diferentes organocatalizadores, no solo en la cinética de polimerización, sino también en la estructura y propiedades de los NIPUs resultantes. Primero, se realizó un estudio cinético de la poliadición de dicarbonato de diglicerol con Jeffamine ED-2003, producido en masa a 120 °C y en presencia de diversos organocatalizadores (bases orgánicas y ácidos, donantes de enlaces de hidrógeno). Este estudio mostró que la reacción está fuertemente influenciada por el tipo de catalizador; las más eficaces son bases fuertes como el fosfazeno P_4 o la guanidina TBD. Además, inesperadamente, se ha comprobado que los grupos de uretano formados inicialmente se han transformado en urea en presencia de estas bases fuertes. A través de un estudio de reactivos modelo, como carbonato de propileno y hexilamina se ha mostrado un nuevo mecanismo para la formación de urea a partir de hidroxiuretano. Posteriormente, esta reacción secundaria se utilizó para desarrollar una nueva ruta sintética que no solo permitía el acceso a una gama de poli(hidroxiurea-uretano)s (PHUUs), sino también para controlar la proporción de urea/uretano. Se sintetizaron diferentes polímeros con diferentes proporciones de urea/uretano. Se descubrió que aumentar la cantidad de urea de conduce a PHUUs con mejores propiedades físicas y morfologías de separación de fases. Estos resultados son de gran interés, considerando no solo la importancia industrial de poliurea-uretanos, sino también las restricciones en el uso de isocianatos.

Por otro lado, es esencial poder sintetizar poliuretanos utilizando reactivos menos nocivos y procesos más sostenibles. Por eso, los poliuretanos en base de agua han recibido mucha atención durante la última década debido a severas

restricciones en el uso de VOC. Debido a la incompatibilidad inherente de los isocianatos con el agua, la síntesis directa de PU en agua no se puede lograr usando técnicas convencionales como pueden por la emulsión o microemulsión. Así industrialmente, se han desarrollado varias estrategias para producir dispersiones acuosas (látex) de PU, entre las cuales, el proceso de acetona, es el más extendido. Sin embargo, a pesar de su interés industrial, los procesos para la preparación de nanopartículas de NIPU en medios acuosos son muy raros. Además, las dispersiones acuosas preparadas a partir de carbonatos cíclicos de 5 miembros exhiben una reacción secundaria predecible, la hidrólisis parcial de dichos carbonatos. Por ello, el desarrollo de nuevas estrategias para obtener nanoparticules de NIPU en agua sin reacciones secundarias, es un campo atractivo para la investigación.

La preparación de dispersiones estables de NIPU se ha estudiado en el siguiente capítulo de esta tesis, a través del proceso de acetona y de la poliadición de carbonatos cíclicos de 5 y 8 miembros con una diamina basada en polidimetilsiloxano (PDMS). En esta reacción, el carbonato cíclico de 8 miembros actúa como un tensioactivo interno. Gracias a la presencia en su estructura, después de la apertura del anillo, de aminas terciarias, que se pueden desprotonizar fácilmente, las partículas de NIPU quedan estabilizadas en agua. Usando esta técnica, ha sido posible obtener dispersiones de PHU estables con un tamaño de partícula promedio de aproximadamente 200 nm. Los resultados mostraron que se requería una concentración mínima de 30% en mol de carbonato cíclico de 8 miembros para estabilizar las partículas de NIPU en el agua. Desafortunadamente, debido a la baja Tg dada por la cadena de PDMS en la diamina, no se pudieron preparar partículas rígidas a partir de estas dispersiones. Uno de los métodos más utilizados para aumentar las propiedades mecánicas de los polímeros es la síntesis de materiales reticulados. Aprovechando las interacciones iónicas dadas por las aminas terciarias presentes en el carbonato cíclico de 8 miembros, se han formado películas que tienen propiedades mecánicas

superiores simplemente incorporando ácidos carboxílicos multifuncionales en la dispersión óptima. En particular, a través del uso del ácido trifuncional ácido cítrico, ha sido posible preparar estructuras dinámicas no covalentes formando enlaces iónicos multidireccionales entre los grupos carboxilato y amonio. Este resultado se confirmó mediante el análisis espectroscópico de infrarrojo (FTIR) y de resonancia magnética nuclear (RMN). Gracias a estas interacciones reversibles, se han obtenido materiales con propiedades de reparación. En general, esta estrategia fácil y versátil, basada en NIPU dispersables en agua, demuestra su potencial para la preparación de nuevos materiales para aplicaciones de revestimientos o adhesivos, por ejemplo.

A pesar del éxito de este proceso para la preparación de dispersiones de NIPU en agua, el proceso de acetona generalmente no permite un buen control sobre la morfología de las partículas. Aunque no es esencial para aplicaciones a gran escala, como pinturas o revestimientos, es muy relevante en aplicaciones relacionadas con la nanomedicina donde el control del tamaño de partícula es crucial. Como una alternativa diferente y una nueva estrategia para la síntesis de NIPU basadas en agua, en el Capítulo 4 de esta tesis se ha estudiando la reacción de policondensación *in situ* a temperatura ambiente de dicarbonatos y diaminas lineales mediante polimerización interfacial. La polimerización interfacial tiene numerosas ventajas sobre la polimerización en miniemulsión. Dado que la reacción en la interfaz fuerza a dos moléculas a experimentar una reacción, que generalmente mejora la cinética de la reacción, las polimerizaciones interfaciales son extremadamente rápidas, ocurren en condiciones generalmente suaves y ofrecen la posibilidad de producir rápidamente polímeros de alto peso molecular. Para este fin, primero se sintetizaros tres dicarbonatos lineales diferentes los cuales contienen pentafluorofenol, nitrofenol y fenol como grupos salientes. Luego se comparó su reactividad con poli(bis)amina (PEG-diamina) para demostrar la influencia del grupo saliente en la cinética de la reacción. Además, se exploraron diferentes condiciones (es decir, aceite en agua y agua en aceite) y se realizó un

exhaustivo estudio computacional para comprender mejor el efecto de las condiciones de solvatación sobre la reactividad de los dicarbonatos y el papel de agua en la reducción de las energías de activación de estas reacciones. La optimización tanto del tipo como de la concentración del tensioactivo utilizado para estabilizar las partículas ha permitido proporcionar nanopartículas de NIPU de tamaños entre 200 y 300 nm. Finalmente, se ha desarrollado un método simple para incorporar funcionalidades en estas nanopartículas de NIPU, tales como grupos de ácido carboxílico. A través de este método se han encapsulado molécula activa, el fármaco quimioterapéutico Doxorrubicina (DOX) por interacciones iónicas, para aplicaciones biomédicas.

Résumé

RESUME

Les polymères sont aujourd'hui omniprésents dans notre société, que ce soit dans les secteurs de l'emballage, de la construction, de l'automobile, de l'électronique, des loisirs ou de la médecine. La production mondiale de matières plastiques a atteint 335 millions de tonnes en 2016 et la croissance de la production a augmenté de 1,5 % en 2018, due principalement à la demande croissante des pays émergents.

Parmi tous les plastiques, les polyuréthanes (PUs) représentent la sixième classe de polymère la plus utilisée dans le monde avec une production mondiale estimée à 18 millions de tonnes en 2016. La demande en PUs augmente en moyenne de 4,5 % par an. En Europe, cette demande a atteint 7,5 % en 2016. Ces polymères ont d'excellentes propriétés physiques et mécaniques telles que leur dureté, leur durabilité, leur biocompatibilité, leur élasticité et leur résistance à l'abrasion. Les PUs sont utilisés, classiquement, en tant que mousses souples et rigides pour l'isolation, en tant que matériaux d'étanchéité, pour des revêtements haute performance, comme adhésifs ou dans le domaine biomédical. Découverts par Otto Bayer en 1947, les PUs sont généralement synthétisés par réaction entre un diol et un diisocyanate en présence d'un catalyseur métallique, et ce même actuellement dans l'industrie. Il est également important de préciser que les PUs sont souvent synthétisés en présence d’un solvant organique pour réduire la viscosité globale de la réaction et obtenir des polymères de forte masse molaire.

Néanmoins, cette synthèse présente des problèmes environnementaux et de santé importants. Tout d'abord, il est reconnu que les isocyanates et les réactifs permettant de les synthétiser tel que le phosgène, sont très toxiques. De plus, la présence de composés organiques volatils (COVs) lors de la synthèse des PUs, pour des applications de revêtements et de peintures se sont révélés dangereux pour la santé humaine avec des effets à long terme ou très nocifs pour

l'environnement. Enfin, les traces métalliques résiduelles provenant du catalyseur peuvent rester dans la matrice du polymère. Ces résidus ont non seulement été associées à des effets néfastes sur les propriétés des polymères, mais restreignent également leur utilisation en tant que polymère haute performance dans des applications biomédicales ou électroniques. La nouvelle réglementation promue par l'Union européenne et l'Environmental Protection Agency (EPA) des États-Unis prévoit d'interdire non seulement l'utilisation de substances contenant plus de 0,1 % en masse de diisocyanate libre, mais aussi de limiter la quantité de COV susceptible de se libérer dans l'atmosphère. Pour ces raisons, la recherche de nouvelles voies de synthèse de polyuréthanes sans isocyanates (NIPUs) en milieux aqueux et en présence d'un catalyseur organique, qui permettent de concurrencer les polyuréthanes conventionnels, constitue un véritable défi pour la science des polymères.

Dans ce contexte, au cours de la dernière décennie, les progrès dans ce domaine ont conduit à un certain nombre de procédés sans isocyanates. Les quatre voies les plus étudiées vers les NIPUs sont (1) la polyaddition de carbonate bis-cycliques avec des diamines, (2) la polycondensation de dicarbonates linéaires avec des diamines, (3) la polycondensation de dicarbamate linéaires avec des diols et (4) la polymérisation par ouverture de cycle de carbamates cycliques. Parmi ces méthodes, la plus populaire et la plus prometteuse, proposée pour la première fois en 1957, est la polyaddition de carbonate bis-cycliques à 5 chaînons avec des diamines pour conduire à la formation de poly(hydroxyuréthanes) (PHUs). Ce système est cependant limité par la faible réactivité des carbonates cycliques, nécessitant souvent des températures élevées, des conditions de polymérisation en masse, des temps de réaction longs et l'utilisation de catalyseurs, pour obtenir des polymères de masse molaires élevées. Ces conditions impliquent souvent la formation de réactions secondaires, telles que les transamidations inter ou intra-moléculaires, conduisant à l'urée. Malgré leur intérêt industriel, ces limitations représentent un véritable obstacle au développement industriel des PHU sans

isocyanates à partir de carbonates cycliques à 5 chaînons. De plus, même si de nombreuses études liées à l'utilisation de catalyseurs dans la polymérisation par étapes, entre les carbonates et les amines cycliques, ont été menées, des études détaillées portant sur l'effet des catalyseurs sur les propriétés finales des PHU résultants, sont très rares.

Par conséquent, une partie de ce manuscrit est dédiée à une étude rationnelle de l'influence des organocatalyseurs, non seulement sur la cinétique de polymérisation, mais aussi sur la structure et les propriétés des NIPUs résultants. Premièrement, une étude cinétique de la polyaddition du diglycerol dicarbonate avec la Jeffamine ED-2003, réalisée en masse à 120 °C et en présence de différents organocatalyseurs (bases et acides organiques, donneurs de liaisons hydrogènes), a été menée. Cette étude a montré que la réaction était fortement influencée par le type de catalyseurs ; les plus efficaces étant les bases fortes telles que le phosphazene P_4 ou la guanidine TBD. De plus, indépendamment de notre volonté, nous avons constaté que les groupements uréthanes formés initialement ont été transformés en urée en la présence de ces bases fortes. Une étude sur des réactifs modèles, tels que le carbonate de propylène et l'hexylamine, a permis de présenter un nouveau mécanisme de formation d'urée à partir d'hydroxuréthane. Par la suite, cette réaction secondaire a été utilisée pour mettre au point une nouvelle voie de synthèse permettant non seulement d'accéder à une gamme de poly(hydroxyurée-uréthane)s (PHUUs), mais également de contrôler le ratio urée/urethane. Différents polymères possédant des ratios urée/urethane différents ont été synthétisés. Nous avons constaté, que l'augmentation de la quantité d'urée conduisait à des PHUUs possédant de meilleurs propriétés physiques et des morphologies de séparation de phase. Ces résultats sont d'un grand intérêt, compte tenu, non seulement de l'importance industrielle des poly(urée-uréthanes), mais aussi des restrictions sur l'utilisation des isocyanates.

Il est indispensable de pouvoir synthétiser les polyuréthanes en utilisant des réactifs moins nocifs et des procédés plus durables. De ce fait, les polyuréthanes à

base d'eau ont beaucoup attiré l'attention au cours de la dernière décennie en raison des restrictions sévères liés à l'utilisation des COVs. En raison de l'incompatibilité inhérente des isocyanates avec l'eau, la synthèse directe de PU dans l'eau ne peut pas être réalisée en utilisant des techniques classiques d'émulsion ou de microémulsion. Par conséquent, plusieurs stratégies ont été développées pour produire des dispersions aqueuses (latex) de PUs, parmi lesquelles, le procédé acétone, est le plus répandu dans l'industrie. A contrario, malgré leur intérêt industriel, les procédés de préparation de nanoparticules de PU sans isocyanates en milieux aqueux sont très rares. De plus, les dispersions aqueuses préparées à partir de carbonates cycliques à 5 chaînons présentent une réaction secondaire prévisible, l'hydrolyse partielle des carbonates cycliques. Par conséquent, d'autres stratégies pour obtenir des nanoparticules de NIPU dans l'eau sans réactions secondaires doivent être développées et testées.

Le chapitre suivant de cette thèse porte donc sur la préparation de dispersions stables de NIPUs. Notre stratégie consiste à adapter le procédé acétone à la polyaddition de carbonates cycliques à 5 et 8 chaînons avec une diamine à base de polydimethylsiloxane (PDMS). Dans cette réaction, le carbonate cyclique à 8 chaînons, joue le rôle de tensioactif interne. Grâce à la présence dans sa structure, après ouverture du cycle, d'amine tertiaires qui peuvent être facilement déprotonées, les particules de NIPU peuvent être stabilisées dans l'eau. En utilisant cette technique, il a été possible d'obtenir des dispersions de PHU stables avec une taille de particule moyenne d'environ 200 nm. Les résultats ont montré qu'une concentration minimum de 30 % en mole de carbonate cyclique à 8 chaînons était nécessaire pour stabiliser les particules de NIPU dans l'eau. Malheureusement, en raison de la faible Tg donnée par la chaîne PDMS dans la diamine, des films rigides n'ont pas pu être préparés à partir de ces dispersions. Une des méthodes connues pour augmenter les propriétés mécaniques des polymères réside dans la synthèse de matériaux réticulés. En tirant parti des interactions ioniques données par les amines tertiaires présent dans le carbonate cyclique à 8 chaînons, des films

possédant des propriétés mécaniques supérieures, ont été formés, par simple incorporation d'acides carboxyliques multifonctionnels dans la dispersion optimale. Notamment, l'utilisation de l'acide citrique, un acide trifonctionnel, a permis de préparer des structures dynamiques non covalentes par formation de liaisons ioniques multidirectionnelles entre les groupements carboxylate et ammonium, comme l'ont confirmé les analyses spectroscopiques IR et RMN. En tirant parti de ces interactions réversibles, des matériaux aux propriétés d'auto-guérison ont pu être obtenus. Dans l'ensemble, cette stratégie facile et polyvalente, basée sur des polyuréthanes sans isocyanates dispersibles dans l'eau, démontre son potentiel pour la préparation de nouveaux matériaux pour des applications de revêtements ou d'adhésifs par exemple.

Malgré le succès de ce procédé pour la préparation de dispersions de NIPUs dans l'eau, le procédé acétone empêche généralement d'avoir un bon contrôle sur la morphologie des particules. Bien que cela ne soit pas essentiel pour des applications à grande échelle, telles que les peintures ou les revêtements, il est très pertinent dans des applications liées à la nanomédecine où le contrôle de la taille des particules est crucial. Comme alternative différente et nouvelle stratégie pour la synthèse de NIPUs à base d'eau, nous avons étudié dans le Chapitre 4 de cette thèse, la réaction de polycondensation *in situ* à température ambiante de dicarbonates linéaires et diamines par polymérisation interfaciale. La polymérisation interfaciale présente de nombreux avantages par rapport à la polymérisation en mini-émulsion. Comme la réaction à l'interface oblige deux molécules à subir une réaction, ce qui améliore généralement la cinétique de réaction, les polymérisations interfaciales sont extrêmement rapides, se produisent dans des conditions généralement douces et offrent la possibilité de produire rapidement des polymères de haut poids moléculaire. À cette fin, nous avons d'abord synthétisé trois différents dicarbonates linéaires contenant du pentafluorophénol, du nitrophénol et du phénol en tant que groupes partants. On a ensuite comparé leurs réactivités envers le polyéthylène (bis) amine (PEG-diamine) pour démontrer l'influence du groupe

partant sur la cinétique de la réaction. Des conditions différentes ont également été explorées (c.-à-d. huile dans eau et eau dans huile) et une étude computationnelle exhaustive a été réalisée pour mieux comprendre l'effet des conditions de solvatation sur la réactivité des dicarbonates et le rôle de l'eau dans la réduction des énergies d'activation de ces réactions. L'optimisation à la fois du type et de la concentration du tensioactif utilisé pour stabiliser les particules, a permis de fournir des nanoparticules de NIPUs de tailles comprises entre 200 et 300 nm. Enfin, une méthode simple pour incorporer des fonctionnalités, tels que des groupes acides carboxyliques, dans ces nanoparticules de NIPU a été développée. Cette méthode a permis d'encapsuler par interactions ioniques des molécules actives, tel que le médicament chimiothérapeutique Doxorubicine (DOX), pour des applications biomédicales.